CHAPTER 2

Applications of Post-Hartree–Fock Methods: A Tutorial

Rodney J. Bartlett and John F. Stanton

Quantum Theory Project, Departments of Chemistry and Physics, University of Florida, Gainesville, Florida 32611

INTRODUCTION

This chapter is meant to be a condensed(!) tutorial on the intelligent use of post-Hartree–Fock (correlated) methods for the determination of molecular structure and spectra.[1] The content is directed at users of the ACES II, GAUSSIAN, CADPAC, HONDO, or GAMESS[2] type of ab initio program, or anyone who would appreciate a broader knowledge of the modern treatment of electron correlation for molecules. The ready availability and applicability of these programs might be said to be one of the principal contributions of ab initio quantum chemistry to science, inasmuch as these systems provide a probe of structural, spectral, and reactivity characteristics frequently unavailable from experiment or, alternatively, facilitate interpretation of available experimental data. However, the ease of using these programs (and their official-looking output!) can mask many difficult situations that might not be recognized by users, resulting in misinterpretation of computational results. Theoreticians who develop such program systems are aware of the potential shortcomings of each approximation, but many users lack a full understanding of the

Reviews in Computational Chemistry, Volume V
Kenny B. Lipkowitz and Donald B. Boyd, Editors
VCH Publishers, Inc. New York, © 1994

theoretical foundations of the various methods. We try to explain some of these considerations, and how they affect the choice of method and basis set for a given application. Clearly, no single chapter can replace several courses in quantum chemistry and years of hands-on experience in the use of correlated electronic structure methods, but we think it is possible to provide a guide that provides much of the essential information required for intelligent application of the current level of post-Hartree–Fock methods without becoming "too theoretical."

At the same time, we must recognize that quantum chemistry is an ongoing research area. Though it is mature enough to provide useful tools for a wide range of applications, even a year ago many of the tools described here and recently incorporated into the ACES II[3] program system did not exist. Among other things, this means that the useful lifetime of any tutorial is finite, but by including some recent developments not widely known to the current user community, we hope that this chapter will have an effective lifetime that is relatively long. No unique recipe for doing post-Hartree–Fock calculations can be offered, but many of the considerations pertinent to such calculations can be identified and emphasized. In the application areas, by following the sequence from self-consistent field (SCF) to the highest current levels of correlated theory, we hope to show how approaches to different problems have evolved, and continue to progress, to provide better and more comprehensive results.

After a discussion of the independent particle or Hartree–Fock (SCF) approximation[4] to introduce some basic concepts, we discuss the correlation problem and available methods for its treatment.[5-10] We then address several topics that cover most of the applications of interest to users of quantum chemical program systems. These include molecular geometries, vibrational spectra, photoelectron spectra, electronic spectra, first- and second-order properties, and nuclear magnetic resonance spectra. In each category of application, we address the range of applicability of SCF methods and the degree of correlation correction required, and we state what can be expected, numerically, from increasing levels of rigor. Our objective is to provide the reader with both a conceptual understanding and some appreciation of the approximate uncertainty for a given level of theory. Our intent is not to present the voluminous results on which these "error bars" are based—that is left to the literature—but instead to pick a few standard and a few difficult molecules that are representative of results one should expect. We do not derive equations, but we do present basic equations to help the reader better appreciate the nature of the approach. Just as a picture can be worth a thousand words, an equation will often do the job of hundreds, and only in this way can we attempt to maintain some brevity while minimizing impreciseness. We assume only that the reader has some familiarity with Hartree–Fock theory.[4] On the other hand, nothing we say should unduly depend on appreciation of mathematical arguments—more conceptual, complementary explanations are employed whenever possible.

To be most useful, we necessarily address the correlated methods that are

most readily applicable to the majority of problems of interest to chemists, thereby imposing several requirements that a method must meet. These include treating different molecular geometries with effectively equal accuracy; equivalent applications to open- and closed-shell systems; treatment of excited, ionized, or electron-attached states as well as ground states; and predictions of other properties such as moments and polarizabilities. Also the term "post-Hartree–Fock" implies a single determinant starting point. Consequently, because of their wide applicability and ease of use, we emphasize methods built upon a single reference when possible. These include many-body perturbation theory[5] (MBPT, also known as MP in some program systems[8]), and its infinite-order coupled-cluster (CC) generalization,[6,11,12] [including quadratic configuration interaction (QCI)[13] as a special case] as well as some configuration interaction (CI) methods.[9] However, we also mention situations for which multi (instead of single) determinant references are appropriate,[14] such as excited states and certain transition states, and provide some alternative readily applicable tools that are no more difficult to understand and use than standard single reference theory.

To avoid being discouraged by discussions of theory, some readers might prefer a "results-oriented" sequence. For those readers, a reasonable sequence would be to start with the section on molecular geometries, continue through the applications areas, and treat the preceding sections as appendices that define the various levels of theory. The sections on theory, however, were written to be clear and thorough.

Most of the results reported here were obtained with the ACES II program system.[3] The program provides CC/MBPT results for molecules, open or closed shell, using UHF, ROHF, RHF and QRHF reference functions (see later for acronyms). It offers analytical gradients for most such methods including MBPT (2), (3) and (4), CCSD, CCSD(T), and analytical Hessians for MBPT(2) with RHF, UHF or ROHF reference functions. ACES II requires only simple Z-matrix (bond distance and angle) input plus key words that identify basis sets (most modern basis sets are catalogued), level of correlation, degrees of freedom to optimize, and other options. The program automatically introduces the available molecular symmetry and employs the largest Abelian subgroup to simplify and speed CC/MBPT calculations. ACES II provides CC methods for excited states (UV-vis spectroscopy), ionized states (photoelectron spectroscopy), molecular properties (ESR, NMR), and relativistic corrections. The program has a number of analysis tools to facilitate interpretation, locate optimum geometries and transition states, and evaluate vibrational spectra.

INDEPENDENT PARTICLE MODEL

The reference framework for most theoretical descriptions of molecular electronic structure and spectra is the independent particle or molecular orbital

(MO) model. In quantum mechanics, the energy of a molecule is based on the Hamiltonian operator

$$\mathcal{H} = -\frac{1}{2}\sum_i \nabla^2(\mathbf{r}_i) - \sum_\alpha \sum_i Z_\alpha / r_{\alpha i} + \frac{1}{2}\sum_{i,j}{}' \frac{1}{r_{ij}} + \frac{1}{2}\sum_{\alpha,\beta}{}' \frac{Z_\alpha Z_\beta}{R_{\alpha\beta}} \qquad [1]$$

(the prime eliminates the $i = j$ and $\alpha = \beta$ term). The first term is the kinetic energy, which is given by a sum over one-particle operators corresponding to each electron $\mathbf{r}_i$. The second one-electron term is the Coulombic electron–nuclear attraction term, where Z_α is the atomic number for the nucleus α, and $r_{\alpha i}$ measures the distance of electron i from the αth nucleus. The third term is the two-electron Coulomb repulsion term, where $r_{ij} = |\mathbf{r}_i - \mathbf{r}_j|$ is the distance between the ith and jth electrons. The final term is the nuclear–nuclear repulsion, where $R_{\alpha\beta} = |\mathbf{R}_\alpha - \mathbf{R}_\beta|$. In the Born–Oppenheimer "clamped nuclei" approximation that underlies nearly all molecular calculations, this term is a constant determined by the nuclear coordinates and is simply added at the end of a calculation. It introduces the characteristic repulsive wall for a potential curve and, thus, is important in the solution of the vibrational Schrödinger equation.

Hence for the electronic Schrödinger equation, our objective is the solution to $\mathcal{H}\Psi_k = E_k\Psi_k$ for the spectrum of electronic states $\{\Psi_k\}$, where

$$\mathcal{H} = \sum_i h(i) + \frac{1}{2}\sum_{i,j}{}' \frac{1}{r_{ij}} \qquad [2]$$

with the two one-electron parts combined into $h(i)$.

The delightful thing about one-electron operators is that we can exactly solve the Schrödinger equation if the Hamiltonian is approximated by its one-electron part ($\mathcal{H} \approx \Sigma_i h(i) = H_0$) since a "separable" wavefunction can be constructed as a product of one-particle functions, $\phi_j(\mathbf{r}_j)$,

$$\Phi_0(r;R) = \phi_1(\mathbf{r}_1)\phi_2(\mathbf{r}_2)\cdots\phi_n(\mathbf{r}_n) \qquad [3]$$

where the notation $\Phi_0(r;R)$ means a function of all electron coordinates collectively indicated by r, that through the Born–Oppenheimer approximation is parametrically dependent on the collective location of the nuclei, R. Using Eq. [3] we would have $[\Sigma_j h(j)]\phi_1(\mathbf{r}_1)\phi_2(\mathbf{r}_2)\cdots\phi_n(\mathbf{r}_n) = [h(\mathbf{r}_1)\phi_1(\mathbf{r}_1)]\phi_1(\mathbf{r}_2)\cdots\phi_n(\mathbf{r}_n) + \phi_1(\mathbf{r}_1)[h(\mathbf{r}_2)\phi_2(\mathbf{r}_2)]\phi_3(\mathbf{r}_3)\cdots + \cdots\phi_1(\mathbf{r}_1)\phi_2(\mathbf{r}_2)\cdots[h(\mathbf{r}_n)\phi_n(\mathbf{r}_n)]$. Then by knowing that each one-particle function was an eigenfunction to $h(\mathbf{r}_j)$ with energy ϵ_j,

$$h(\mathbf{r}_1)\phi_j(\mathbf{r}_1) = \epsilon_j\phi_j(\mathbf{r}_1) \qquad [4]$$

we would have

$$H_0\Phi_0 = E_0\Phi_0 \qquad [5]$$

$$E_0 = \sum_{j=1}^{n} \epsilon_j \qquad [6]$$

However, we can do even better without sacrificing this convenient separability. If we are able to approximate the two-particle term as some "average" one-particle operator, $u(\mathbf{r}_j)$, where, for example, we might average over the repulsion of all other electrons in the system toward electron j, then we obtain the expression

$$\begin{aligned} \mathcal{H} &= \sum_{j=1}^{n} [h(\mathbf{r}_j) + u(\mathbf{r}_j)] + \frac{1}{2}\sum_{i,j}{}' \frac{1}{r_{ij}} - \sum_{j=1}^{n} u(\mathbf{r}_j) \\ &= \sum_{j=1}^{n} \mathcal{F}(\mathbf{r}_j) + V = H_0 + V \end{aligned} \qquad [7]$$

If V is small (and it is clearly smaller than the two-particle term itself), then we might expect that replacement of $\mathcal{H}$ by H_0 (which is a separable sum of one-particle Hamiltonians, $\mathcal{F}(\mathbf{r}_j)$) to be a good approximation. This simplification allows us to reduce the n-particle problem to a set of one-particle eigenvalue problems,

$$\mathcal{F}(\mathbf{r}_j)\phi_j(\mathbf{r}_j) = \epsilon_j\phi_j(\mathbf{r}_j) \qquad [8]$$

and is the basis of molecular orbital theory. An MO is an eigenfunction of an effective one-particle Hamiltonian, and the electron in the MO is considered to have an orbital energy of ϵ_j. Eigenfunctions to a Hermitian operator $\{\phi_j\}$ are either orthonormal or may be chosen to be orthonormal in degenerate cases, so $\langle\phi_i|\phi_j\rangle = \delta_{ij}$.

Although the basic concept will not change, two additional modifications must be made to this simple theory to make it consistent with other aspects of quantum mechanics. First, to fully characterize electrons we need to include spin. Consequently, this requires that to each spatial one-particle function $\phi_j(\mathbf{r}_j)$ we attach α (spin-up) or β (spin-down). Hence, each one-particle function becomes $\phi_j(\mathbf{r}_j)\alpha(\omega_j)$ or $\phi_j(\mathbf{r}_j)\beta(\omega_j)$, where ω_j indicates a coordinate in spin space. We can use an even shorter notation by specifying $\varphi_j(x_j) = \phi_j(\mathbf{r}_j)\alpha(\omega_j)$ to be spin orbitals, where the combined space-spin coordinate is x_j. It is still true that $\mathcal{F}(x_j)\varphi_j(x_j) = \epsilon_j\varphi_j(x_j)$.

Second, suitable solutions to the Schrödinger equation for electrons must have appropriate permutational symmetry. That is, an interchange of the space-spin coordinates x_i and x_j must not alter the probability density $|\Psi|^2$.[15] For this to be true, the interchange operator P_{ij} has to have the effect, $P_{ij}\Psi = \pm\Psi$. For

electrons and other fermions, the minus applies (the Pauli exclusion principle), requiring that our wavefunctions be antisymmetrized products that assume the determinantal form

$$\Phi_0 = \frac{1}{\sqrt{n!}} \begin{vmatrix} \varphi_1(x_1) & \varphi_2(x_2) \cdots & \varphi_n(x_n) \\ \varphi_2(x_1) & \cdots & \cdots \\ \vdots & & \vdots \\ \varphi_n(x_1) & \cdots & \varphi_n(x_n) \end{vmatrix} = \mathcal{A}(\varphi_1(x_1) \cdots \varphi_n(x_n)) \qquad [9]$$

The operator $\mathcal{A} = (1/\sqrt{n!}) \sum_P (-1)^p P$, where P presents a permutation of electron labels. $\mathcal{A}$ forms a determinant by permuting all the space-spin labels in the simple product multiplied by the parity factor $(-1)^p$ and normalizing the wavefunction.

It is fairly easy to see that each of the $n!$ products introduced by the determinant will behave in exactly the same way (i.e., H_0 and $\mathcal{A}$ commute) resulting in the same one-particle equations (suppressing the x),

$$\mathcal{F}(1)\varphi_j(1) = \epsilon_j \varphi_j(1) \qquad [10]$$

and in particular

$$\begin{aligned} H_0 \mathcal{A}(\varphi_1(1) \cdots \varphi_n(n)) &= E_0 \mathcal{A}(\varphi_1(1) \cdots \varphi_n(n)) \\ H_0 \Phi_0 &= E_0 \Phi_0 \end{aligned} \qquad [11]$$

In this simple scheme, such other eigenstates of H_0 as Φ_j^a are formed by replacing one of the molecular orbitals $\varphi_j(j)$ occupied by electron j by some orbital unoccupied in the ground state, call it $\varphi_a(j)$, that is also an eigenfunction of $\mathcal{F}(i)$. Thus we would have

$$\begin{aligned} H_0 \Phi_j^a &= H_0 \mathcal{A}(\varphi_1(1) \cdots \varphi_a(j) \cdots \varphi_n(n)) \\ &= E_j^a \mathcal{A}(\varphi_1(1) \cdots \varphi_a(j) \cdots \varphi_n(n)) \\ &= E_j^a \Phi_j^a \end{aligned} \qquad [12]$$

where the eigenvalue is written

$$\begin{aligned} E_j^a &= \left(\sum_{k(\neq j)} \epsilon_k \right) + \epsilon_a \\ &= E_0 + \epsilon_a - \epsilon_j \end{aligned} \qquad [13]$$

The general independent particle model described above becomes the Hartree–Fock, self-consistent field (SCF) approximation when Φ_0 is the ener-

getically "best" single determinant approximation to Ψ. (In some SCF approaches, Φ_0 is energetically optimal subject to certain constraints on the orbitals.) That is, we use the variational principle, $E = \langle\Phi_0|\mathcal{H}|\Phi_0\rangle \geq E_{\text{exact}}$ to vary the form of the n-spin orbitals $\{\varphi_i\}$ subject to maintaining their orthogonality $\langle\varphi_i|\varphi_j\rangle = \delta_{ij}$ until we obtain the lowest possible energy, E_{SCF}. In the course of the energy variation, we find that

$$\mathcal{F}(1) = h(1) + u(1) = h(1) + \sum_{j=1}^{n} \int \varphi_j^*(2) \frac{1}{r_{12}} (1 - P_{12})\varphi_j(2) d\tau_2 \qquad [14]$$

which defines the operator, $u(1)$. The volume element in space-spin coordinates is $d\tau$. Self-consistency in the solution of Eq. [10] is necessary because the form of $\mathcal{F}$ is dependent on the form of the spin orbitals, $\{\varphi_j\}$ via the $u(1)$ operator of Eq. [14].

Furthermore,

$$\begin{aligned} E_{SCF} &= \langle\Phi_0|\mathcal{H}|\Phi_0\rangle = Tr(\mathcal{H}\rho) \\ &= \sum_i \langle\varphi_i|h(1)|\varphi_i\rangle + \frac{1}{2}\sum_{i,j}\langle\varphi_i\varphi_j\|\varphi_i\varphi_j\rangle \\ &= \sum_i \langle i|h|i\rangle + \sum_{i<j} \langle ij\|ij\rangle \\ &= \sum_i \epsilon_i - \sum_{i<j} \langle ij\|ij\rangle \\ &= E_0 + \langle\Phi_0|V|\Phi_0\rangle \end{aligned} \qquad [15]$$

so E_{SCF} is not a simple sum of orbital energies. The double bar means $\langle ij\|ij\rangle = \langle ij|ij\rangle - \langle ij|ji\rangle$, where $\langle ij|ij\rangle = \int \varphi_i^*(1)\varphi_j^*(2)(1/r_{12})\varphi_i(1)\varphi_j(2)d\tau_1 d\tau_2 = (ii|jj)$.

These particular spin-orbital equations are termed the unrestricted Hartree-Fock (UHF) equations, since variation here does not assume that all spatial orbitals are doubly occupied. That is, we permit $\varphi_j = \phi_j\alpha$ and $\varphi_{j+1} = \phi_j'\beta$, where $\phi_j \neq \phi_j'$. For a closed-shell system, we can insist on getting the best energy while having $\phi_j = \phi_j'$, which defines the restricted Hartree–Fock (RHF) solution. Hence, UHF is formally the same for open and closed shells, whereas RHF applies only to the latter. For high spin open shells, we can also insist that our solutions have maximum double occupancy as shown in Figure 1. These are referred to as restricted open-shell Hartree–Fock (ROHF) solutions. For such a case there is a more complicated $\mathcal{F}(1)$ operator,[4] but the orthonormal orbitals that emerge are degenerate. These different SCF models may be succinctly compared by inspection of Figure 1. We collectively refer to any of the foregoing approaches as "SCF" methods.

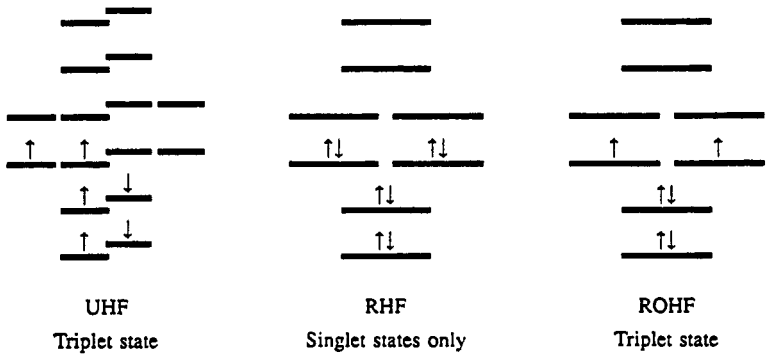

Figure 1 Orbital energy level diagrams for UHF, RHF, and ROHF reference functions.

The result of an SCF calculation is the wavefunction $\Phi_0 = \Phi_{SCF}$, consisting of the MOs $\{\varphi_i\}$, the density $\rho = \Phi_i \Phi_i^*$, from which properties for some operator θ are given by $Tr(\theta\rho)$; the total energy E_{SCF}; and in the canonical UHF or RHF case, the orbital energies ϵ_i, which provide an (unrelaxed) estimate of the ionization potential via Koopmans' theorem, $\epsilon_i = -I(i)$, for an electron in the ith MO. The approximation of interelectronic repulsion by the effective one-particle operator, $u(1)$ in Eq. [14], represents the potential one electron feels when moving in an average field generated by the remaining electrons. This follows because in the sum over j in Eq. [15], when $j = i$, we have $\langle ii \| ii \rangle = 0$.

All the SCF methods mentioned above are independent particle models. Since they serve as the reference for the post-Hartree–Fock methods discussed in this chapter, we should be aware of their properties. RHF applies only to closed-shell systems and is a singlet eigenfunction of spin. (Some authors insist that "restricted" must pertain to spatial symmetry as well as spin symmetry, but GAUSSIAN, ACES II, and other program systems can in principle converge to broken spatial symmetry solutions even for closed shells, so we will not insist that RHF solutions be restricted to spatial symmetry eigenfunctions, too.) As is well known, and shown in Figure 2 for H_2, an RHF solution does not separate correctly to open-shell fragments on a potential energy curve. (RHF separates correctly for closed-shell products such as $B_2H_6 \rightarrow 2BH_3$, or $Be_2 \rightarrow 2Be$, or $HeH^+ \rightarrow He + H^+$.) That is because RHF uses equal orbitals for different spins at all internuclear separations, which does not allow the orbitals to localize on the individual atoms. The RHF wavefunction for H_2 is $|1\sigma_g\alpha 1\sigma_g\beta|$. Yet to get two H(1s) atoms at separation we must have $1s_A = 1\sigma_g + 1\sigma_u$ and $1s_B = 1\sigma_g - 1\sigma_u$, where *g* and *u* refer to *gerade* (even) and *ungerade* (odd). Hence, correct separation would require the two determinants $C_1|1\sigma_g\alpha 1\sigma_g\beta| \pm C_2|1\sigma_u\alpha 1\sigma_u\beta|$, where $C_1 = C_2$ at separation but $C_1 \gg C_2$ at R_e. This two-determinant wave-

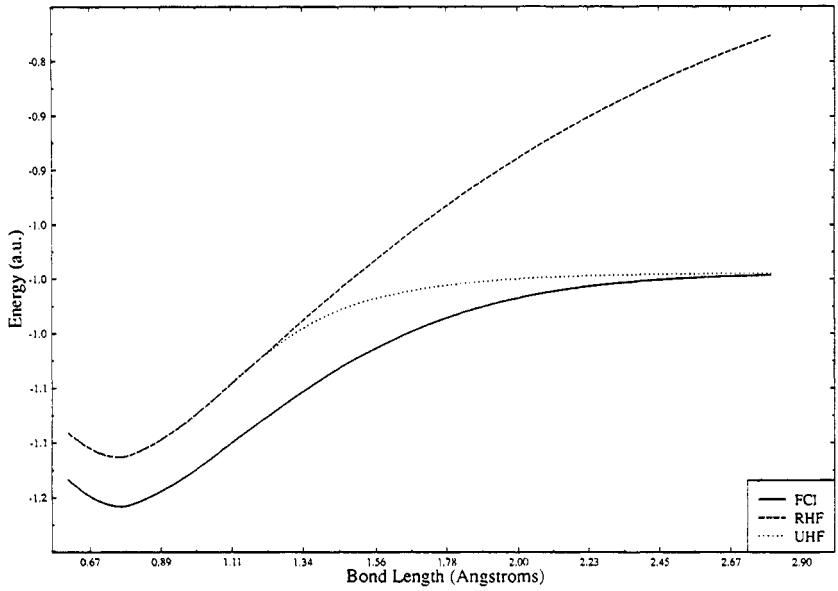

Figure 2 Potential energy curves for H_2.

function is an example of a generalized valence bond (GVB) function. Compare the GVB result with the two SCF results in Figure 2.

A high spin ROHF wavefunction is also an eigenfunction of spin: that is, $\hat{S}^2|\text{ROHF}\rangle = S(S+1)|\text{ROHF}\rangle$. The designation "high spin" is meant to eliminate such situations as an open-shell singlet (illustrated in Figure 3), which cannot be written as a single determinant. We would require two determinants, that is, $(|\phi_1\alpha\phi_1\beta\phi_2\alpha\phi_3\beta| - |\phi_1\alpha\phi_1\beta\phi_2\beta\phi_3\alpha|)$, to be a spin eigenfunction. Similar situations pertain to the low-spin doublets also shown in Figure 3, whereas the "maximum" double-occupancy doublet is an eigenfunction of spin. Like RHF, an ROHF wavefunction usually will not separate correctly on a potential energy surface, as shown for $O_2(^3\Sigma_g^-)$ in Figure 4. (An open-shell example like

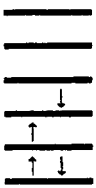

Open-shell singlet

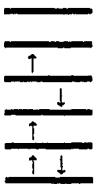

Low-spin doublet

Figure 3 Orbital energy level diagrams for the open-shell singlet and low-spin doublet cases.

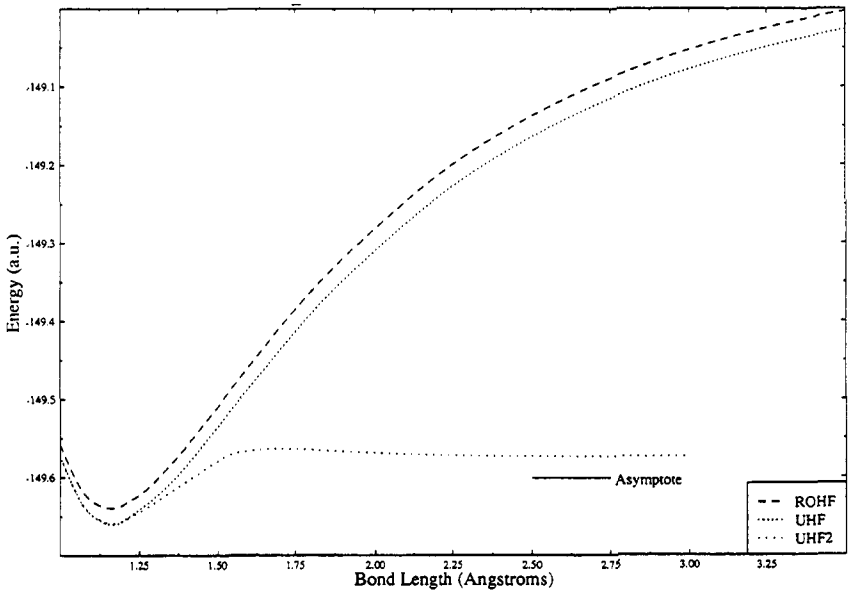

Figure 4 SCF potential curves for O_2.

$AB^+ \rightarrow A^+ + B$, where B is a closed-shell system, will separate correctly in ROHF.)

UHF is a fully unconstrained SCF method and actually represents several different solutions, depending on what symmetries are broken. First, it allows the wavefunctions to be impure spin states. Also, because the various kinds of spatial and spin symmetry are frequently broken in UHF wavefunctions, we can often obtain correct asymptotic separation on a potential energy curve as in Figure 2. For example, the UHF solution for H_2 breaks g and u symmetry to give localized $1s_A$ and $1s_B$ functions, but, unlike the GVB solution, the UHF wavefunction does not have the symmetry of the molecule (see Figure 5; it is half of the correct solution!). To construct a proper wavefunction, the UHF solution must be mixed with its phase-reversed partner. The change in energy brought about by this process of symmetrization is related to the singlet–triplet splitting. However, this gap goes to zero in the limit of infinite separation, since the two UHF wavefunctions are degenerate. As a result, UHF and GVB energies are asymptotically degenerate.

The UHF solutions for O_2 in Figure 4 illustrate another aspect as the higher energy UHF only breaks spin symmetry, whereas the lower energy solution, UHF2, breaks spatial symmetry, too. However, unlike H_2, there is no UHF solution that correctly separates to two UHF $O(^3P)$ atoms for $O_2(^3\Sigma_g^-)$.

In making practical SCF calculations we introduce a basic set $\{\chi_\mu\}$, which usually consists of contracted Gaussian-type orbitals centered on each atom γ,

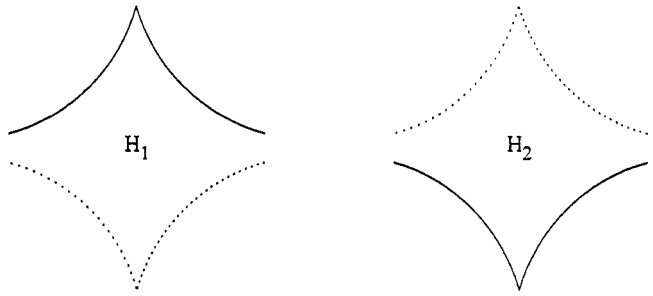

Figure 5 Solid lines, UHF solution for H_2 at $R = \infty$; dashed lines, degenerate UHF solution.

that is, $\chi_s(R_\gamma) = \Sigma_k \eta_{s_k} \exp(-\xi_{s_k} r_\gamma^2)$, $\chi_{p_x}(R_\gamma) = \Sigma_k \eta_{x_k} x \exp(-\xi_{x_k} r_\gamma^2)$, etc., where the coefficients η_k and ξ_k are fixed typically from prior atomic Hartree–Fock calculations, but other prescriptions are possible. Using UHF as an example, spatial orbitals are associated with each spin via

$$\begin{aligned} \phi_j^\alpha &= \sum_{\mu=1}^{M} \chi_\mu c_{\mu_j}^\alpha = |\tilde{\chi}\rangle c_j^\alpha \\ \phi_j^\beta &= \sum_{\mu=1}^{M} \chi_\mu c_{\mu_j}^\beta = |\tilde{\chi}\rangle c_j^\beta \end{aligned} \qquad [16]$$

Inserting Eq. [16] into the canonical SCF equation $\mathcal{F}\varphi_i = \epsilon_i \varphi_i$, leads to the matrix formulation of the UHF equations

$$\begin{aligned} \mathbf{F}^\alpha \mathbf{c}_p^\alpha &= \mathbf{S}\mathbf{c}_p^\alpha \epsilon_p^\alpha \\ \mathbf{F}^\beta \mathbf{c}_p^\beta &= \mathbf{S}\mathbf{c}_p^\beta \epsilon_p^\beta \end{aligned} \qquad [17]$$

where $\mathbf{F} = \langle \tilde{\chi} | \mathcal{F} | \tilde{\chi} \rangle$ and $\mathbf{S} = \langle \tilde{\chi} | \tilde{\chi} \rangle$, and the α or β dependence in F arises from the explicit spin integrated $u(1)$ part of $\mathcal{F}$. For RHF $\mathcal{F}^\alpha = \mathcal{F}^\beta$, of course. For ROHF there are two different forms of $\mathcal{F}$ to consider, one for the α-spin open-shell orbitals, and one for the α- or β-spin doubly occupied orbitals.

Because the matrix $\mathbf{F}^\alpha$ or $\mathbf{F}^\beta$ has dimension $M \times M$, we obtain M α-spin and M β-spin spatial orbitals via diagonalization. But we only use n_α and n_β of these orbitals to construct the SCF solution. This leaves us with $M - n_\alpha = N_\alpha$ and $M - n_\beta = N_\beta$ spin orbitals unoccupied in the SCF solution. We identify these orbitals collectively by the letters *a, b, c, . . .*, whereas *i, j, k, . . .* indicate orbitals occupied in the SCF solution, and *p, q, r, s, . . .* indicate any orbital. The orbitals *a, b, c, . . .* are frequently called "virtual" orbitals because they

are obtained as a by-product of diagonalizing the F matrix. They are not determined by the variational principle as are the occupied SCF orbitals. Physically, an electron in a virtual orbital feels the average field of all n electrons instead of the $n - 1$ felt by an electron in an occupied orbital. The virtual orbitals are, however, a convenient orthogonal set of one-particle functions that satisfy $\mathcal{F}(1)\varphi_a(1) = \epsilon_a\varphi_a(1)$ for all a (like the occupied orbitals) and, combined with the occupied orbitals, span the space represented by the contracted Gaussian functions. The virtual orbitals play a critical role in correlated methods.

CORRELATION PROBLEM

An investigation of the potential curves for N_2 (Figure 6) and F_2 (Figure 7) tells us a great deal about the deficiencies of a model of the Hartree–Fock, independent particle type. The inability of a restricted (RHF or ROHF) solution to correctly separate to open shells causes the curve to rise too quickly, leading to a gross overestimate of the dissociation energy. Hence, RHF usually will underestimate equilibrium bond lengths (R_e). For the same reason, the curvature (force constant) at R_e will be larger than it should be, resulting in an overprediction of the vibrational frequency. UHF does not rectify this problem, even though it will often separate correctly, as in the N_2 example. The reason is

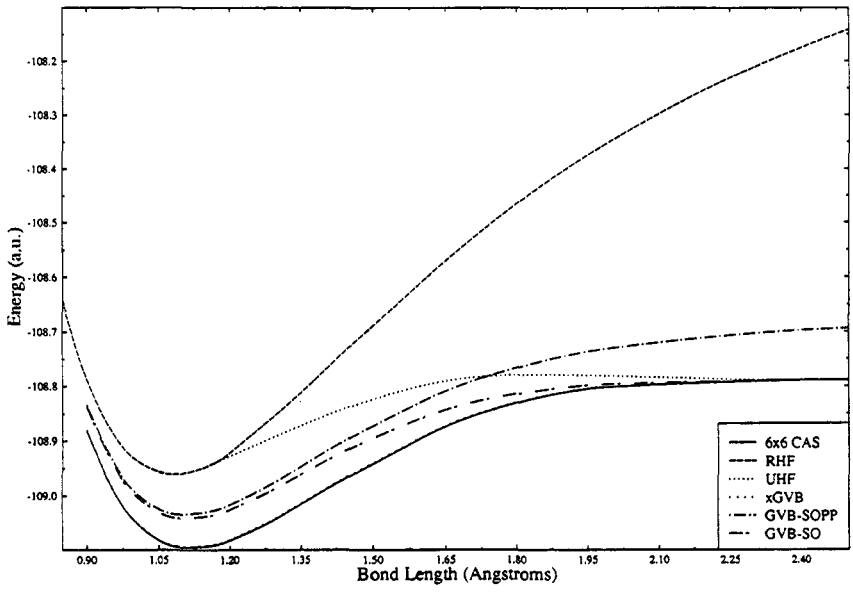

Figure 6 SCF, GVB, and CASSCF potential curves for N_2.

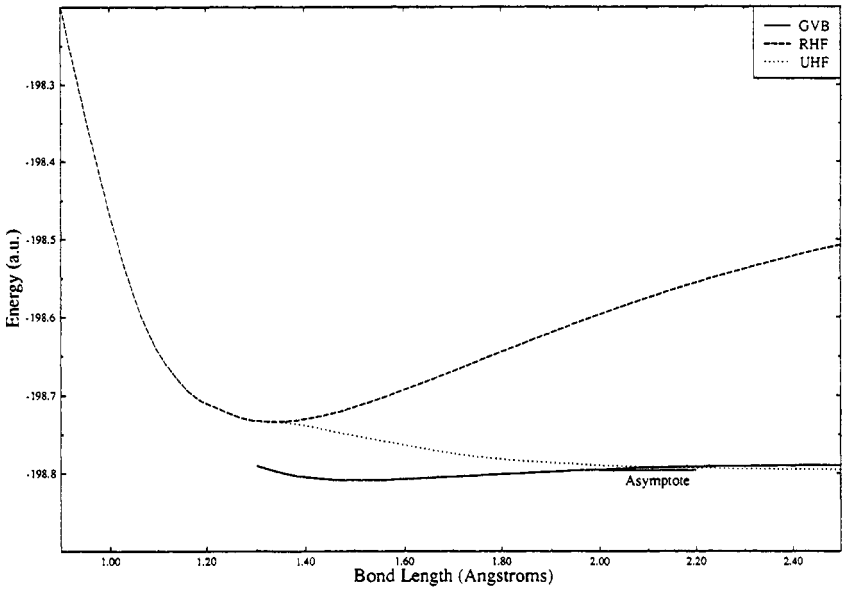

Figure 7 SCF and GVB potential curves for F_2.

that for closed-shell systems, the UHF solution and the RHF are usually the same at R_e, so the RHF deficiencies apply. (For some closed-shell examples a UHF solution which is necessarily below the RHF solution can be obtained, but that will not change our conclusion.) Furthermore, even when the UHF differs from the RHF, its lack of spin symmetry can affect the shape of the potential curve. For closed-shell cases in particular, where UHF is being used to effect correct separation, all triplet, quintet, and higher odd-spin states, which have higher energies, contaminate the UHF solution, causing the curve to rise too steeply slightly beyond equilibrium. (Because the UHF solution is not an eigenfunction of spin, we can resolve the UHF solution into its pure spin eigenstates, via $|\text{UHF}\rangle = \Sigma_{s_k}|s_k\rangle c_{s_k}$ and $c_{s_k} = \langle s_k|\text{UHF}\rangle$. If $S_z = 0$, as for a closed shell, then only triplet, quintet, etc., can have $S_z = 0$ components.) Because the UHF solution is separating correctly in this case, the curve can even show a slight artificial barrier to separation for some examples (see Figure 6). On the other hand, at the UHF separated atom limit, the several spin states all become degenerate. Hence, even though the spin multiplicity is erroneous, the energy is correct at the asymptote, as in the H_2 example (Figure 2).

Another failing of UHF is less frequent but pertinent for some examples. This is demonstrated by the F_2 UHF curve (Figure 7), which is not bound. That is, two F atoms are lower in energy than is the F_2 molecule, causing UHF not to predict the existence of the F_2 molecule!

To correct the foregoing deficiencies of a Hartree-Fock reference, we have to introduce "electron correlation." What is electron correlation? As discussed above, in the SCF method we attempt to describe the contribution of the two-electron part of the Hamiltonian by one electron moving in an average field of the $n - 1$ other electrons. Overall, this is not a bad approximation, inasmuch as the SCF energy is usually more than 99% of the total (nonrelativistic) electronic energy of an atom or molecule. However, chemists are interested in much smaller energy differences, such as bond dissociation energies, and we see from Figures 4, 6, and 7 that these are poorly described by SCF methods. Other quantities of interest (ionization potentials, electron affinities, electronic excitation energies, vibrational energies, etc.) are sensitive in varying degrees to the "average" electron interaction approximation of SCF theory. An average field neglects the fact that electrons, as charged particles, have instantaneous Coulombic interactions that keep them apart. That is, the motion of electrons is "correlated." The movement of one affects the movement of all others, so we have a complicated many-body system to describe. Because the instantaneous interactions serve to keep electrons apart better than an average interaction, the interelectronic repulsion is reduced, causing the energy for the molecule to be lower than the SCF value. The energy difference is called the *correlation energy:*

$$E_{\text{corr}} = E_{\text{exact}} - E_{\text{SCF}} \qquad [18]$$

where E_{SCF} can be any of our independent particle models, RHF, UHF, or ROHF. [Some authors use E_{RHF} (or E_{ROHF}) as the reference, so that E_{UHF} already includes some degree of electron correlation by relaxing the double-occupancy restriction on the spatial orbitals. For our purposes, "correlation" will be the correction for any SCF reference.]

To improve on a single determinant reference we must develop a superior treatment of the two-electron interaction. Logically, this would involve explicit use of the two-particle operator r_{ij} in a trial wavefunction, and such Hylleraas-type trial wavefunctions have been used to obtain the best results (for, e.g., He, Li, Be, H_2, and LiH).[15] Analysis of certain other analytic properties of the correlation cusp $1/(|\mathbf{r}_i - \mathbf{r}_j|)$[16] have also been exploited to develop better descriptions without having to use wavefunctions that are explicitly dependent on r_{ij}, but such methods also have many computational restrictions.

Electron correlation can be introduced solely with one-particle functions if we construct a wavefunction with the flexibility to allow electrons to stay away from each other. That means we need functions in regions of space different from just that sampled by the SCF calculation. As the SCF wavefunction spans only the occupied space, we can introduce different regions of space by admitting the "virtual" orbitals that are unoccupied in the SCF into the wavefunction. We do this by constructing a configuration interaction (CI) wavefunction

$$\Psi_{CI} = \Phi_0 + \sum_{i,a} C_i^a \Phi_i^a + \sum_{\substack{i<j \\ a<b}} C_{ij}^{ab} \Phi_{ij}^{ab} + \cdots \qquad [19]$$

which in addition to the SCF solution introduces single, double, and higher excitations. Φ_0 is called the *reference state* wavefunction. The single excitation $\Phi_i^a = \mathcal{A}(\varphi_1(1) \cdots \varphi_a(i) \cdots \varphi_n(n))$ corresponds to replacing the occupied SCF orbital φ_i by the unoccupied orbital, φ_a. Φ_{ij}^{ab} represents the double excitation, $\mathcal{A}(\varphi_1(1) \cdots \varphi_a(i) \cdots \varphi_b(j) \cdots \varphi_n(n))$, and so forth through triple Φ_{ijk}^{abc}, quadruple Φ_{ijkl}^{abcd}, . . . all the way to n-tuple excitations $\Phi_{ijk\ldots n}^{abc\ldots z}$ for n electrons. The CI coefficients (C_i^a, C_{ij}^{ab}, etc.) are then optimized to give the lowest variational energy,

$$E_{CI} = \frac{\langle \Psi_{CI} | \mathcal{H} | \Psi_{CI} \rangle}{\langle \Psi_{CI} | \Psi_{CI} \rangle} \qquad [20]$$

Because the CI wavefunction is a much more flexible wavefunction than is Φ_0, $E_{CI} < E_{SCF}$ and we lower the energy in line with the effect of correlating electron motions. [If we add only single excitations, there can be no improvement of the RHF or UHF energy, since singles do not directly mix with these solutions (Brillouin's theorem). Double excitations have to be included to introduce electron correlation.]

The "full CI" is defined as the wavefunction that includes all possible excitations through n-fold for n electrons. If the $\{\chi_\mu\}$ basis used to represent the MOs were complete (which usually means infinite), then the full CI would be the "complete" CI, which is the exact solution to the nonrelativistic Schrödinger equation. In a practical case $\{\chi_\mu\}$ is finite, so the full CI is the best that can be done in the basis set. Different correlated methods are recommended according to how closely they approach full CI results.

In the full CI wavefunction we have three (not mutually exclusive) categories of correlation corrections relative to Φ_0 that should be distinguished:

1. Excitations whose individual contributions are small, but because of an excessive number, their cumulative contributions are quite significant.
2. Excitations required to provide a correct zeroth-order description as dictated by spin-symmetry considerations.
3. Excitations whose coefficients will be comparatively large, as required to enable a molecule to separate correctly into fragments, in some excited states, and for certain other cases.

Category 1 is called *dynamic correlation* because its function is to enable the electrons to stay apart. It usually represents the largest part of the total correlation energy.

Category 2 occurs for the open-shell singlet example discussed earlier. A single determinant is not an eigenfunction of spin, so such states should always

be preferentially described using a two-determinant reference. We will refer to this as symmetry required, or *static correlation*. When these states are described by a single UHF determinant $|\phi_1\alpha(1)\phi_2\beta(2)|$ the wavefunction corresponds to a 50:50 mixture of the $|\phi_1\alpha(1)\phi_2\beta(2)| \pm |\phi_1\beta(1)\phi_2\alpha(2)|$ singlet (minus) and triplet (plus) state. Because the latter state can also be described by the high spin single determinant $|\phi_1\alpha(1)\phi_2\alpha(2)|$, the triplet energy can be obtained, and, aided by that information, approximate methods can be used to subtract the triplet contamination from the energy for the single UHF determinant,[17] but this is far less desirable than a treatment using the two-determinant reference.

Category 3 is often called *nondynamic correlation* and is perhaps best described by considering the simplest possible correlated wavefunction for F_2 and N_2 that can correctly dissociate. In the F_2 case (Fig. 7) this is a GVB wavefunction,[10] which in the orthogonal orbital form for F_2 consists of the two-determinant wavefunction $C_1|\text{core } 2p\sigma_g\alpha 2p\sigma_g\beta| + C_2|\text{core } 2p\sigma_u\alpha 2p\sigma_u\beta|$.

As discussed above for H_2, a σ_u must be mixed with a σ_g function to allow the electrons to localize on the two separated atoms in a model that, unlike UHF, preserves spin and spatial symmetry. Furthermore, the GVB result requires that the form of the orbitals $2p\sigma_g$ and $2p\sigma_u$ be determined together with the configuration coefficients C_1 and C_2. GVB is the simplest example of a multiconfiguration (MCSCF) calculation.[18,19] The GVB result for F_2, shown in Figure 7 is qualitatively correct as a function of internuclear distance R.

Similarly, in Figure 6 we show results for N_2 with analogous GVB wavefunctions for the triple bond,[20] which requires a product of wavefunctions consisting of two orbitals for each of the three bonds. This means we mix the $2p\sigma_g$ and $2p\sigma_u$ orbitals and also mix the $2p\pi_{xu}$, $2p\pi_{xg}$, $2p\pi_{yu}$, and $2p\pi_{yg}$. This results in a set of determinants starting with $\Phi_0 = |\text{core } 2p\sigma_g\alpha 2p\sigma_g\beta 2\pi_{xu}\alpha\pi_{xu}\beta 2\pi_{yu}\alpha 2\pi_{yu}\beta|$ through all other symmetry-allowed combinations including the hextuple excitation $|\text{core } 2p\sigma_u\alpha 2p\sigma_u\beta 2\pi_{xg}\alpha 2\pi_{xg}\beta 2\pi_{yg}\alpha 2\pi_{yg}\beta|$. If we allow the three two-determinant products to be singlet coupled (GVB-SO-PP) (8 configurations) only, we do not get the correct asymptote. Allowing singlet and triplet coupling among the three bonds, GVB-SO (14 configurations) and xGVB (20 configurations), both of which arise from singlet and triplet coupled combinations including the open-shell singlets, correctly separate N_2 into two ^4S N atoms as shown in Figure 6. The complete active space SCF (CASSCF)[14] takes this one step further. It recognizes that N_2 requires six orbitals, $3\sigma_g$, $3\sigma_u$, the pair $1\pi_u$, and the pair $1\pi_g$, and distributes the six electrons among them in all possible ways. This gives the xGVB set plus others (32 configurations) and clearly effects proper separation to two N(^4S) atoms. In Fig. 6, the CASSCF is nearly indistinguishable from the xGVB result.

This nondynamic correlation does not pertain to keeping electrons apart, which is a dynamic effect, but instead emphasizes having the appropriate sets of excitations in the wavefunction that requires a "large coefficient" to permit a more proper zeroth-order description. ["Large" is not well defined. In practice a coefficient for a determinant greater than 0.2 in an intermediately normalized wavefunction (see later) is frequently cause for concern, while for well-defined

dynamical correlation effects all determinants have coefficients < 0.1.] Other examples include O_3, where the competing resonance structures require at least two determinants in its zeroth-order solution (see section entitled Electronic Spectra).

These different categories of correlation effects are not mutually exclusive because the full CI is the exact result in a basis for any situation. Hence, even when a single determinant SCF model is a poor approximation to the right answer (e.g., RHF for N_2 at a large internuclear separation), the full CI solution would properly weight the other important configurations to give the right result. Similarly, even for the open-shell singlet example we could start with just the $|\phi_1\alpha\phi_2\beta|$ determinant, and since the double excitation $|\phi_1\beta\phi_2\alpha|$ is in the full CI solution, we will obtain both terms with the same coefficient but opposite sign in the full CI for the singlet solution.

Thus, we have two operational choices:

1. We can take the dynamic correlation route and always start with a single determinant reference, even when it is a poor approximation, and introduce higher categories of excitations until we believe our wavefunction is flexible enough to obtain satisfactory results.
2. We can insist on first introducing the relevant static or nondynamic correlation to have a qualitatively correct zeroth-order solution and then augment it by dynamic correlation to obtain quantitative results.

The preferable route will depend on the problem, the ease of implementation, and the computational efficiency.

The single reference (dynamic correlation) approaches will lead us to CI approximations such as all single and double excitations from a single determinant (CISD);[9] or many-body perturbation theory (MBPT)[5] [also known as Møller–Plesset (MP) perturbation theory[8]]; or coupled-cluster (CC) methods[6] for single and double excitations like CCSD[21] and its approximation termed quadratic CI (i.e., QCISD);[13] or coupled-cluster single, double, and triple excitations (CCSDT).[22] The second operational choice above will introduce multi–reference (MR) methods like MCSCF,[18,19] GVB,[10] or CASSCF[14] [the latter is also known as full-optimized reaction space (FORS)[23]]. Each of these references may then be augmented by additional dynamic correlation via CI, as when single and double excitations from a selection of reference determinants are included to define a MR-CISD wavefunction.[9] More specific designations are GVB-CISD and CASSCF-CISD and so on. Furthermore, there are similar MR-MBPT[24-26] and MR-CC methods.[29-32]

Whereas CI methods are variational, giving upper bounds to the total energy, the other discriminating factor in choice of correlated method is whether a method scales correctly with size, or, equivalently, the number of electrons. This (size) extensive property,[33] which can be quite significant numerically, is satisfied by many-body methods (e.g., MBPT, CC, and QCI methods) but not by CI methods other than full CI. "Truncated" CI ap-

proaches are often subject to semiempirical extensivity corrections[34] in an attempt to alleviate this failing. We will further discuss the consequences of inextensivity in the next section. MR-CC has the attraction of being extensive while including nondynamic correlation. One particularly useful development in MR-CC is the recently developed two-determinant reference open-shell singlet (TD-CCSD) method[31]. Another is the Fock space MR-CC[27-29] for excited, ionized, and electron-attached states, both in ACES II.[29,30]

METHODS FOR ELECTRON CORRELATION

Methods

Given a set of $n = n_\alpha + n_\beta$ molecular spin orbitals $i, j, k, \ldots$ occupied in Φ_0, and a set of $N = N_\alpha + N_\beta$ molecular spin orbitals $a, b, c, \ldots$ that are unoccupied in Φ_0, to allow for electron correlation our objective is to introduce the excited molecular orbitals $a, b, c, \ldots$ that do not appear in Φ_0 to make an improved wavefunction

$$\Psi = \Phi_0 + \sum_{i,a} C_i^a \Phi_i^a + \sum_{\substack{i<j \\ a<b}} C_{ij}^{ab} \Phi_{ij}^{ab} + \sum_{\substack{i<j<k \\ a<b<c}} C_{ijk}^{abc} \Phi_{ijk}^{abc} + \cdots$$
$$= (1 + \hat{C}_1 + \hat{C}_2 + \hat{C}_3 + \cdots)\Phi_0 \qquad [21]$$

In the limit of all possible n excitations (since m_s is a good quantum number—we can only excite to orbitals with the same spin), we have the full CI (FCI) solution. Notice that this CI wavefunction applies equally well for open and closed shells and, for the latter, permits either ROHF, UHF, or other orbitals. The full CI solution has several attractive properties:

1. It gives the best solution for the energy and density in the contracted (AO) basis set for any states.
2. It is "extensive" (i.e., it scales properly with molecular size and the number of electrons).
3. It is invariant to any change in the form of the MOs, so any orbitals are satisfactory.
4. It provides an upper bound to the exact electronic energy for any state.

The full CI is impractical except as a reference because the number of determinants is asymptotically $\sim N^n$. That means its application is possible only for small molecules and small basis sets. In practice, calculations using $\sim 25 \times 10^6$ determinants for H_2O in a double zeta plus polarization (DZP) basis have been made[35] and $\sim 10^8$ determinants for CH_3 in a triple zeta plus polarization (TZP) basis.[36]

The three most popular methods for introducing electron correlation are (truncated) CI such as CISD, MBPT, and CC theory. Other correlated methods (e.g., propagator methods,[37,38] which are related to the last two) have also been widely used for excitation and ionization energies. All can be viewed as different ways of building in some of the excitations that are present in the FCI. The comparative merits of the methods depend on how rapidly they converge to the FCI solutions for energies, densities, and other quantities of interest.

Configuration Interaction

CI methods are straightforward. Once truncated to some subset of excitations, the coefficients, $C_i^a, C_{ij}^{ab}, \ldots$ are determined from the variational principle $E_{CI} = \langle \Psi_{CI} | \mathcal{H} | \Psi_{CI} \rangle / \langle \Psi_{CI} | \Psi_{CI} \rangle \geq E_{exact}$ to give the lowest energy for the ground state (or lowest state of a given symmetry). Introducing only double excitations defines CID, whose wavefunction is $\Psi_{CID} = (1 + \hat{C}_2)\Phi_0$. The variational condition is equivalent to the matrix equation

$$\begin{bmatrix} \mathbf{H}_{OO} & \mathbf{H}_{OD} \\ \mathbf{H}_{DO} & \mathbf{H}_{DD} \end{bmatrix} \begin{bmatrix} 1 \\ \mathbf{C}_D \end{bmatrix} = \begin{bmatrix} 1 \\ \mathbf{C}_D \end{bmatrix} E_{CID} \qquad [22]$$

$$E_{CID} = \langle \Phi_0 | H | \Psi_{CID} \} \qquad [23]$$

where **D** in

$$\begin{aligned} \mathbf{H}_{OD} &= \langle \Phi_0 | H | \mathbf{D} \rangle \\ \mathbf{H}_{DD} &= \langle \mathbf{D} | H | \mathbf{D} \rangle \end{aligned} \qquad [24]$$

indicates all double excitations, Φ_{ij}^{ab}. Furthermore, in CI, each member of a subset of excitations will improve the energy somewhat, so adding singles, E(CISD) < E(CID). Similarly, if the most important few triples are added (call it CISDT′) then E(CISDT′) might be a good approximation to the full E(CISDT). Truncated CI methods also provide upper bounds to all electronic states. However, in chemistry we are interested in energy differences (dissociation energies, excitation energies, activation barriers, etc.), and there is seldom a bound on them. Furthermore, unlike MBPT and CC methods (see below), CI methods are not "extensive," and this can cause numerically significant errors.

Because the full CI (FCI) is the ultimate result in a given basis set, we can partly assess the comparative quality of different correlated methods by comparing with the limited number of full CI results available for molecules.[35,39,40] These are available for BH, FH, and H_2O at the equilibrium bond length R_e,1.5 R_e, and 2.0 R_e in a DZP basis (see later). As discussed earlier, the RHF reference function separates incorrectly when going to open-shell fragments, so as bonds are stretched, it offers a particularly poor approximation to the correct answer. Because the FCI is the best possible answer, this behavior has no effect on those results, but for a truncated CI, MBPT, or CC calculation, a poor

Table 1 Differences (millihartrees[a]) Between FCI Energies and Various Truncations at Three Internuclear Separations (DZP Basis)

	BH			FH			H_2O			Mean absolute error
CI method	R_e	1.5 R_e	2.0 R_e	R_e	1.5 R_e	2.0 R_e	R_e	1.5 R_e	2.0 R_e	
CID	6.02	9.63	20.8	10.3	18.6	35.5	13.7	34.5	84.8	25.9
CISD	5.21	7.51	14.5	9.38	14.9	27.6	12.9	30.4	75.6	22.0
CISDT	3.60	5.19	10.1	7.01	11.1	19.2	10.6	23.5	60.3	16.7
CISDTQ	0.03	0.06	0.16	0.28	0.49	0.92	0.40	1.55	6.29	1.13

[a]One millihartree is 0.6275 kcal/mol.

reference places extreme demands on the method. The ability of a correlated method to overcome such a poor reference is a testament to its accuracy and applicability. The errors in the energy relative to FCI for various truncated CI methods are shown in Table 1.

The correlation energy error in these examples ranges from 102 to 370 millihartrees, with an average of 213. CID accounts for about 88% of the correlation.

We can make a few observations. The variational condition guarantees that the error is above the exact result. Because of incorrect separation of the RHF reference, the errors are greatest at twice the equilibrium R_e. Comparing the different CI truncations, we see that on average single excitations account for ~4, triples for ~5, and quadruples for a whopping ~15 millihartrees. The vast improvement of CISDTQ compared to CISDT emphasizes the numerical importance of quadruple excitations in CI. Very accurate methods should include these effects, and MBPT and CC methods do so in a convenient way.

Many-Body Perturbation Theory

The next method we consider is many-body perturbation theory (MBPT).[41,42] This approach exploits the form of the Hamiltonian in Eq. [7]

$$\mathcal{H} = H_0 + V \qquad [25]$$

$$H_0 = \sum_i \mathcal{F}(i) \qquad [26a]$$

$$V = \frac{1}{2} \sum_{i,j} \frac{1}{r_{ij}} - \sum_i u(i) \qquad [26b]$$

so that we attempt to solve the correlation problem by introducing the perturbation, V. In other words, the exact (FCI) wavefunction can be written as a perturbation expansion

$$\Psi = \Phi_0 + \psi^{(1)} + \psi^{(2)} + \cdots \qquad [27]$$

instead of the form in Eq. [21]. Similarly, we have the eigenvalue $E = E_0 + E^{(1)} + E^{(2)} + \cdots$. Inserting into the Schrödinger equation, with $\Phi_0 = \psi_0$, we obtain

$$\begin{aligned}(H_0 + V)(\psi_0 + \psi^{(1)} + \psi^{(2)} + \cdots) \\ = (E_0 + E^{(1)} + E^{(2)} + \cdots)(\psi_0 + \psi^{(1)}) \cdots\end{aligned} \qquad [28]$$

All the terms in such an expansion are linearly independent, so this equation must be satisfied for each order m. Therefore,

$$0th: (E_0 - H_0)\psi_0 = 0 \tag{29a}$$

$$1st: (E_0 - H_0)\psi^{(1)} = (V - E^{(1)})\psi_0 \tag{29b}$$

$$2nd: (E_0 - H_0)\psi^{(2)} = (V - E^{(1)})\psi^{(1)} - E^{(2)}\psi_0 \tag{29c}$$

$$3rd: (E_0 - H_0)\psi^{(3)} = (V - E^{(1)})\psi^{(2)} - E^{(2)}\psi^{(1)} - E^{(3)}\psi_0 \tag{29d}$$

$$\vdots$$

$$mth: (E_0 - H_0)\psi^{(m)} = (V - E^{(1)})\psi^{(m-1)} - \sum_{k=2}^{m} E^{(k)}\psi^{(m-k)} \tag{29e}$$

By multiplying on the left by ψ_0 and using the zeroth-order equation and ($\langle\psi_0|\psi_0\rangle = 1$, $\langle\psi_0|\psi^{(m)}\rangle = 0$), we find that

$$\begin{aligned} E^{(1)} &= \langle\psi_0|V|\psi_0\rangle \\ E^{(2)} &= \langle\psi_0|V|\psi^{(1)}\rangle \\ &\vdots \\ E^{(m+1)} &= \langle\psi_0|V|\psi^{(m)}\rangle \end{aligned} \tag{30}$$

In the energy expression we are using intermediate normalization. Remember that all wavefunctions are determined only up to an arbitrary constant, which is frequently chosen to make $\langle\Psi|\Psi\rangle = 1$ to provide a convenient probability interpretation. In perturbation theory (and in CI as we are doing it here), it is more convenient to choose the intermediate normalization $\langle\psi_0|\Psi\rangle = 1$, which is equivalent to $\langle\psi_0|\psi^{(k)}\rangle = 0$ for all $k > 0$. The relationship between a fully normalized wavefunction, $\langle\Psi|\Psi\rangle = 1$, and an intermediately normalized one is straightforward. If $\Psi = \Sigma_k C_k\Phi_k$ and $\langle\Psi|\Psi\rangle = 1$, for $\{\Phi_k\}$ a set of functions orthogonal to Φ_0, then $\Psi' = \Phi_0 + \Sigma_{k\neq 0}(C_k/C_0)\Phi_k$ is intermediately normalized, since $\langle\Phi_0|\Psi'\rangle = 1$. This normalization has the effect of simplifying the energy expression to that in Eq. [30].

Consistent with the intermediate normalization condition, we want all our perturbed n-particle functions $\Psi^{(m)}$ to be orthogonal to Ψ_0. Just as in the case of CI, a natural set to represent these functions is the set of single, double, etc., excitations.

To obtain $\psi^{(1)}$ consider its expansion in double excitations,

$$\psi^{(1)} = \sum_{\substack{i>j \\ a>b}} C_{ij}^{ab(1)}\,\Phi_{ij}^{ab} \tag{31}$$

where the $^{(1)}$ on the coefficient emphasizes its first-order character. Because every excitation like Φ_{ij}^{ab} is an eigenfunction of H_0 (i.e., $H_0\Phi_{ij}^{ab} = E_{ij}^{ab}\Phi_{ij}^{ab}$),

$$E_{ij}^{ab} = \sum_{k\neq i,j}^{n} \epsilon_k + \epsilon_a + \epsilon_b$$

$$= E_0 - \epsilon_i - \epsilon_j + \epsilon_a + \epsilon_b = E_0 - \varepsilon_{ij}^{ab}$$

it follows that

$$(E_0 - H_0)\Phi_{ij}^{ab} = \varepsilon_{ij}^{ab}\,\Phi_{ij}^{ab} \qquad [32]$$

Consequently, inserting $\psi^{(1)}$ from Eq. [31] into Eq. [29b] and left-multiplying by another double excitation Φ_{kl}^{cd} and integrating, via orthonormality of the excitations, we obtain

$$\varepsilon_{kl}^{cd}\,C_{kl}^{cd(1)} = \langle\Phi_{kl}^{cd}|V|\Phi_0\rangle \qquad [33]$$

or

$$\psi^{(1)} = \sum_{\substack{i>j\\a>b}} \frac{\langle\Phi_{ij}^{ab}|V|\Phi_0\rangle}{\varepsilon_{ij}^{ab}}\,\Phi_{ij}^{ab} \qquad [34]$$

and

$$E^{(2)} = \sum_{\substack{i>j\\a>b}} |\langle\Phi_{ij}^{ab}|V|\Phi_0\rangle|^2/\varepsilon_{ij}^{ab} = \sum_{\substack{i>j\\a>b}} |\langle ij\|ab\rangle|^2/\varepsilon_{ij}^{ab} \qquad [35]$$

This second-order correction defines MBPT(2), and it is the simplest correlation correction. It should be clear that triple and higher excitations cannot contribute to $\psi^{(1)}$ because V includes only a two-particle operator. Following the same procedure as above for single excitation contributions, Φ_i^a, the results depend on $\langle\Phi_0|V|\Phi_i^a\rangle = \langle\Phi_0|H|\Phi_i^a\rangle = \langle i|\mathcal{F}|a\rangle = \mathcal{F}_{ia} = 0$, which is why no single excitations can mix with an RHF or UHF Φ_0. For an ROHF reference MBPT, however, $\mathcal{F}_{ia} \neq 0$. This introduces an additional term in $E^{(2)}$ and various additional terms in higher order. These have to be included in ROHF-MBPT applications, but that has been accomplished in our ROHF-MBPT method.

Remembering that the average correlation energy correction for the full CI examples is 213 millihartrees MBPT(2) typically accounts for 85–95% of the correlation energy obtainable in a given basis set, as seen in Table 2. Because MBPT(2) depends only on the relatively small subset of two occupied

Table 2 Differences (millihartrees) Between FCI and MBPT Energies (DZP Basis)

Perturbation theory	BH			FH			H_2O			Mean absolute error
	R_e	1.5 R_e	2.0 R_e	R_e	1.5 R_e	2.0 R_e	R_e	1.5 R_e	2.0 R_e	
MBPT(2)	28.6	36.1	52.8	7.80	10.6	24.0	13.0	23.3	53.7	27.8
MBPT(3)	11.1	15.7	27.1	5.44	11.9	27.0	7.22	26.4	74.6	22.9
SDQ-MBPT(4)	5.69	8.20	15.0	2.75	5.39	12.5	4.40	13.3	34.2	11.3
MBPT(4)	5.06	7.23	13.3	−0.26	0.77	4.84	0.92	5.76	14.9	5.89
MBPT(5)[a]	2.52	3.60	6.07	0.81	2.29	8.10	0.70	4.98	17.0	5.12

[a]Reference 44.

and two virtual orbital two-electron integrals $\langle ij\|ab\rangle$ (most integrals would be four-virtual $\langle ab\|cd\rangle$ type) and the SCF orbital energies, it is computationally easy to evaluate $E^{(2)}$. $E^{(2)}$ itself is an $\sim n^2N^2$ procedure but the transformed integral $\langle ij\|ab\rangle$ requires an $\sim Mn^2N^2$ step, where $M = n + N$. Because MBPT(2) offers such a large percentage of the correlation correction, it typically provides much better results than SCF alone. We will see that in many applications.

Higher orders of perturbation theory are not conceptually too different from $E^{(2)}$. To get third order we have to consider $\psi^{(2)}$, but for RHF and UHF cases, it depends only on double excitations. We would have to evaluate terms that depend on integrals like $\langle ab\|cd\rangle$, $\langle ia\|jb\rangle$, and $\langle ij\|kl\rangle$ in addition to the $\langle ij\|ab\rangle$ used in $E^{(2)}$. For example, the particle–particle ladder (PPL) part of $E^{(3)}$ is

$$E^{(3)}_{PPL} = \sum_{\substack{a>b \\ c>d \\ i>j}} \langle ij\|ab\rangle\langle ab\|cd\rangle\langle cd\|ij\rangle / \varepsilon^{ab}_{ij}\,\varepsilon^{cd}_{kl}$$

This term causes MBPT(3) to require an $\sim n^2N^4$ algorithm, like CID (or CISD). In fact, the CID coefficients are $C^{ab}_{ij} \approx C^{ab(1)}_{ij} + C^{ab(2)}_{ij}$ through second order; so we would expect CID and MBPT(3) to usually give similar results. From Table 2 we see that the average absolute error of MBPT(3) is 22.9 millihartrees, which is close to the CID error of 25.9.

Some important distinctions emerge in fourth order. First, even for RHF or UHF $E^{(4)}$ has contributions from single, triple, and quadruple excitations in addition to double excitations.

$$E^{(4)} = \langle\Phi_0|V|\psi^{(3)}\rangle = E^{(4)}_{\mathrm{D}} + E^{(4)}_{\mathrm{S}} + E^{(4)}_{\mathrm{T}} + E^{(4)}_{\mathrm{Q}} - E^{(2)}\langle\psi^{(1)}|\psi^{(1)}\rangle$$

Now we see the consequences of (size)-extensivity for the first time. The last term, which depends on $E^{(2)}$, arises from the second term on the right in Eq. [29c] after multiplying on the left by $\langle\psi^{(1)}|$ and using the fourth-order energy formula. This term plays a critical role in distinguishing MBPT from CI. If we continued approximating the CID coefficients by higher order perturbation theory, we would have

$$C^{ab}_{ij} \approx C^{ab(1)}_{ij} + C^{ab(2)}_{ij} + C^{ab(3)}_{ij} - E^{(2)}C^{ab(1)}_{ij}$$

because $E^{(2)}$ arises only from double excitations.

To understand what is wrong with this, it is convenient to consider a noninteracting system of $m\mathrm{H}_2$ molecules. For such a system, the exact wavefunction for $m\mathrm{H}_2$ would be $\Psi(m\mathrm{H}_2) = [\psi(\mathrm{H}_2)]^m$. Furthermore, the exact en-

ergy $E(mH_2) = mE(H_2)$. Since the exact energy must be written in terms of perturbation corrections, it follows that $E_{SCF}(mH_2) = mE_{SCF}(H_2)$, $E^{(2)}(mH_2) = mE^{(2)}(H_2)$, $E^{(3)}(mH_2) = mE^{(3)}(H_2)$, etc. But notice, the negative (renormalization) term depends on $E^{(2)}$ and $\langle\psi^{(1)}|\psi^{(1)}\rangle$ and since $E^{(2)}(mH_2) = mE^{(2)}(H_2)$ and since $\psi^{(1)}(mH_2) = [\psi^{(1)}(H_2)]^m$, $\langle\psi^{(1)}(mH_2)|\psi^{(1)}(mH_2)\rangle = m\langle\psi^{(1)}(H_2)|\psi^{(1)}(H_2)\rangle$, the quantity $E^{(2)}\langle\psi^{(1)}|\psi^{(1)}\rangle$ depends on m^2! How can this be, because we must have $E^{(4)}(mH_2) = mE^{(4)}(H_2)$? This can happen only if somehow the m^2-dependent part of the $E^{(2)}\langle\psi^{(1)}|\psi^{(1)}\rangle$ term cancels another part of $E^{(4)}$ to eliminate the m^2 dependence. This is exactly what happens. Part of $E_Q^{(4)}$ cancels $E^{(2)}\langle\psi^{(1)}|\psi^{(1)}\rangle$. (There are actually two parts to $E^{(2)}\langle\psi^{(1)}|\psi^{(1)}\rangle$; an m^2-dependent "disjoint part" and an m-dependent "conjoint or EPV part." The former is canceled while the latter contributes to $E_Q^{(4)}$.) However, because $E^{(2)}$ and $\langle\psi^{(1)}|\psi^{(1)}\rangle$ depend only on double excitations, the cancellation can occur only when quadruple excitations are allowed to be in the wavefunction! Hence, CID is not extensive[5] because it does not scale correctly with m units because of the absence of quadruple excitations. Higher orders would similarly require even higher excitations until the FCI is reached! This failing of CI causes the paradoxical situation that a finite-order approximation to CID [e.g., MBPT(2) or MBPT(3)] frequently can be superior to the converged E(CID) result because the CI retains such nonextensive terms as $E^{(2)}\langle\psi^{(1)}|\psi^{(1)}\rangle$.

Although illustrated by CID, the inextensivity failing obviously pertains to any truncated CI, since the cancellations that must occur always involve the higher excitations that are not included in the truncated CI. The numerical effects of these nonextensive terms is important even for small molecules; and, today, most CI calculations include an estimate for these terms that allows their value to be subtracted from the CI energy (Davidson's approximation[34]). Many-body methods, instead, make the intelligent decision to eliminate all such nonphysical terms from the equations before calculation. This makes the method formally suited to describing many-bodies (i.e., many electrons). The term *many-body perturbation theory* emphasizes this cancellation of terms (also known as unlinked diagrams) that are not in the full CI solution. This leaves just the appropriate (linked) ones, in the energy and wavefunction: the so-called *linked-diagram theorem.*[45] Now, by building approximations on that equation we are already closer to the exact solution. This is a vastly better approach formally, operationally, and in terms of numerical accuracy for a given level of computation. Though extensive, MBPT is not variational, however, as negative corrections in Table 2 show.

The SDQ-MBPT(4) method, which includes all terms except the triple excitations, requires only an $\sim n^2N^4$ algorithm compared to $\sim n^3N^4N_{it}$ (N_{it} = number of iterations) for CISDT. Allowing for its nonvariational character, it is generally better than CISDT (Table 2) because it has already incorporated most of the effects of quadruple excitations. Full MBPT(4) also benefits from the effect of triple excitations, is a noniterative $\sim n^3N^4$ procedure, and is considerably closer to the full CI than is CISDT. In fifth order the additional "con-

nected" effects of quadruple excitations are introduced, but these are comparatively small compared to those already in SDQ-MBPT(4). MBPT(5)[44] is an $\sim n^3N^5$ method but shows little numerical improvement over MBPT(4), despite its much greater expense. CISDTQ, which is also correct through fifth order, is still better than MBPT(5) because it includes all orders of perturbation theory among those categories of excitations.

Clearly, extensivity pays important dividends numerically, but it should be remembered that extensivity is only one possible source of error, and others can be equally or more important for a given problem. In particular, for some problems we might prefer the nonextensive multireference CI method instead of single reference MBPT or CC.

Coupled-Cluster Theory

The failing of MBPT is that it is basically an order-by-order perturbation approach. For difficult correlation problems it is frequently necessary to go to high orders. This will be the case particularly when the single determinant reference function offers a poor approximation for the state of interest, as illustrated by the foregoing examples at 2.0 R_e. A practical solution to this problem is coupled-cluster (CC) theory.[46] In fact, CC theory simplifies the whole concept of extensive methods and the linked-diagram theorem into one very simple statement: the exponential wavefunction ansatz,

$$\Psi_{CC} = \exp(\hat{T})\Phi_0 = (1 + \hat{T} + \frac{1}{2}\hat{T}^2 + \frac{1}{3!}\hat{T}^3 + \cdots)\Phi_0 \qquad [36]$$

where

$$\hat{T} = \hat{T}_1 + \hat{T}_2 + \hat{T}_3 + \cdots + \hat{T}_n$$

Just as in $\hat{C}_p$ in a CI wavefunction, $\hat{T}_p$ generates p-fold excitations. Hence, CCD gives

$$\begin{aligned}\psi_{CCD} &= (1 + \hat{T}_2 + \frac{1}{2}\hat{T}_2^2 + \cdots)\,\Phi_0 \\ &= \Phi_0 + \sum_{\substack{i<j \\ a<b}} t_{ij}^{ab}\,\Phi_{ij}^{ab} + \sum_{\substack{i<j<k<l \\ a<b<c<d}} t_{ij}^{ab}\,t_{kl}^{cd}\,\Phi_{ijkl}^{abcd} + \cdots\end{aligned} \qquad [37]$$

Unlike CID, even CCD[33] introduces quadruple excitations Φ_{ijkl}^{abcd} and hextuples Φ_{ijklmn}^{abcdef}, etc., up to all n-tuples for n electrons. However, the number of coefficients to determine in CCD (t_{ij}^{ab}) is exactly the same as in CID (C_{ij}^{ab}), because the coefficients of the higher excitations are products of the same coefficients. Since they arise from $\hat{T}_2^2/2$, $\hat{T}_2^3/3!$, etc., we call the latter "disconnected" terms (not unlinked; all terms in the exact wavefunction are linked!), which will lead us to a nonlinear set of equations for the determination of the t_{ij}^{ab}. "Connected" quadruples come from $\hat{T}_4$.

The correct scaling or extensive property is manifestly obvious in CC methods because for noninteracting H_2 molecules (described with localized orbitals),

$$\Psi(mH_2) = [\psi(H_2)]^m \qquad [38]$$

and in CC theory

$$\begin{aligned} \Psi_{CC} &= \exp(T(1) + T(2) + \cdots T(m))\Phi_0(mH_2) \\ &= \exp(mT)[\Phi_0(H_2)]^m \\ &= [\exp(T)\Phi_0(H_2)]^m \end{aligned} \qquad [39]$$

This means

$$E_{CC}(mH_2) = mE_{CC}(H_2) \qquad [40]$$

Note that Eq. [40] is true regardless of the subset of CC excitations (T_p) included (CCD,[33] CCSD,[21] CCSDT,[22] etc.). Similarly, it is true for such approximations as CCSD + T(CCSD)[47] and CCSD(T)[48,49] (see below), where the initial contributions of triple excitations are computed noniteratively after a CCSD calculation, as well as essentially any other approximation based on CC and MBPT theory. [The CEPA (coupled electron-pair approximations)[50] are approximations to CC theory but do not necessarily retain all the invariance properties required to ensure rigorous extensivity.]

The use of the noninteracting limit above is pedagogical, but the consequences of the exponential ansatz clearly pertain to the interacting case, since there are no "unlinked" terms. It is important to recognize that it pertains to a high density electron gas, too, which mimics a metal. Then the exponential ansatz guarantees correct scaling with the number of electrons. *Extensivity,* whose rigorous definition is the absence of "unlinked diagrams,"[5,33] is a very general and important consistency condition for a correlated method, and it is absolutely essential for applications of quantum chemistry to extended systems.

The CC equations are obtained by inserting the wavefunction from Eq. [36] into the Schrödinger equation projected by the reference function Φ_0 and single, double, and higher excitations. Using

$$H_N = H - \langle\Phi_0|H|\Phi_0\rangle$$

for CCD we have

$$\begin{aligned} &\langle\Phi_0|H_N \exp(T)|\Phi_0\rangle = \Delta E \\ &\langle\Phi_{ij}^{ab}|H_N \exp(T)|\Phi_0\rangle = \Delta E\langle\Phi_{ij}^{ab}|e^T|\Phi_0\rangle \text{ for all } i,j;\ a,b \end{aligned} \qquad [41]$$

where ΔE is the correlation energy. The equations projected by excitations provide equations for the coefficients, $\{t_{ij}^{ab}\}$. The actual equations are

$$\Delta E = \langle \Phi_0 | H_N \hat{T}_2 | \Phi_0 \rangle = \sum_{\substack{i>j \\ a>b}} t_{ij}^{ab} \langle \Phi_{ij}^{ab} | H_N | \Phi_0 \rangle = \sum_{\substack{i>j \\ a>b}} t_{ij}^{ab} \langle ab \| ij \rangle \qquad [42]$$

$$\Delta E t_{ij}^{ab} = \langle \Phi_{ij}^{ab} | H_N | \Phi_0 \rangle + \langle \Phi_{ij}^{ab} | H_N \hat{T}_2 | \Phi_0 \rangle + \langle \Phi_{ij}^{ab} | H_N \hat{T}_2^2 | \Phi_0 \rangle \qquad [43]$$

Notice, no higher terms than $\hat{T}_2^2$ can contribute to the CC equations because $\hat{T}_2^3$ would generate hextuple excitations, which would have vanishing matrix elements with Φ_{ij}^{ab}. Therefore, even though the exponential CC wavefunction consists of all terms up to n-fold excitations, the equations for the coefficients $\{t_{ij}^{ab}\}$ are lower order.

Explicitly, the canonical orbital CCD equations can be further simplified to

$$\begin{aligned} \varepsilon_{ij}^{ab} t_{ij}^{ab} = {} & \langle ab \| ij \rangle + \frac{1}{2} \sum_{c,d} \langle ab \| cd \rangle t_{ij}^{cd} + \frac{1}{2} \sum_{k,l} \langle ij \| kl \rangle t_{kl}^{ab} \\ & + \sum_{k,c} \left(\langle ak \| jc \rangle t_{ik}^{cb} - \langle bk \| jc \rangle t_{ik}^{ca} - \langle ak \| ic \rangle t_{jk}^{cb} + \langle bk \| ic \rangle t_{jk}^{ca} \right) \\ & + \frac{1}{4} \sum_{\substack{k,l \\ c,d}} \langle kl \| cd \rangle [t_{kl}^{ab} t_{ij}^{cd} - 2(t_{ij}^{ac} t_{kl}^{bd} + t_{ij}^{bd} t_{kl}^{ac}) \\ & - 2(t_{ik}^{ab} t_{jl}^{cd} + t_{ik}^{cd} t_{jl}^{ab}) + 4(t_{ik}^{ac} t_{jl}^{bd} + t_{ik}^{bd} t_{jl}^{ac})] \end{aligned} \qquad [44]$$

Notice the elimination of ΔE from the CCD equations, unlike those for CID. Having *algebraic* instead of eigenvalue equations is a consequence of extensivity. If we include T_1 in addition to T_2, we would obtain coupled equations for t_i^a and t_{ij}^{ab}. Including T_3 and its coefficients t_{ijk}^{abc}, we have coupled equations for t_i^a, t_{ij}^{ab}, t_{ijk}^{abc}, etc. Given a set of transformed two-electron integrals, the solution of the nonlinear CC equations is obtained by iteration exploiting various acceleration techniques. Table 3 compares results for CCD, CCSD, CCSDT, and CCSDTQ[51] to full CI. These are clearly the most accurate results we have yet considered. Like MBPT, CC results are not variational, and negative errors compared to full CI are possible.

The low order iterations of the CC equations recover MBPT approximations. For example, taking the first approximation to Eq. [44] and inserting it into Eq. [42],

Table 3 Differences (millihartrees) Between FCI Energies and Coupled-Cluster Results (DZP Basis)

Method	BH			FH			H_2O			Mean absolute error
	R_e	1.5 R_e	2.0 R_e	R_e	1.5 R_e	2.0 R_e	R_e	1.5 R_e	2.0 R_e	
CCD	2.72	5.00	12.8	3.76	8.13	21.9	5.01	15.9	40.2	12.8
CCSD	1.79	2.64	5.05	3.01	5.10	10.2	4.12	10.2	21.4	7.06
CCSD(T)[a]	0.41	0.55	0.41	0.40	0.88	−0.26	0.72	2.09	4.63	1.15
CCSDT-1[b]	0.46	0.62	0.96	0.16	0.48	0.56	0.59	1.96	−2.88	0.96
CCSDT[c]	0.07	0.03	−0.09	0.27	0.65	1.13	0.53	1.78	−2.47	0.78
CC5SD(TQ*)[d]	0.05	0.01	−0.59	0.33	0.56	−0.18	0.19	0.13	−1.96	0.44
CCSDTQ[e]	0.00	0.00	+0.00	0.02	0.04	0.06	0.02	0.14	−0.02	0.03

[a] Reference 49.
[b] Reference 52.
[c] Reference 22.
[d] Reference 49, 53.
[e] Reference 51.

$$t_{ij}^{ab(1)} = \frac{\langle ab \| ij \rangle}{\varepsilon_{ij}^{ab}}$$
$$E^{(2)} = \sum_{\substack{i>j \\ a>b}} t_{ij}^{ab(1)} \langle ab \| ij \rangle \qquad [45]$$

Plugging $t_{ij}^{ab(1)}$ into the second, third, and fourth summations on the right of Eq. [44] gives $t_{ij}^{ab(1)}$ and $E^{(3)} = \Sigma_{i>j} t_{ij}^{ab(2)} \langle ab \| ij \rangle$. Fourth-order quadruple excitations arise from inserting $t_{ij}^{ab(1)}$ into the term quadratic in t, along with $t_{ij}^{ab(2)}$ inserted into the terms linear in t, because both terms contribute to $t_{ij}^{ab(3)}$. This order defines the DQ-MBPT(4) approximation, which continuing to convergence must give CCD. Including singles via the CCSD equations gives SDQ-MBPT(4), which at convergence gives CCSD. Similarly, if we also introduce the triple excitation T_3 equations, we obtain SDTQ-MBPT(4) or just MBPT(4) as the fourth-order approximation to CCSDT.

Computationally, CCD and CCSD are $\sim n^2N^4N_{it}$ methods, whereas CCSDT is $\sim n^3N^5N_{it}$ and if T_4 were added to give CCSDTQ, we would require an $\sim n^4N^6N_{it}$ algorithm. The corresponding CI methods have the same computational dependence but do not introduce the higher excitations that are found in the CC methods.

It is possible to combine some aspects of MBPT with CC theory to retain much of the infinite-order aspect of CC while saving significantly in the computational cost for higher cluster operators. This may be done iteratively or noniteratively. Taking just the most important contributions of T_3 (as judged by order in perturbation theory) and coupling to all T_1 and T_2 terms, we obtain CCSDT-1.[52] This still requires an $\sim n^3N^4N_{it}$ algorithm, though. Results are shown in Table 3.

If we further consider only these T_3 terms in CCSDT-1 noniteratively (i.e., we do not let the T_3 coefficients change), we obtain highly accurate but considerably less expensive methods. This is done as follows. The fourth-order triple excitation correction may be written as

$$\sum_{\substack{i>j>k \\ a>b>c}} (t_{ijk}^{abc(2)})^2 \varepsilon_{ijk}^{abc} \qquad [46]$$

where $t_{ijk}^{abc(2)}$ would consist of several terms derived from T_2 coefficients of the form $\Sigma_e \langle bc \| ei \rangle t_{jk}^{ae(1)}$ and $\Sigma_m \langle ma \| jk \rangle t_{mi}^{bc(1)}$. The former requires an n^3N^4 evaluation. If we simply use the converged t_{jk}^{ae} and t_{mi}^{bc} coefficients from CCSD instead of their first-order approximations (Eq. [45]) in Eq. [46], we would have higher than fourth-order terms. In this manner we evaluate the n^3N^4 step just one time and obtain CCSD + T(CCSD)[47]. If, in addition, we introduce a term like $t_i^a \langle bc \| jk \rangle$ that arises in CCSDT-1 from considering the contribution of T_3 to the T_1 equation, (a fifth-order term), we obtain CCSD(T).[48] Both are

clearly correct through fourth order and should be an improvement over MBPT(4). In this manner much of the often important effect of T_3 can be introduced without solving the full CCSDT equations, which is a substantial savings. Similar noniterative methods have been developed that include the initial T_4 contributions and are correct through fifth order, CCSD + TQ*(CCSD) = CC5SD(TQ*),[49] whose rate-determining step is a single n^3N^5 step.

Again recalling that unlike CI, CC methods are not variational, we can compare various CC methods with full CI and the prior approximations in Table 4. In terms of the energies, it is apparent that CC methods are closer to full CI than the corresponding CI or MBPT results, as must be clear from the theory. For example, CCSDT is closer than even CISDTQ. Even CCSD(T) is competitive with CISDTQ, yet the latter requires an $n^4N^6N_{it}$ computational dependence, while CCSD(T) is $n^2N^4N_{it}$ with a single n^3N^4 step. Also, CISDTQ is still not extensive. Similarly, the extensive fourth-order MBPT methods, SDQ-MBPT(4), which is the fourth-order approximation to CCSD, and MBPT(4), which is the fourth-order approximation to CCSDT or CCSD(T), differ from the infinite-order methods by ~5 millihartrees. Notice the improvement by a factor of better than 3 by CCSD compared to CISD and factor of ~16 improvement of CCSD(T) compared to CISDT. Whereas triples are important in CC theory, their improvement in CISDT is small. Although Table 4 is for just the energy, the overall relative quality of the various methods tends to

Table 4 Comparison of Mean Absolute Errors for Different Correlated Methods Versus Full CI for BH, FH, and H_2O[a]

Method	Mean absolute error (millihartrees)
CID	25.9
CISD	22.0
CISDT	16.7
CISDTQ	1.13
MBPT(2)	27.8
MBPT(3)	22.9
SDQ-MBPT(4)	11.3
MBPT(4)	5.89
MBPT(5)	5.12
CCD	12.8
CCSD	7.06
CCSD(T)	1.15
CCSDT-1	0.96
CCSDT	0.78
CC5SD(TQ*)	0.44
CCSDTQ	0.03

[a]Summary of data from Tables 1–3.

follow the errors shown. Hence we expect CCSD(T) > MBPT(4) > CCSD > SDQ-MBPT(4) > CISD > MBPT(2).

The Brueckner orbital variant of CC should also be mentioned.[54] CCSD puts in all single excitation effects via the wavefunction $\exp(T_1 + T_2)\Phi_0$. We can instead change the orbitals $\{\varphi_i\}$ in Φ_0 in this wavefunction until $T_1 = 0$. These orbitals are called Brueckner orbitals and define a single determinant reference B instead of Φ_0 that has maximum overlap with the correlated wavefunction. Since B-CCD[54] (or BD)[55] effectively puts in T_1, it will give results similar but not identical to those from CCSD (they differ in fifth order). For BH, the corresponding B-CCD errors are 1.81, 2.88, and 5.55, compared to 1.79, 2.64 and 5.05, for CCSD as a function of R_e. See also B-CCD for symmetry breaking problems.[56]

Quadratic configuration interaction (QCISD)[13] is an approximation to CCSD methods (it is also the same up to fifth-order terms) and will give similar results. Generally E(QCISD) < E(CCSD) because the higher order nonlinear terms in CCSD tend to be positive. For the purposes of the present discussion, we do not need to consider it separately. The details and numerical results compared to full CI are presented in the Appendix.

Numerical Results for Potential Energy Curves

Besides FCI comparisons discussed above, correlated results for the N_2 and F_2 potential energy curves are informative. Because of the importance of nondynamic correlation in correctly separating the N_2 potential curve to two N(^{4}S) atoms, the reference result shown in Figures 8 and 9 is the MR-CI, which is the same as CASSCF-CISD. Recall from Figure 6 that the CASSCF solution is qualitatively correct as a function of R, so augmenting it with all the single and double excitations that can be formed from excitations among the 32 spin-adapted configurations in the CASSCF should be excellent (even though not an extensive) approximation to the FCI. In this case it consists of 77,558 configurations. For the correctly separating UHF-based correlated methods, all the purely single reference, purely dynamic correlation methods go to the correct asymptotic limit except for MBPT(2) (Figure 8). The characteristic spin contamination of the UHF that persists into the correlated calculations is apparent from the erroneous, too steep, curvature near 1.3 Å. The latter is never alleviated by finite-order MBPT results, but is once the CCSD result has been obtained. That is, despite no explicit consideration of nondynamic correlation, UHF-CCSD offers a perfectly reasonable approximation to the N_2 curve all the way to separation. Adding triples either noniteratively, CCSD(T), or completely, CCSDT, provides results that follow the CASSCF-CISD curve very accurately. Notice that the CCSD(T) and CCSDT energies (along with MBPT(4)) are actually lower in the vicinity of equilibrium and, if we had the full CI result, would be closer to it than the CI. This reflects the remaining

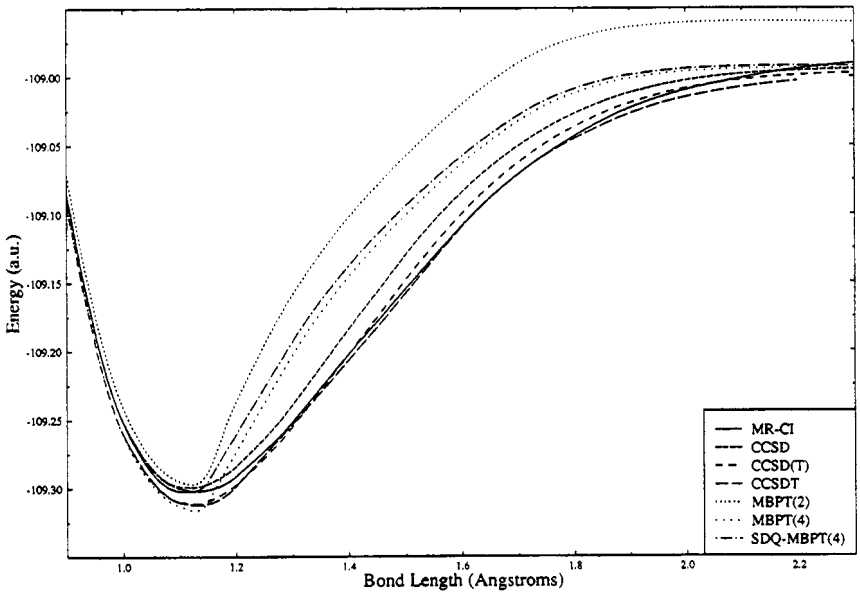

Figure 8 Correlated potential curves for N_2 using a UHF reference.

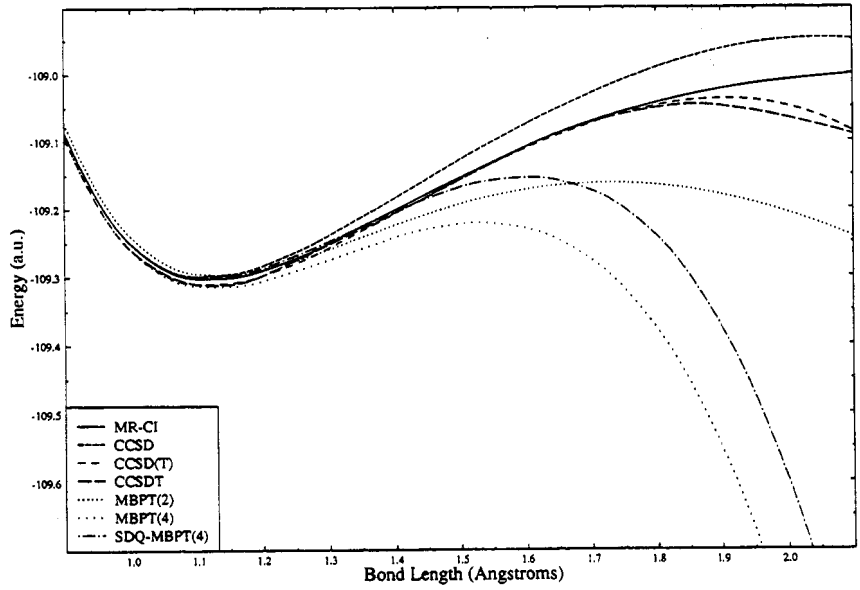

Figure 9 Correlated potential curves for N_2 using an RHF reference.

inextensivity error even in a large CASSCF-CISD calculation. The CI still does not have all the benefit of triple and quadruple excitations, which is why most such calculations will still be augmented by a semiempirical estimate of the extensivity correction. It is clear from the above that whereas CC methods should be able to describe the curvature accurately, MBPT frequencies will suffer from spin contamination.

Considering the RHF-based CC and MBPT methods (Figure 9), to obtain a reasonable curve, the CC and MBPT methods must overcome a reference that is incorrectly separating. From Figure 6 that means correcting for about 0.8 hartree (or ~500 kcal/mol!). The fact that CCSD(T) and CCSDT can largely do that is rather remarkable! In practice that means that CCSD and CCSD(T) are fairly good to about 1.5 Å and CCSDT is nearly superimposable upon the CASSCF-CISD result until about 1.9 Å. Once again near the minimum where UHF and RHF coincide, the many-body methods with triples have lower energies. Here, finite-order MBPT shows the characteristic turnover that results when an energy denominator $\epsilon_i + \epsilon_j - \epsilon_a - \epsilon_b$ approaches zero where $\epsilon_i + \epsilon_j \approx \epsilon_a + \epsilon_b$, as some orbitals are exactly degenerate at separation. The denominator is negative, which causes the result to go to negative infinity. Unlike the UHF-based results, finite-order RHF-MBPT is qualitatively correct near equilibrium, however.

Figures 10 and 11 show a similar set of curves for F_2. Figure 12 shows the differences in dissociation energies. F_2 is complicated by its small dissociation energy and its unbound UHF solution. However, it is simpler than N_2 in that only a single bond is being broken. For single bond breaking, CC methods will not show the turnover observed for the N_2 RHF-based examples. Comparisons with the GVB-CISD = CASSCF-CISD demonstrate the general accuracy of nondynamic CC methods for single bond breaking. In particular, results from the simplest iterative triples model, CCSDT-1[52] (Figure 12) are in good agreement with the GVB-CISD at separation and better than those from its noniterative counterpart, CCSD(T). As for N_2, the many-body results give deeper minima and better dissociation energies for F_2 than does CASSCF-CISD. Here, of course, the CAS space consists of only two orbitals and the CI contains only 6620 configurations. The RHF-MBPT curves still turn over (Figure 10), but farther out on the potential curve than for N_2. Because of UHF's qualitative failure for F_2, UHF-MBPT shows no binding either (Figure 11). However, once again, CCSD and CCSD(T) provide qualitatively correct potential energy curves (Figure 12) although the former is too steep near 1.8 Å as it is for N_2.

To summarize, CC/MBPT methods are usually more accurate near equilibrium geometries than are nondynamic correlated methods, but less accurate asymptotically. These two examples are extreme cases chosen to show failures. Correctly breaking a C—H bond in CH_4 or C—C bond in ethane is not too demanding for these methods. Because chemistry is mostly accomplished by breaking single bonds, most situations involving bond cleavage are amendable to single-reference CC methods. In particular, there are no particular problems

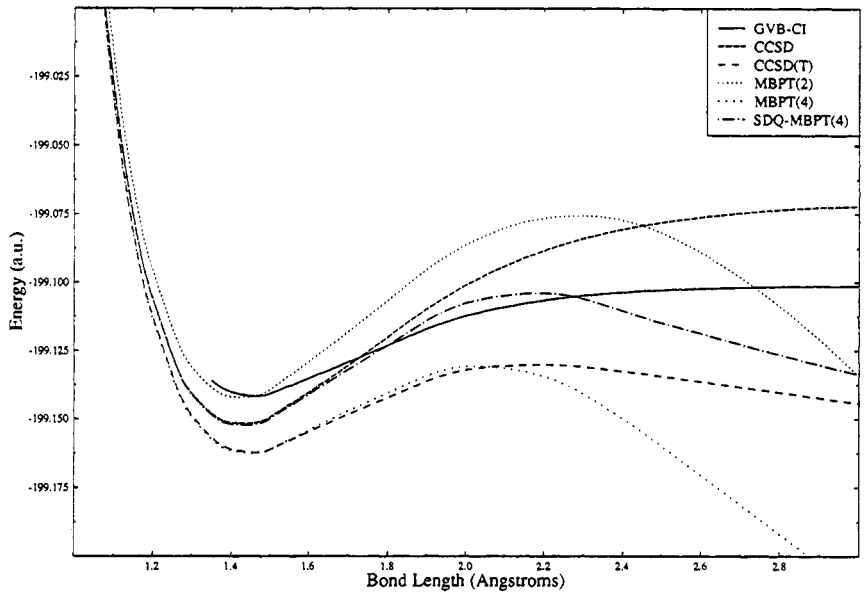

Figure 10 Correlated potential curves for F_2 using an RHF reference.

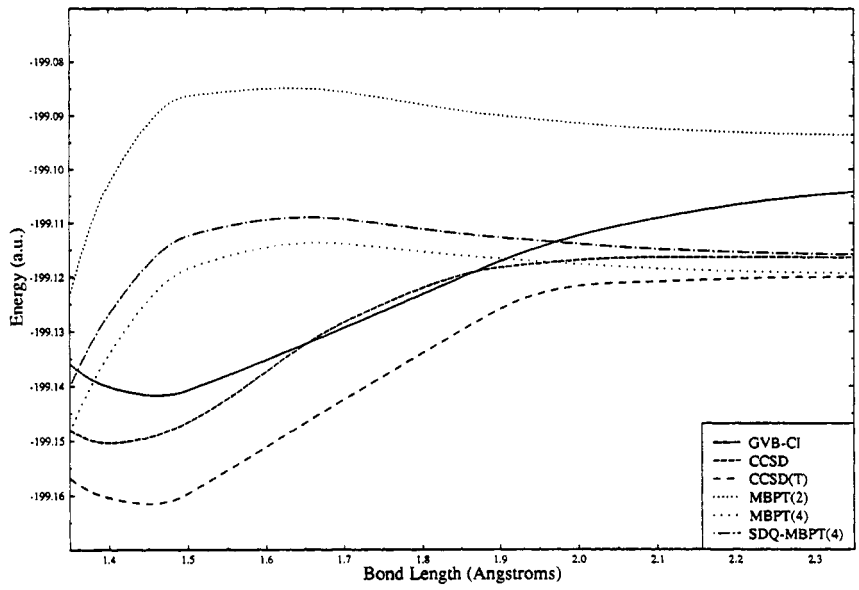

Figure 11 Correlated potential curves for F_2 using a UHF reference.

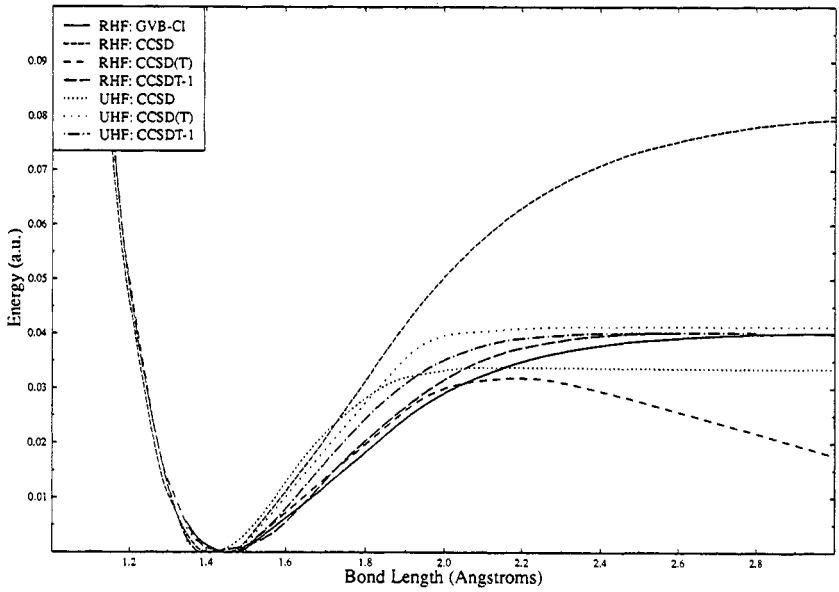

Figure 12 Correlated potential curves for F_2.

in the vicinity of equilibrium for most molecules, which is why even MBPT will usually give quite good answers. We will see many such examples in later sections.

Basis Sets

We have seen that the solution of the correlation problem within an "atomic orbital" (AO) basis set $\{\chi_\mu\}$ is given by the full CI. The full CI's agreement with experiment for various properties is a function of the choice of basis set. Since the whole mechanism for introducing electron correlation is to allow the wavefunction enough flexibility to let electrons avoid each other, the contracted Gaussian basis must include spatial flexibility.[57] This is introduced by (1) having multiple s functions for atoms that have s electrons; p functions for atoms that have p electrons, etc., and (2) by including higher angular momentum functions like d functions for B, C, O, N, F, p functions for H, f functions for the first-row transition series, etc., which are not normally required for the conceptual bonding description involving that atom. Both additions give extra flexibility to the wavefunction. Type (1) basis functions allow the correlated method to introduce "radial" correlation because we have extra flexibility in spatial regions along a bond in a molecule, while type (2) basis functions introduce polarization into the wavefunction and particularly allow for "angular correlation." While such higher angular functions will also give

improved SCF results for molecules, they are critical to the treatment of electron correlation for the obvious reason that d functions introduce areas of space that are not usually covered by s and p functions, and the more spatial flexibility, the better the electron correlation description. Similarly, f functions would introduce additional spatial flexibility, as would even higher angular momentum functions. Consequently we have to be concerned with the level of correlated theory and the quality of the basis set as shown in Table 5. The actual distance from the "truth" for a particular level of calculation and a particular property is a *"calibration"* step, largely determined by comparing results from a given level of correlated theory and basis to experiment. Calibration is discussed for several different categories of problems in later sections.

The minimum level AO basis that is meaningful for ab initio correlated treatments is at least a 6-31G*,[58] 6-31G**,[59] or, better, DZP basis.[60] The first two bases are in the GAUSSIAN program system, and the notation indicates that the core orbitals are represented by a single basis function involving a contraction of six Gaussian functions, while the valence s and p orbitals are described by two functions. The innermost, or least diffuse, function is a linear

Table 5 Basis Set Versus Quality of Theory in ab Initio Calculations

	Basis set							
Method	DZ	6-31G**	DZP	TZ2P	PVTZ	PVQZ	· · ·	Complete basis
SCF								
MBPT(2)								
CISD								
MBPT(3)								
CCD								
CCSD								
MBPT(4)								
CISDTQ								
CCSD(T)								
CCSDT								
CC5SD(TQ*)								
CCSDTQ								
MR-CI								
MR-CC								
⋮								
FULL CI								Truth

combination of three Gaussians, while the outermost is represented by a single uncontracted Gaussian. The exponents of the primitive Gaussians are the same for the valence s and p basis functions. (Many programs routinely put all six of the Cartesian components of d functions like x^2, y^2, z^2, xy, yz, xz into a calculation, and similarly 10 functions for f functions. The designation "spherical" limits the basis to the usual 5 d and 7 f functions.) The single asterisk (*) means that a set of six (Cartesian) functions is added to the heavy atom (i.e., B, C, N, O, F), while the double (**) means that a set of three p functions is added to all hydrogen atoms. Without the polarization functions, the basis sets (i.e., STO-3G, 4-31G, 6-31G, DZ, etc.) do not adequately include the most important physical effects of electron correlation. As a consequence, although there will be some energy reduction, the change will be relatively constant as a function of geometry or for ionization or excitation energies, etc., instead of introducing the physically significant differential effects of correlation.

The double zeta (DZ) basis[60] means choose twice as many s and p contracted functions as are occupied in the ground state of the atom (i.e., 2 s for H, but 4 s for Li, and 2 p for B, C, N, O, F). In practice we usually use 2 p for Be and Li, as well. The DZ plus polarization basis (DZP) means add a set of six d functions to the heavy atom and a set of three p functions to H. Unlike 6-31G**, there is no restriction to s and p contracted Gaussians having the same exponent, which gives the DZP basis additional flexibility. The primitive functions are not specified in the DZP designation, but usually the basis is derived from the 9s5p primitive optimized atomic Gaussian sets of Huzinaga.[61] This DZP basis (preferably with the polarization function exponents optimized at the correlated level for small molecules)[62] is the simplest reasonable level and will be widely used for illustrative calculations in this chapter. Obviously we could add larger primitive sets from which to define a DZP contraction, with some marginal improvement. More generally, we can use a larger contracted basis like TZP,[63] meaning 5s3p1d per atom (triple zeta in valence region), TZ2P (5s3p2d), TZ2Pf (5s3p2d1f), etc. We can use the same primitives or expanded sets. We can also add diffuse functions, which are sometimes indicated as 6-31G**++, for example.

The recently developed atomic natural orbital (ANO)[64,65] and "correlation consistent" (ccPVDZ, ccPVTZ, ccPVQZ, . . .) bases[66] use a large number of primitives and then form a contraction guided by results of correlated calculations. In the latter designation the P means polarization and the VDZ means "valence double zeta," which translates into 3s2p1d contracted Gaussians for first-row atoms, while PVTZ is 4s3p2d1f and PVQZ is 5s4p3d2f1g, etc. Even with more extensive primitive sets, the PVDZ basis tends to be slightly inferior to a DZP basis. Another useful basis is the POL1 basis of Sadlej[67] determined to accurately describe polarizabilities.

Note that for correlated calculations the number of primitive functions (n_p) is not of great concern because that number affects only the integral time (an $\sim n_p^4$ step), while the number of contracted functions $M = n + N$ deter-

mines the scale factor in correlated calculations, and that is greater than M^5. [All the integrals do not need to be transformed for MBPT(2), so then we have $\sim Mn^2N^2$ integrals.]

The larger the basis, the better the treatment of electron correlation. We cannot expect any monotonic convergence for most properties with either basis or correlated treatment, but larger basis sets and more correlation effects give methods that are "theoretically" more complete. However, the dimension of the basis is critical for post-Hartree–Fock calculations. For M contracted Gaussian (AO) functions, and n the number occupied, then $M - n = N$ unoccupied spatial orbitals left over after the SCF calculation. In typical polarized basis correlated calculations, N is more than three times the dimension of n. The cost of the SCF calculation is proportional to the number of primitive integrals $\langle \mu\nu|\lambda\delta\rangle$ (i.e., $\sim n_p^4/8$) that have to be evaluated. (For sufficiently large molecules, strategies can be exploited to make the scaling more like $\sim n_p^2$.) Regardless of what the correlated method is (CI, CC, MBPT, etc.), all such calculations start by transformating the AO two-electron integrals to the MO two-electron integrals $\langle \phi_i\phi_j|\phi_k\phi_l\rangle$. This requires a procedure proportional to $\sim M^5/4$. Molecular symmetry can be exploited to reduce the cost of integral evaluation by h, where h is the order of the point group, e.g., $h = 8$ for D_{2h}, and the integral transformation by a factor of h^2. CISD, CCSD and MBPT(3) require an n^2N^4 step, while other widely used higher order methods like MBPT(4) and CCSD(T) are $\sim n^3N^4$. By using molecular symmetry, all such methods with the exception of MBPT(2) can be reduced by a factor of h^2, which can result in a critical savings for large-scale correlated calculations.[68] Despite the advantages of symmetry when applicable, the nonlinear dependence on N (which even for a DZP basis is typically a factor 3–4 times n; for a TZP basis the factor is $\sim 5n$ and TZ2P, about $\sim 6n$, etc.) seriously impedes our ability to do correlated calculations. Doubling the size of the basis set requires $\sim 2^3$ as much computer time for MBPT(2), $\sim 2^4$ for MBPT(3), CCSD or CISD and $\sim 2^5$ for MBPT(4) or CCSD(T).

The nonlinear dependence on basis size greatly limits either the size of molecule or the basis set in a correlated calculation. To help some, inner shell electrons, which are known to have little effect on the formation of chemical bonds, are frequently not correlated. This means that the lowest occupied orbital (largely the 1s core AO) and the corresponding virtual orbital (V1s) are deleted from the basis before making the correlated calculation. For CH_4, this saves just two functions, but for C_6H_6, it would be 12. Similarly, for systems containing heavier atoms like Fe, several lower orbitals like 1s, 2s, and 2p can frequently be left uncorrelated without serious error. That usually means deleting the V1s, V2s, and V2p orbitals as well, because their primary function is to correlate the core orbitals; so 10 orbitals would be dropped from the correlated calculation. Most programs allow the automatic exclusion of such orbitals prior to the transformation for the correlated calculation.

Another option that reduces the number of functions, particularly when heavy atoms are involved, is the replacement of inner shell electrons by effective (or pseudo) potentials.[69] Such procedures have been incorporated into many ab initio program systems including ACES II. Since the core electrons are not explicitly considered, effective potentials can drastically reduce the computational effort demanded by the integral evaluation. However, because the $\sim n_b^4$ step is an inexpensive part of a correlated calculation, the role of effective potentials in correlated calculations is less important, due to the fact that dropping orbitals is tantamount to excluding them via effective potentials. An exception occurs when relativistic effects are important, as they would be in a description of heavy atom systems. Most such chemically relevant effects are due to inner shell electrons; their important physical effects, like expanding the Pt valence shell, can be introduced via effective potentials that are extracted from Dirac–Fock or other relativistic calculations on atoms.[70] Similarly, some effective potentials introduce some spin-orbital effects as well.[71] Thus, besides simplifying the computation, effective potential calculations could include important physical effects absent from the ordinary nonrelativistic methods routinely applied.

MOLECULAR GEOMETRIES

Because the concept of structure is central to chemistry, it is only natural that prediction of molecular geometries has historically been the most frequent area of application for quantum chemical methods. For the most part, these studies can be loosely grouped into two categories. In the first, rather general questions of structure are addressed, such as the point group symmetry of the molecule (e.g., is cyclobutadiene D_{2h} or D_{4h}?). Other investigations are directed toward predictions of the fine details of structure (bond lengths, bond angles, torsional angles, etc.), and it is this second group we discuss here.

Unlike some of the topics addressed in this chapter, the study of molecular geometries does not force us to explicitly consider more than one electronic state. Hence, correlation effects do not involve unpredictable differential correlation between states, but rather only changes in the correlation energy as one moves along the potential energy surface. As it turns out, the qualitative effects of correlation on geometrical structures tend to be systematic.

A definition of molecular structure is actually fairly complicated. For the most part, we tend to view this question from a classical perspective in which structure is defined by an arrangement of nuclei that minimizes the potential energy. The geometrical parameters that characterize these special points on the potential energy surface constitute an "equilibrium structure," where forces on the atoms vanish (i.e., $\partial E/\partial X_\alpha = 0$ for all Cartesian coordinates X_α). This is

the geometry the molecule might assume in the absence of available energy. However, in the real (quantum mechanical) world, molecules are never at rest and molecular structure is a dynamical concept involving oscillations of the nuclear positions about equilibrium geometries.

While quantum chemists typically calculate equilibrium geometries, experimentalists can only measure average structures in a direct fashion. For example, rotational spectroscopy yields moments of inertia that are related to average geometries in specific vibrational states, whereas electron diffraction provides internuclear distances averaged over a statistical ensemble of vibrational and rotational states. Extraction of equilibrium geometries from experimental data is an exceedingly difficult task for all but diatomic molecules because the anharmonic force field of the molecule must be known. Reliable equilibrium geometries are available for several triatomic molecules and a scant number of larger systems. For the most part, however, differences between equilibrium and vibrationally averaged structures are small ($\leq$0.01 Å for bond lengths, $\leq 0.5°$ for angles), and it is therefore possible to make meaningful comparisons between theoretical calculations and experimental results, provided we are careful.

The determination of equilibrium geometries involves the location of minima on the potential energy surface. At such a point, all first derivatives of the energy vanish (i.e., there is no net force on the nuclei) and the matrix of second derivatives (the Hessian) has no negative eigenvalues. For small molecules (particularly diatomics and triatomics), the potential energy surface is of small dimension, and it is not difficult to locate stationary points. Even the relatively crude procedure of evaluating the energy over a grid of points followed by interpolation works well. However, as molecular size grows, the potential surface rapidly becomes complex and more sophisticated approaches are warranted.

The intractability of simple energy-grid-based approaches is most easily communicated by means of an example. Suppose that one wanted to determine the equilibrium structure of 3-fluorotoluene. Even if C_s symmetry is imposed, there are still 22 distinct degrees of conformational freedom for the molecule. Consequently, if we want to perform a Newton–Raphson step to improve the geometry, we will have to determine the 22 components of the gradient and 253 unique Hessian elements. To calculate the derivatives with sufficient numerical accuracy, so-called double-sided differentiation must be used. (Such a procedure, which means taking equal $+\delta_q$ and $-\delta_q$ displacements for derivatives, removes the contaminating effects of the next higher derivatives and therefore improves numerical accuracy.) This would require that a grid of $\sim$500 energy points be evaluated, which is clearly not a practical procedure! However, a number of useful numerical techniques exist that allow us to estimate the Hessian, based on information from preceding geometry steps. Thus, it is practical to begin with a reasonable estimate of the Hessian and evaluate only

the first derivatives. Nevertheless, a numerical evaluation of the gradient by the double-sided method

$$\left.\frac{\partial E}{\partial q_i}\right|_{q_i=q_0} = \frac{E(q_0 + \delta) - E(q_0 - \delta)}{2\delta} \qquad [47]$$

requires 44 energy calculations.

The bottleneck in geometry optimizations alluded to above has yielded to one of the most important advances in quantum chemistry—the development of methods to calculate the gradient of the energy analytically.[72-76] An efficient formalism for the calculation of SCF derivatives was developed more than 20 years ago, and the first analytic derivative formulation for correlated methods followed a decade later. For the MBPT and CC approaches advocated by us, analytic gradient methods have been implemented for all the computational levels typically used in practice—MBPT(2), MBPT(3), SDQ-MBPT(4), MBPT(4), CCD, CCSD, CCSD + T(CCSD), CCSD(T), QCISD, and QCISD(T).[77-83] The ACES II program system allows the routine calculation of gradients at all these levels for both RHF and UHF reference functions, while ROHF-based MBPT(2),[80] CCSD,[79] and CCSD(T)[83] derivatives are also available. Other program packages permit analytic evaluation of UHF and RHF-based MBPT(2) derivatives and RHF-CISD, although no package other than ACES II has CC/MBPT gradient capabilities beyond MBPT(2). The GAUSSIAN program system is capable of evaluating gradients at the QCISD level.

In general, analytic gradient calculations scale only weakly with the number of degrees of freedom and typically require roughly 1–3 times the CPU time as the energy calculation itself. Gradients for SCF and correlated methods may be evaluated from the formula

$$\frac{\partial E}{\partial X_\alpha} = \mathrm{Tr}\left(\frac{\partial H}{\partial X_\alpha}\,\rho\right) + \mathrm{Tr}\left(\frac{\partial S}{\partial X_\alpha}\,I\right) \qquad [48]$$

where $\partial H/\partial X_\alpha$ is a derivative of the Hamiltonian matrix for one of the $3N$ Cartesian coordinates, ρ is a suitably defined density matrix, $\partial S/\partial X_\alpha$ are the derivatives of the overlap integrals, which serve to preserve the orthonormality of the wavefunction, and I is a one-particle-like quantity.

For SCF methods, ρ represents elements of the one- and two-particle density matrices. In correlated methods, the one-particle part of ρ is the sum of the actual reduced density and a contribution that is proportional to the derivative of the energy with respect to orbital rotations. For the MCSCF method, the orbitals are variationally optimum, and this latter term vanishes. Similarly, for FCI there is no orbital contribution. However, it is required for other CI, CC, and MBPT correlated methods, because the energy in these approaches is not stationary with respect to first-order changes in the molecular orbitals. This

latter term is said to account for "orbital relaxation," and the composite ρ is called a "relaxed" or "effective" density. Hence, all gradient calculations consist of evaluating density matrices and I intermediates and contracting them with matrix elements of an appropriately differentiated operator. For SCF methods, construction of ρ and I involves negligible computational expense, and timings are therefore dominated by integral derivative evaluation, which typically requires about twice the CPU time as the calculation of undifferentiated integrals.

For MBPT and CC methods, evaluation of the reduced density requires determining a response vector (Λ) as well as T. This defines a response density $\rho' = e^T|\Phi_0\rangle\langle\Phi_0|(1 + \Lambda)e^{-T}$. In addition, we want to allow the molecular orbitals to relax. The latter consideration adds another term, ρ'', to the one-particle density. This "relaxed" density, $\rho = \rho' + \rho''$, is the critical quantity in CC and MBPT analytical gradient (and property) methods.[84] For just the one-particle part, we have $\rho(1) = \rho'(1) + \rho'' = D(1)$ which will show up again when we discuss properties.

For all methods besides MBPT(2) and MBPT(3), the evaluation of Λ requires a fair amount of additional computation. However, even for CC methods this step requires only about half the CPU time of the CC calculation itself. Hence, for calculations in which the integral evaluation time is negligible the ratio of timings between MBPT/CC energy and energy plus gradient calculations is expected to be between ~1:1 and 1:1.75. Thus, it may be seen that the availability of efficient analytic gradient methods greatly facilitates the study of potential energy surfaces. Indeed, the development of such techniques now seems to be a prerequisite for any method intended for use in chemical applications.

The accuracy of molecular geometries predicted by the SCF approximation has received considerable attention in the literature. On the whole, the neglect of electron correlation causes bond lengths to be underestimated, as seen in the basis set study for water in Table 6. This statement about underestimated bond lengths applies to exact SCF calculations, namely those in which the basis set is complete. As seen in Table 6, SCF calculations performed with

Table 6 Optimized SCF Molecular Geometry Data for H_2O as a Function of Basis Set

Basis	R_e, O—H (Å)	θ, H–O–H (degrees)
STO-3G	0.989	100.0
3-21G	0.967	107.7
DZ	0.951	112.5
6-31G*	0.947	105.5
DZP	0.944	106.6
TZ2P	0.941	106.2
Experimental	0.957	104.5

poor basis sets often overestimate the distance between bonded atoms. The underestimation, of course, is a manifestation of deficiencies of the SCF model for potential energy surfaces discussed previously. In SCF calculations, the electron–electron repulsion terms are not treated properly, and electrons tend to bunch together too closely. This results in compact bonds with favorable Coulombic attractions between the electrons and nuclei. However, when interelectronic repulsion is treated properly, the electrons move apart, which causes the bond lengths to increase. The overestimation of bond angles observed in SCF calculations for many molecules may be rationalized as a consequence of the considerations discussed above. That is, underestimation of the bonded distances causes an increased (and unfavorable) interaction between the nonbonded atoms. Therefore, bond angles increase.

Another ubiquitous trend in SCF geometry studies, which is illustrated by the data in Table 6 is a marked inverse relationship between the quality of the basis set and the predicted bond lengths. In our water example, SCF bond lengths monotonically decrease from 0.989 Å to 0.941 Å as the basis set is improved from STO-3G to TZ2P. In water as well as many other molecules, small basis sets usually overestimate the experimental bond lengths, which are in turn longer than those obtained at the SCF level with extensive basis sets. Therefore, it is often possible to select a basis set of intermediate quality (DZ in the present example) which gives an accurate "prediction" of R_e. This is an example of a *Pauling point*—a level of theory that provides better results than those obtained in more sophisticated calculations—and is due to the opposing nature of correlation and basis set corrections, which tend to increase and decrease bonded distances, respectively. [This situation should contrast with the calculation of excitation energies, in which both correlation and basis set effects tend to act in concert with improvements in both leading to lower values (see later).] Indeed, SCF geometry optimizations in a split-valence polarized basis set, such as 3-21G or DZ, have long been used to predict geometries of organic molecules. For the most part, this approach works reasonably well, because the errors tend to be highly systematic provided lone-pair electrons are not present. However, the results for our water example clearly illustrate that polarization functions are needed to predict bond angles, so one must exercise a certain amount of care in choosing basis sets for geometry optimizations. It is very difficult to predict the location of Pauling points a priori; instead *one must rely on experience gained in studies of similar molecules.* For example, one should not expect the equilibrium bond length of ozone predicted at the SCF level with a DZ basis set to be as accurate as that for the O—H bond in water. Indeed, at the DZ-SCF level the equilibrium for ozone is predicted to be R_e(O—O) = 1.259 Å; θ = 119.7°, as compared to the experimental results of 1.272 Å and 116.8°, respectively. Whereas our experience for water is consistent with the overestimation of the bond angle with this unpolarized basis set, the error in bond length (−0.012 Å) is about twice that found for water (−0.006 Å).

The only reliable way to obtain molecular structures that converge toward the correct result is to use increasingly larger basis sets and more complete treatments of electron correlation. For water, the results of calculations using a variety of basis sets (STO-3G, 3-21G, DZ, 6-31G*, DZP, and TZ2P) and computational methods [SCF, MBPT(2), CCSD, and CCSD(T)] are listed in Table 7. The equilibrium bond lengths and bond angles predicted by these calculations clearly demonstrate the trends discussed above, namely the tendency for electron correlation to increase bond lengths (and by consequence reduce bond angles), while basis set expansion exhibits the opposite behavior. Nevertheless, the magnitudes of the changes are relatively modest once a reasonable level of theory has been surpassed, such as MBPT(2) with the DZP basis set.

Having results obtained at a few correlated levels with different basis sets, it is usually possible to estimate the direction of the residual error with a fair degree of confidence. As an example, let us consider water once again. Because water has a well-isolated electronic ground state and no significant nondynamical electron correlation effects, the CCSD(T) approximation should provide a nearly quantitative treatment of correlation. Hence, the error in our most sophisticated calculation [CCSD(T) with the TZ2P basis set] should be due almost entirely to deficiencies in the basis. The structure obtained in this calculation [R_e (O—H) = 0.959 Å and θ = 104.2°] is therefore expected to have an overestimated bond length and underestimated bond angle, as verified by comparison with the experimental values.

In Table 8, we list errors in bond length (Å) and bond angles (degrees) calculated at various correlated levels with a DZP basis set for a set of molecules. The equilibrium geometries of the systems studied here have been reasonably well determined experimentally, so comparisons between the present values and the experimental results are relevant.

The effects of correlation (Table 8) exhibit the same qualitative behavior we have noted for water. (One should note that the rationalization provided for the behavior of the bond angle in water does not apply to formaldehyde,

Table 7 Optimized Geometries (in angstroms and degrees) for H_2O as a Function of Basis Set

	SCF		MBPT(2)		CCSD		CCSD(T)	
Basis	R_e	θ	R_e	θ	R_e	θ	R_e	θ
STO-3G	0.989	100.0	1.013	97.3	1.028	96.8	1.028	96.8
3-21G	0.967	107.7	0.989	105.2	0.993	104.9	0.994	104.8
DZ	0.951	112.5	0.979	110.5	0.979	110.3	0.980	110.3
6-31G*	0.947	105.5	0.969	104.0	0.969	104.0	0.971	103.9
DZP	0.944	106.6	0.963	104.4	0.961	103.7	0.962	103.6
TZ2P	0.941	106.3	0.958	104.2	0.956	104.5	0.959	104.2
Experimental							0.957	104.5

Table 8 Errors in Bond Lengths and Angles for Various Levels of Theory (DZP Basis)

SCF	MBPT(2)[a]	SDQ-MBPT(4)[a]	CCSD[b]	MBPT(4)[a]	CCSD(T)[c]	Molecule	Bond or angle
			Bond lengths (Å)				
−0.006	0.005	0.004	0.004	0.005	0.005	H_2O	OH
−0.011	0.002	0.003	0.003	0.004	0.004	NH_3	NH
−0.001	0.003	0.005	0.005	0.006	0.006	CH_4	CH
−0.002	0.006	0.006	0.007	0.008	0.008	C_2H_2	CH
−0.012	0.024	0.017	0.016	0.025	0.023		CC
−0.005	0.003	0.004	0.004	0.008	0.006	CH_2O	CH
−0.015	0.022	0.017	0.015	0.023	0.021		CO
−0.003	0.004	0.005	0.005	0.006	0.006	HCN	CH
−0.017	0.032	0.020	0.019	0.030	0.024		CN
−0.008	0.007	0.005	0.006	0.007	0.008	HNC	NH
−0.010	0.025	0.020	0.017	0.031	0.024		CN
−0.015	0.022	0.016	0.012	0.028	0.018	CO_2	CO
			Average absolute error				
−0.009	0.013	0.010	0.009	0.015	0.013		
			Bond angles (degrees)				
2.1	−0.1	0.1	0.1	0.0	0.0	H_2O	H–O–H
1.5	0.0	−0.2	−0.2	−0.3	−0.4	NH_3	H–N–H
−0.3	−0.2	−0.3	−0.2	−0.6	−0.2	CH_2O	H–C–O
			Average absolute error				
1.3	0.1	0.2	0.2	0.3	0.2		

[a] Reference 85.
[b] Reference 86.
[c] Reference 87.

because variation of the H–C–H bond angle involves changes in three distinct nonbonded interactions.) Due to the nature of the basis set used in these calculations, the bond lengths obtained with the most sophisticated treatment of correlation [CCSD(T)] are systematically longer than the experimental values. Absolute errors in bond length are largest for multiple bonds (CN, CC, and CO) at both the SCF and correlated levels. Assuming that the majority of error in the CCSD(T) results is due to basis set deficiencies, this observation suggests that both basis set and correlation effects are more pronounced for multiple bonds than for single bonds as discussed previously. The basis set sensitivity results from the more pronounced correlation effects, because larger basis sets provide a more flexible set of the virtual orbitals required to describe correlation. This reflects a statement made early in this chapter. To paraphrase: *when correlation effects are important, a large basis set is needed to describe them properly!* This is one of the important messages we are trying to convey.

We conclude this section with a brief discussion on a related topic—the optimization of transition state structures at the correlated level. In these calculations, the stationary points of interest are those that have precisely one significant negative eigenvalue of the Hessian matrix. Such points always represent the energy maximum along a minimum energy pathway linking two local minima on the potential energy surface. Points with more than one negative eigenvalue never represent transition states because there is always a lower energy path between the minima. In some sense, these other points (which are only of academic interest) represent transition states between transition states. Location of saddle points on potential energy surfaces is more difficult than finding local minima. However, a number of clever algorithms have been developed in the past decade.[88,89]

As chemical reactions proceed via pathways that are either allowed or disallowed by orbital symmetry considerations,[90] studies of transition states may also be broadly categorized in this way. In the former case, orbitals of the reactants map smoothly into those of the products and MBPT/CC calculations based on a single determinant reference should therefore be appropriate for studying the reaction pathway. However, for "forbidden" reactions, the region of the potential energy surface near the transition state is usually very poorly described by a single determinant starting point, and multi-reference-based methods are warranted. Many interesting chemical reactions (particularly those with low barrier heights) are allowed by orbital symmetry, and the single reference correlated methods discussed in this chapter may readily be applied to a study of these reactions.

A prototypical example of a transition state amenable to single determinant MBPT/CC methods is the unimolecular dissociation of formaldehyde

$$CH_2O \rightarrow H_2 + CO \qquad [49]$$

which has been the subject of a number of theoretical and experimental studies. Structural parameters of the transition state calculated with a DZP basis and a

Table 9 Internal Coordinates (in angstroms and degrees) for the Transition State in the Decomposition of Formaldehyde

Correlation treatment	$R(CO)$	$R(CH_1)$	$R(CH_2)$	$\theta(OCH_2)$	$\theta(H_2CH_1)$
SCF	1.151	1.102	1.583	112.5	49.4
MBPT(2)	1.192	1.096	1.596	111.6	50.7
CCSD	1.188	1.094	1.595	110.2	51.4
CCSD(T)	1.193	1.092	1.621	110.3	52.2

number of different treatments of correlation are listed in Table 9. For topological features of molecules that are common to both reactants and products, the considerations of basis set and correlation effects discussed earlier in this section still apply. For example, in the formaldehyde decomposition reaction, the C—O bond length increases from 1.151 Å to 1.193 Å as the level of theory is increased from SCF to CCSD(T). The magnitude of this expansion (0.042 Å) is comparable to that found for the C—O bond in ground state formaldehyde using the same basis (0.035 Å). However, the simple systematic behavior we have observed for ground state structures usually does not hold for bonds that are broken or otherwise transformed by the reaction. In this transition state, for example, the two C—H distances behave quite differently as the treatment of correlation is improved. With respect to the SCF structure, the distance between the carbon and the proximal hydrogen actually decreases by 0.010 Å while the other C—H distance increases by 0.038 Å at the CCSD(T) level.

VIBRATIONAL SPECTRA

For rigid molecules, energy differences between the ground and singly excited vibrational states are relatively small with respect to barrier heights on the potential energy surface. Hence, the nuclei tend to undergo only small-amplitude vibrations about their equilibrium positions in both the ground and excited states and therefore do not sample a large region of the potential surface. As a result, the part of the potential energy surface that governs these states and the transitions between them can be reasonably approximated by the potential function of a multidimensional harmonic oscillator. In the theory of vibrational spectroscopy, this "harmonic" approximation plays a role similar to that of the Hartree–Fock approximation in electronic structure theory. Both these simplifying approximations lead to separable and therefore exactly soluble Schrödinger equations, the solutions of which ("normal" vibrational modes and molecular orbitals, respectively) represent useful paradigms for our understanding of the respective phenomena. However, we must be careful to remember that both normal coordinate theory and molecular orbital theory are approximations, and exact calculations must go beyond these models.

Because of the properties noted above, most quantum chemical studies of vibrational frequencies are carried out within the "double" harmonic approximation (i.e., using only second derivatives for the force constants and the derivative of the dipole moment for the intensities; see below). This neglects the so-called mechanical and electrical anharmonicities. As is the case for theoretical predictions of molecular structures, we must once again be careful when comparing experimental and theoretical results. In structural predictions, one is usually forced to compare equilibrium geometries obtained by theory to some sort of averaged geometry obtained from experiment, whereas vibrational calculations produce harmonic frequencies that do not include anharmonic effects. Hence, to rigorously assess the quality of harmonic force fields obtained theoretically, it is necessary to compare results to "experimental harmonic frequencies." We believe that the difficulty of obtaining harmonic frequencies experimentally is not as widely appreciated among the quantum chemical community as it should be. Indeed, the amount of information required to determine harmonic frequencies from experimental data is the same as that needed to determine the equilibrium geometry. Therefore, the number of systems for which accurate harmonic frequencies have been determined is even smaller than that for which the equilibrium geometry is known with precision. The point of this section is to assess how accurately different quantum chemical methods can predict harmonic frequencies, so we will concern ourselves primarily with such systems.

The quantities we require in a calculation of harmonic vibrational frequencies are the second derivatives (i.e., the force constants) of the electronic energy with respect to nuclear displacement, $\partial^2 E/\partial q_\alpha \partial q_\beta$. In terms of Cartesian coordinates there are $3N$ such terms, for N atoms. Elimination of translational and rotational degrees of freedom gives the familiar $3N - 6(5)$ independent nuclear coordinates. We refer to the force constant matrix as the Hessian matrix. The eigenvalues of the Hessian matrix must all be positive at a minimum energy geometry, while at a transition state (which corresponds to a saddle point), one will be negative. The corresponding eigenvector identifies the reaction path, while the remaining eigenvalues are positive. Operationally, we can evaluate second derivatives of the electronic energy in one of three ways:

1. Obtain the energy at several points and determine the second derivatives from numerical second derivatives. If we insist on "double-sided" numerical differentiations, which is recommended because it benefits from eliminating any third-derivative contaminant, we require $E(0)$ and $E(\pm\delta q_\alpha)$ for each Cartesian displacement, δq_α. Clearly, symmetry can be used to reduce the number of calculations by replacing q_α by symmetry coordinates (S_α). This is done automatically in ACES II.
2. Evaluate the gradient to provide analytic first derivatives $\{\partial E/\partial q_\alpha\}$ from which $\partial^2 E/\partial q_\alpha \partial q_\beta$ can be obtained by a displacement in $\pm\delta q_\beta$. Again, symmetry can be exploited to reduce the number of gradient evaluations.
3. Evaluate the second derivative matrix analytically.

Each level is more efficient and numerically accurate than the preceding one. For most polyatomic molecules, ab initio calculations using approach 1 are not feasible because of the large number of independent degrees of freedom: they require roughly $(3N - 6) \times (3N - 5)/2 \times 2$ energy calculations. Approach 2 is used for many applications of interest at correlated levels. Approach 3 is readily used in SCF calculations, and although some attempts have been made for MCSCF, CI, and CCSD methods; in practice, correlated analytical Hessians have been largely limited to MBPT(2).[91-93] Analytic MBPT(2) Hessian evaluation for RHF,[91] UHF,[92] and ROHF[93] reference functions have now been presented and will be available in ACES II.

At uncorrelated levels, the frequently incorrect separation of the RHF wavefunction or spin contamination in a UHF solution will cause too large a curvature, illustrated in the diatomic potential curves discussed earlier. Hence, SCF will normally overestimate the second derivatives, causing the resultant harmonic frequencies to be too high. (Note that pathological situations, such as the UHF curve for F_2 and "symmetry breaking" where the RHF, ROHF, or UHF solution for some small displacement fails to connect to that at the higher symmetry point, have to be recognized. The latter frequently prohibits calculating second derivatives with finite displacement, although analytical second derivatives can be obtained at the high symmetry point.) The SCF-predicted frequencies are found to be about 10% above the fundamental vibrational frequencies observed experimentally, recommending an *empirical scaling factor* of 0.9. Some workers use different scale factors for different frequency modes (symmetric stretches, asymmetric stretches, bends, etc.) or applied to the force constants for these modes. We show the differences between experimental harmonic frequencies and DZP basis SCF theory for several ordinary closed-shell molecules in Table 10. Also in Table 10 are results from several different levels of electron correlation. Any level of electron correlation reduces the SCF error to about 5%. (In this table, the "experimental" values correspond to actual harmonic frequencies, but the reader should remember that these are rarely available for polyatomic molecules.) Most of the error is recovered at the simplest MBPT(2) level, with more modest improvements at higher levels.

In terms of computational requirements, MBPT(2) is a highly applicable level of correlated theory. The results are somewhat better than the infinite-order CISD. Unlike CISD, MBPT(2) is an extensive method, and that means that even though it corresponds to the first iteration of CISD, it is also the first iteration of CCSD, and it tends to give results closer to those for CCSD than for CISD. Second, as discussed previously, MBPT(2) tends to overestimate bond lengths and angles compared to experiment. Because longer bonds tend to diminish the force constants, MBPT(2) vibrational frequencies usually move closer to experimental values. That, together with the ready availability of analytical Hessians, makes MBPT(2) a highly useful method for extensive (!) applications to molecules.

Concerning the scaling of the SCF frequencies, another point should be made. An implicit assumption underlying the use of empirical scaling factors is

Table 10 Differences Between Theoretical and Experimental Harmonic Frequencies ω (cm^{-1}) for Several Small Molecules (DZP Basis)

Molecule		Experimental	SCF[a]	CISD[a]	MBPT(2)[b]	SDQ-MBPT(4)[b]	CCSD[a]	MBPT(4)[b]	CCSD(T)[c]
H_2O	ω_1	3832	332	135	77	89	80	73	64
	ω_2	1649	102	44	15	33	34	26	28
	ω_3	3943	344	147	112	107	98	92	83
NH_3	ω_1	3506	218	91	67	56	45	40	27
	ω_2	1022	97	98	78	97	97	99	100
	ω_3	3577	295	165	164	135	123	121	107
	ω_4	1691	111	204	12	27	25	20	18
CH_4	ω_1	3026	148	90	86	71	61	62	50
	ω_2	1583	88	18	11	5	3	−1	−4
	ω_3	3157	137	100	117	85	73	77	63
	ω_4	1367	90	30	16	20	18	14	11
C_2H_2	ω_1	3497	84	94	54	53	41	30	22
	ω_2	2011	194	70	−58	3	8	−60	−29
	ω_3	3415	162	77	49	40	28	23	10
	ω_4	624	146	−4	−78	−58	−61	−109	−106
	ω_5	747	116	22	−16	−10	−13	−35	−37
H_2CO	ω_1	2978	171	102	62	47	51	19	26
	ω_2	1778	228	99	−8	28	41	−26	3

	ω_3	1529	127	71	39	41	44	19	30
	ω_4	1191	144	56	23	21	20	4	1
	ω_5	2997	229	165	132	108	113	78	88
	ω_6	1299	68	11	−18	−14	−12	−30	−24
HCN	ω_1	3440	196	109	64	61	53	35	31
	ω_2	2128	276	96	−131	−15	17	−119	−25
	ω_3	727	131	35	−11	0	−1	−28	−35
CO_2	ω_1	1354	159	75	−28	−10	25	−95	−13
	ω_2	2397	193	116	59	27	51	−28	−12
	ω_3	673	94	37	−17	−2	9	−38	21
C_2H_4	ω_1	3139	191		108	172		159	
	ω_2	1655	165		44	57		32	
	ω_3	1371	101		21	21		6	
	ω_4	1047	87		18	5		−5	
	ω_5	3212	183		120	99		7	
	ω_6	1245	94		15	20		10	
	ω_7	968	113		−9	−12		−29	
	ω_8	959	130		−148	−130		−172	
	ω_9	3234	187		126	105		92	
	ω_{10}	843	47		−12	−10		−18	
	ω_{11}	3138	165		85	72		57	
	ω_{12}	1473	113		33	40		30	
Error, %			8.7	3.7	3.2	2.5	2.2	3.1	2.4

[a] Reference 86.
[b] Reference 85.
[c] Reference 87.

that the order of the vibrational frequencies is correctly predicted at the SCF level. However, for many molecules, correlation effects interchange the order, as illustrated by C_2H_4 in Table 10. Experimentally, the $\omega_7(b_{1u})$ mode has a higher frequency than $\omega_8(b_{2u})$, but SCF has the reverse ordering. MBPT(2) and all higher correlated levels have the correct order. This also seems to be a characteristic of several proposed nitrogen analogs of cyclopropane and cyclopentadiene, N_3H_3[94] and N_5H,[95] where the SCF order (and intensities) are significantly changed at the MBPT(2) level. MBPT(2) is not always right, however, as unwarranted changes from SCF for the open-shell OCBO molecule[96] were rectified at higher order CC levels.

In addition to the frequencies, the infrared intensities may be determined by evaluating $\partial\mu_i/\partial X_\alpha$ where μ_i is a component of the dipole moment and X_α is a Cartesian nuclear displacement. The dipole moment itself can be viewed as the gradient of the electronic energy with respect to an electric field ϵ_i (see later discussion of molecular properties), so $\partial\mu_i/\partial X_\alpha = \partial^2 E/\partial\epsilon_i\partial X_\alpha$ requires a cross-second derivative. Just as for force constants, analytical evaluation is preferred and is now routine for MBPT(2). For higher correlated methods, analytical evaluation of μ_i from the relaxed density at finite nuclear displacements is used to obtain the intensities. Whereas the calculated frequencies only are subject to the accuracy of the energy as a function of displacement, intensities are more sensitive to diffuse regions of the electronic density through the dipole matrix elements, placing greater demands on the quality of the basis set.[97,98]

Mean absolute errors for IR intensities determined from the standard molecules discussed above are shown in Table 11 for different levels of approximation and a DZP basis. Of course, errors for relative intensities are much smaller.

Once again, it appears that for a modest basis set like DZP, MBPT(2) is on average about as good as more sophisticated correlated methods. This does not necessarily follow once the basis has been improved, however. To illustrate this we present frequencies and intensities with DZ, DZP, and TZ2P basis sets for H_2O in Table 12. As the level of correlation and basis are improved, there is a fairly regular convergence toward the experimental values. In particular,

Table 11 Errors in Intensities at Various Levels of Theory (DZP Basis)[a]

Method	Mean absolute error (%)
SCF	96
MBPT(2)	41
CISD	47
SDQ-MBPT(4)	34
CCSD	41
MBPT(4)	40
CCSD(T)	34

[a]Extracted from same references as in Table 10.

Table 12 Vibrational Frequencies (cm^{-1}) and Intensities (km mol^{-1}) for H_2O as a Function of Basis Set

Basis sets	ω_1	ω_2	ω_3	I_1	I_2	I_3
DZ						
SCF	4028	1711	4204	3.4	135.8	65.0
MBPT(2)	3674	1624	3872	0.4	100.4	27.0
SDQ-MBPT(4)	3668	1638	3848	1.7	95.1	15.3
CCSD	3653	1639	3831	2.2	93.6	13.0
DZP						
SCF	4164	1751	4287	20.5	108.0	73.8
MBPT(2)	3909	1664	4055	4.5	80.9	45.6
SDQ-MBPT(4)	3905	1687	4020	5.9	65.8	30.7
CCSD	3898	1687	4012	5.6	65.9	29.8
CCSD(T)	3879	1681	3994	4.3	63.5	26.6
TZ2P						
SCF	4133	1752	4237	20.9	88.0	98.7
MBPT(2)	3864	1653	3987	10.6	61.6	77.5
SDQ-MBPT(4)	3883	1678	3991	8.0	62.7	61.3
CCSD	3886	1679	3991	8.0	63.4	61.0
CCSD(T)	3848	1670	3955	6.4	60.1	56.1
Experimental	3832	1649	3943	2.2	53.6	44.6

larger basis sets with higher level correlated methods generally show significant improvement over MBPT(2). In the case of the symmetric stretch mode ω_1 the small "experimental" value for I_1 is likely to be as much in error as the calculation, so the error value might not be too meaningful. In fact, several other "experimental" values are available for these intensities.

Table 13 shows a few more examples of results using a larger TZ2Pf basis,[99] that contains f functions.[100] The average error for CCSD(T) results for frequencies is 0.7%, while the intensities have an average absolute error of 16%.

The customary accuracy of MBPT(2) has now been extended to purely analytical second-derivative methods for open shells using UHF[93] or ROHF reference functions. The latter requires some new (noncanonical MBPT/CC) theory recently developed.[80,93] As discussed previously, unlike ROHF, which is an eigenfunction of spin for high spin cases, UHF reference functions can sometimes suffer from spin contamination. For low order correlated methods like MBPT(2) (unlike CCSD, e.g.), the UHF spin contamination can drastically affect the answers obtained.

As an example, consider the methylene imidogen molecule, CH_2N.[93] This system, which is isoelectronic with the vinyl radical, has a multiplicity $2S + 1 = 2.256$ at the UHF level. Its vibrational frequencies are shown in Table 14.[101] There are several messages in Table 14. First there are differences between UHF and ROHF of ~200 cm^{-1} for ω_2 and ~100 cm^{-1} for ω_3 and ω_6. Second, the order of the ω_5 and ω_6 frequencies is interchanged. Third, the

Table 13 Correlated Vibrational Frequencies (cm^{-1}) and Intensities (km mol^{-1}) in Parentheses for HCN, CO_2, and C_2H_2 in a TZ2Pf Basis[a]

	HCN			CO_2			C_2H_2				
Method	$1(\sigma)$	$2(\sigma)$	$3(\pi)$	$1(\sigma_g)$	$2(\sigma_u)$	$3(\pi_g)$	$1(\sigma_g)$	$2(\sigma_g)$	$3(\sigma_u)$	$4(\pi_g)$	$5(\pi_u)$
MBPT(2)	3481	2044	726	1356	2421	659	3544	1986	3451	613	756
	(85.8)	(0.22)	(74.1)	(0)	(561.0)	(50.0)	(0)	(0)	(99.0)	(0)	(179.2)
CCSD(T)	3450	2126	723	1351	2393	663	3514	2010	3416	599	749
	(71.8)	(0.09)	(73.4)	(0)	(625.8)	(58.6)	(0)	(0)	(84.9)	(0)	(178.4)
Experimental	3440	2128	727	1354	2397	673	3497	2011	3415	624	747
	(62)	(0)	(58)	(0)	(551)	(48)	(0)	(0)	(71)	(0)	(175)

[a] Reference 99.

Table 14 Harmonic Vibrational Frequencies (Intensities) of CH_2N (DZP and TZ2P Basis)[a]

	$\omega_1(a_1)$	ω_2	ω_3	$\omega_4(b_1)$	ω_5	$\omega_6(b_2)$
UHF	3207.2 (0.6)	1606.4 (17.1)	1402.4 (0.0)	3301.0 (13.1)	1051.8 (13.6)	1012.7 (39.5)
ROHF	3235.9 (2.2)	1879.3 (1.1)	1511.7 (16.5)	3328.7 (12.6)	1067.4 (13.9)	1135.0 (33.8)
UHF-MBPT(2)	3099.9 (0.2)	2041.5 (12.0)	1430.1 (19.2)	3182.2 (8.5)	954.4 (7.5)	1153.8 (34.7)
ROHF-MBPT(2)	3100.0 (0.0)	1677.4 (3.8)	1407.5 (7.2)	3197.1 (6.8)	931.3 (6.5)	981.4 (39.4)
ROHF-MBPT(2)(TZ2P)	3079.1 (0.9)	1681.9 (5.6)	1409.6 (12.2)	3176.1 (0.7)	956.2 (9.6)	988.0 (37.3)
UHF-CCSD	3066.0 (0.5)	1693.6 (1.8)	1409.1 (8.1)	3144.8 (13.3)	952.4 (7.9)	982.8 (35.4)
ROHF-CCSD	3064.9 (0.5)	1689.3 (2.0)	1408.5 (7.8)	3143.9 (13.4)	953.1 (8.0)	979.1 (35.1)
UHF-CCSD(T)	3043.8 (0.4)	1671.1 (2.4)	1396.9 (7.6)	3121.8 (13.8)	938.3 (7.3)	963.7 (36.1)
ROHF-CCSD(T)	3041.8 (0.4)	1651.8 (3.0)	1394.2 (7.1)	3119.8 (13.8)	936.9 (7.2)	953.9 (36.1)
Experimental[b]	2820	1725	1337	3103	913	954

[a] Reference 93.

[b] Actual (nonharmonic) frequencies from reference 101.

intensity distribution between the ω_2 and ω_3 mode is vastly different. Once we have performed an MBPT(2) calculation, the UHF-MBPT(2) multiplicity is still poor ($2S + 1 = 2.203$), but ROHF-MBPT(2) does not suffer from this failing. We see drastic changes of ~400 cm^{-1} for the ω_2 mode and ~200 cm^{-1} for ω_6 between the two approaches. The usefulness of a method depends on how rapidly it converges to the full CI solution, and as we have seen, CCSD and CCSD(T) go a long way toward the full CI. From the data in Table 14, therefore, it is clear that ROHF-MBPT(2) is much closer to the CCSD and CCSD(T) results, differing by only 12–26 cm^{-1} for ω_2 and 2–27 cm^{-1} for ω_6; and intensity for ω_2 is 3.8 versus 2.0 and 3.0. Notice that the CCSD and CCSD(T) results scarcely change with the choice of reference function. The reason is that CCSD and higher CC methods benefit from the orbital property of Eq. [53], below, making the methods relatively independent of orbital choice. [This feature makes it possible to use quasi–restricted Hartree–Fock orbitals (QRHF) in CCSD calculations, when the orbitals are taken from a different system and are not at all the optimum set for the problem.] As the failing of UHF-MBPT(2) is largely due to spin contamination, we can also see this from noting that the UHF-CCSD $2S + 1 = 2.018$, which is close to a perfect doublet.

The new development of ROHF-MBPT(2) analytical Hessians offers an important tool for the theoretical description of vibrational spectra but it, too, is not a panacea. Although ROHF does not suffer from spin contamination, ROHF does tend to localize unpaired electrons in unphysical ways, which can cause it to offer a poorer reference than UHF for such problems. A case in point is the $^3\Sigma_g^-$ C_4 molecule, where UHF-MBPT(2) is superior to the ROHF-MBPT(2) description.

One final informative example is offered by the O_3 molecule. As discussed O_3 possesses resonance structures and biradical character, which usually recommends at least two reference functions in its zeroth-order description. We can expect this to be a demanding case for single reference methods,[102] although multireference methods have their own problems. These results are presented in Table 15.

The first observation is that the single determinant RHF-SCF harmonic frequencies have an average error of 19% instead of the usual ~10%. A two-reference (2R or GVB) CI would appear to offer a more correct description,[103] and, although it seems to significantly reduce the error for the symmetric stretch (ω_1) and bend (ω_2), it is still substantially in error for the asymmetric stretch (ω_3), which causes an average error of 12%. In addition, the 2R-CISD calculation gives the wrong order of the levels, having $\omega_3 > \omega_1$. The CASSCF (9 orbital, 12 electron) calculation regains the relative order while underestimating each frequency.

The usually reliable MBPT(2) method shows its customary agreement for the two symmetric stretch modes in Table 15 but badly exceeds the asymmetric stretch frequency ω_3. MBPT(4) improves on ω_3, but still overestimates its value,

Table 15 Vibrational Frequencies (cm^{-1}) of O_3 at Various Levels of Theory (DZP Basis)[a]

Method	ω_1	ω_2	ω_3
SCF	1547	859	1428
2R-CISD[b]	1234	745	1352
CASSCF[c]	1098	689	989
MBPT(2)	1167	739	2373
MBPT(4)	1123	695	1547
CCSD	1256	748	1240
CCSD + T(CCSD)	1097	685	128i (327)[d]
CCSDT-1	1076	674	680
QCISD(T)[e]	1128	697	934
CCSD(T)[f]	1129	703	976
CCSDT-2[g]	1158	712	1182
CCSDT-3[f]	1149	707	1118
CCSDT[f]	1141	705	1077
Experimental	1135	716	1089

[a] Results from reference 102 except as indicated.
[b] Reference 103.
[c] Reference 104.
[d] A nonimaginary result is obtained in a larger (5s4p2d) basis.
[e] Reference 105.
[f] Reference 106.
[g] Reference 107.

causing the wrong ordering of levels to persist. The infinite-order effects in CCSD correct the ordering and reduce the average error to be below 10%; but when estimates of triple excitations are introduced, the agreement can worsen. The noniterative triples correction CCSD + T(CCSD) even gives an imaginary frequency for ω_3 that would imply that O_3 does not have C_{2v} symmetry! Though not imaginary, the iterative CCSDT-1 method gives an unreasonably low value for ω_3. The CCSD(T) noniterative approximation to CCSDT-1 gives a much better value and the correct order, whereas the QCISD(T) approximation to CCSD(T) is slightly worse. If we add even higher order terms, which would define the iterative model, CCSDT-2, we get relatively good agreement overall, except the order of ω_3 and ω_1 is wrong. CCSDT-3 with still higher order triple contributions is good. Finally, the full CCSDT method gives excellent (too good!) agreement (< 1% error) with experimental harmonic frequencies. CCSDT is an $n^3N^5N_{it}$ procedure, so it is not yet suited to large-scale application. It is, however, the reference point for all other less expensive triple excitation approximations in CC theory, and it is clear from this example that results for difficult cases can hinge on small, usually negligible contributions. Furthermore, we expect that the DZP basis used in this study makes the CCSDT agreement with experiment partly fortuitous. Much larger basis CCSD(T) results increase the frequencies by 23, 31 and 62 cm^{-1},[108] which suggests that CCSDT in a larger basis would overshoot by a like amount.

The primary problem in O_3 seems to be that the asymmetric stretch introduces two singly excited configurations that are forbidden by symmetry from mixing into the symmetric modes.[102] This causes the multireference (nondynamic) character to be worse for asymmetric stretches. Only at very high levels of purely dynamic correlation are all these factors properly handled in O_3.

An example of the removal of the harmonic force constant approximation is a study of the quartic force field for H_2O at various CC, MBPT, and CI levels.[109,110] The energy of 18 vibrational levels are correctly described to within 18 cm^{-1}, and, with an empirical correction, to within 6 cm^{-1} at the CCSDT-1 level.[111]

PHOTOELECTRON SPECTRA

Ionization Potentials

Photoelectron spectra concern energy changes involved in the process

$$h\nu + M(Q) \rightarrow M^+(Q') + e^- + KE(e^-) \qquad [50]$$

where Q indicates the quantum state of M and Q' that for M^+, and $KE(e^-)$ is the kinetic energy of the ejected electron. For N_2 in its ground state $^1\Sigma_g^+(1\sigma_g^2 1\sigma_u^2 2\sigma_g^2 2\sigma_u^2 3\sigma_g^2 1\pi_u^4)$, Eq. [50] might correspond to removing an electron from the $1\pi_u$ orbital, the $3\sigma_g$, or any other. It usually requires X-ray energies to eject electrons from inner shell orbitals, so we usually speak of XPS or ESCA for inner shell ionization and ultraviolet photoelectron spectroscopy, UPS, using less energetic UV photons for the valence shell. The SCF independent particle model readily gives an approximate interpretation of the ionization potential for an electron via *Koopmans' theorem.*[4] This assumes that the state of the ion can be approximated by simply deleting an electron from the relevant orbital in the original SCF solution $|\text{core } 3\sigma_g 3\bar{\sigma}_g 1\pi_{u_x} 1\bar{\pi}_{u_x} 1\pi_{u_y} 1\bar{\pi}_{u_y}|$ to give, for example, either $|\text{core } 3\sigma_g 1\pi_{u_x} 1\bar{\pi}_{u_x} 1\pi_{u_y} 1\bar{\pi}_{u_y}|$ or $|\text{core } 3\sigma_g 3\bar{\sigma}_g 1\pi_{u_x} 1\bar{\pi}_{u_x} 1\pi_{u_y}|$. It is assumed that the orbitals do not change from their form in the neutral species. If we work out the energy expectation values for M and M^+ within this approximation, we find that

$$\bar{E}_M = \sum_{i=1}^{n} \epsilon_i - \sum_{i,j}^{n} \langle ij \| ij \rangle$$

$$\bar{E}_{M+} = \sum_{i=1}^{n-1} \epsilon_i - \sum_{i,j}^{n-1} \langle ij \| ij \rangle \qquad [51]$$

$$E_M - \bar{E}_{M+} = \epsilon_k = -I_p(k)$$

where ϵ_k is the orbital energy associated with orbital k in the canonical SCF approximation,

$$\mathcal{F}(1)\varphi_k(1) = \epsilon_k\varphi_k(1) \qquad [52]$$

This, in fact, gives meaning to the orbital energies of an SCF calculation and is often used as a justification for the MO (instead of valence bond) model of electronic structure.

There are two approximations in interpreting ϵ_i as the negative of an I_p: (1) the MOs for the ion are not allowed to change (i.e., there is no relaxation), and (2) there is no difference in the correlation energies of M and M^+. However, correlation will lower the energy of M relative to M^+, simply because M has one more electron to correlate with all other electrons. As a result, correlation effects will tend to increase the ionization potential. On the other hand, admitting orbital relaxation will tend to lower the energy of M^+ relative to M, diminishing the I_p. In many cases these two factors fortuitously cancel for valence electrons, with Koopmans' theorem offering a reasonably good measure of the actual I_p. However, for other cases this is untrue, and N_2 is a well-known example. From Table 16 we see that Koopmans' theorem gives the wrong order, as the lowest I_p experimentally corresponds to ionization from the $3\sigma_g$ orbital instead of the $1\pi_u$ highest occupied molecular orbital (HOMO).

For core ionization the approximate cancellation that makes Koopmans' theorem work clearly does not apply because ejecting an electron from the core causes a much greater degree of orbital relaxation error. The effect of a core electron is to decrease the effective nuclear charge (via screening) by one unit. This causes large changes in the M^+ MOs. Furthermore, correlation effects are dominated by the valence electrons. The appropriate solution for SCF treatments of core ionization requires separate SCF calculations for M and M^+, which is called ΔE_{SCF}. Such values are shown in the RHF-UHF column in Table 16. Though there is no correlation in either calculation, the core relaxation effect accounts for an enormous improvement (7.34 eV). For the valence ionizations, though, this is not as pronounced, although the results are improved over

Table 16 SCF Vertical Ionization Potentials (eV) of N_2 (5s4p1d Basis)[a,b]

Leading configuration	RHF-UHF ΔE_{SCF}	RHF-QRHF (Koopmans)	RHF-ROHF ΔE_{SCF}	Experimental
$3\sigma_g^{-1}$	15.69	17.27	15.96	15.5
$1\pi_u^{-1}$	15.34	16.78	15.42	16.8
$2\sigma_u^{-1}$	19.95	21.12	20.15	18.6
$1\sigma_g^{-1}$	419.46	426.80		409.9

[a] RHF-UHF refers to a calculation for which the ground state calculation is based on an RHF reference and the ionic state calculations on a UHF reference. RHF-QRHF indicates that the ionic calculations are based on a QRHF reference (i.e., the orbitals for the ion are the same as the neutral), and RHF-ROHF indicates that they are based on an open-shell RHF reference function.
[b] Reference 112.

Koopmans' theorem. However, the order of the ΔE_{SCF} level is still erroneous. (Much better results are offered if the core ionized state is described by a broken symmetry SCF solution that corresponds to an "atomic" 1s-type core hole, rather than ejection from the $1\sigma_g$ MO.)

To improve on both SCF approximations, correlation is essential. Such results are shown in Table 17. Note that correlation effects amount to more than 1 eV for the valence ionizations, which also corrects the order, while the effect on the core ionization is about 8 eV.

The simplest way to introduce correlation into ionization potentials is to compute $E(M)$ and $E(M^+)$ with some correlated method. (For a molecule, if the energy difference is computed at the geometry of M, we obtain vertical ionization energies; or if we allow M^+ to relax to its optimum geometry before evaluating its energy, we get adiabatic ionization energies where zero-point vibrational energy differences are ignored.) Provided the correlated method is applicable to open and closed shells, this approach has the advantage that nothing new is required to calculate ionization ionization potentials beyond that needed to evaluate energies. Because such routine, widely applicable methods are usually built on a single determinant, independent particle reference, this is usually possible for the lowest (i.e., HOMO) ionization potential of closed-shell neutral molecules, or, in fact, for any ionization from a closed-shell system where the electron is ejected from the highest orbital of a particular symmetry.

In our N_2 example, energies corresponding to ionization from the $1\pi_u$, $3\sigma_g$, or $2\sigma_u$ orbitals can readily be obtained by such an approach. The reason is that the independent particle Hartree–Fock solution for the ion, whether it is UHF or ROHF, is readily converged to such states and correlated calculations can be carried out straightforwardly. Such results for N_2 are shown in Table 17. However, it is more difficult to describe an ionized state where the electron has been ionized from an orbital of the same symmetry like the $2\sigma_g$ (or $1\sigma_g$) that is lower in energy than another, as shown in Figure 13. The reason is that it is more difficult to converge a "hole" state of the ion. Remember, Hartree–Fock methods are intended to provide the lowest possible energy for a single determinant, independent particle wavefunction. That is obtained when the SCF

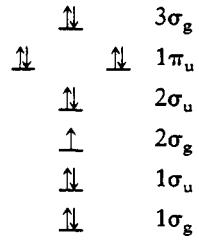

Figure 13 Orbital diagram of N_2.

Table 17 Correlated Vertical Ionization Potentials (eV) of N_2 (5s4p1d Basis)[a]

Leading configuration	RHF-UHF			RHF-QRHF			RHF-ROHF		Experimental
	CCD	CCSD	CCSDT-1	CCD	CCSD	CCSDT-1	CCSD	CCSDT-1	
$3\sigma_g^{-1}$	15.54	15.44	15.29	17.08	15.39	15.36	15.46	15.29	15.5
$1\pi_u^{-1}$	16.72	16.72	16.85	18.24	16.69	16.87	16.72	16.85	16.8
$2\sigma_u^{-1}$	18.88	18.78	18.50	20.24	18.71	18.57	18.80	18.50	18.6
$1\sigma_g^{-1}$		411.43	410.93		411.07	411.29			409.9

[a]Reference 112.

procedure interchanges orbitals $3\sigma_g$ and $2\sigma_g$, to give the $2\sigma_g^2 3\sigma_g^1$ occupancy instead, but that is just the HOMO ionized state. If this happens, we do not have an appropriate reference function to study the second ionization.

Certain algorithms can sometimes be used to force convergence to this hole state (that is how the $1\sigma_g^{-1}$ level is obtained in Tables 16 and 17), but it would be better to avoid the SCF hole state calculation altogether. In particular, it is conceptually and operationally appealing if all ionized states are described in terms of the same set of reference orbitals, namely those for the neutral, while occupying them as needed for the various possible principal ionizations. This means that we will describe the $2\sigma_g$ ionization in our example by $|\text{core}\ 2\sigma_g 2\sigma_u^2 3\sigma_g^2 1\pi_u^4|$ which we call a quasi-RHF, or QRHF wavefunction, because this is clearly not the energetically optimum determinant. This choice follows the spirit of Koopmans' theorem and does not allow the ionized state orbitals to relax.

Yet, we pointed out earlier that neglect of relaxation effects causes important errors. How do we resolve the apparent dilemma? CCSD gives us a solution. The role of $\exp(T_1)$ in CCSD and further generalizations of CCSD like CCSD(T), CCSDT-1, and CCSDT is to permit orbital rotations. That means, if we operate on a single determinant Φ_0 composed of orbitals $\varphi_1\varphi_2 \cdots \varphi_n$ we can form any other Φ_0' composed of orbitals $\varphi_1'\varphi_2' \cdots \varphi_n'$ with $\exp(T_1)\Phi_0 = \Phi_0'$. [Any Φ_0' can be obtained from Φ_0 via the action of $\exp(T_1)$, provided Φ_0' and Φ_0 are not orthogonal. This is known as the Thouless theorem.] Because the relaxed and unrelaxed orbitals are related by such an orbital rotation, we have (for CCSD),

$$\exp(T_2)\exp(T_1)\Phi_0 = \exp(T_2)\Phi_0' \qquad [53]$$

Though we never explicitly obtain Φ_0' (it could actually be constructed from the T_1 coefficients), most of the relaxation and correlation effects are introduced by solving the CCSD equations. The coupling between relaxation and correlation is incomplete until all possible excitations (i.e., those due to T_3, T_4, . . .) are also included. But CCSD is usually adequate because most correlation effects are found at just the T_2 level. This is apparent from Table 17. The difference between using the QRHF reference[112] (which is a spin eigenfunction) and the fully relaxed (but spin-contaminated) UHF reference for the ion is 0.03 to 0.07 eV for the valence levels. Even for the core, which is most sensitive to relaxation, the difference of 0.36 eV amounts to less than 0.1%!

It should be remarked that the CISD method does not share this property. The reason is that the exponential form of T_1 is critical in describing orbital rotations. Approximating $\exp(T_1)$ by $1 + T_1 = 1 + C_1$, which would be the CI form for single excitations, provides only a small part of the net effect because CI is linear and terms that are nonlinear in T_1 appear as parts of C_2, C_3, . . . , in CI approaches. Also, there is less coupling through the higher excitations because CISD, for example, would not include the T_1T_2 triple and T_2^2 quadruple excitation terms of CCSD. Similarly, no conventional finite-order perturba-

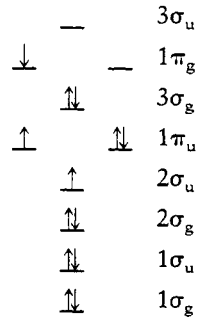

Figure 14 Example of a shake-up ionization for N_2.

tion method (even fourth-order) has a similar degree of invariance, because it is the infinite-order aspect of CC theory that is critical here. After T_2, the most important contributions come from T_3. In the N_2 example, its effect can range up to 0.5 eV. For highly accurate work, T_3 should be included and the basis should incorporate multiple polarization functions.

Before discussing even more sophisticated photoionization correlated methods, we need to mention another area in which correlation is important, namely the "shake-up" processes.[113] A shake-up ionization means that electrons are excited (or de-excited) while another is ejected, as shown in Figure 14. As the energy relative to the ground state M^+ species is changed because of excitation upon ejection of the electron, such states typically appear as satellites on the principal photoelectron peak. In a favorable case, their intensity can be comparable to that for a primary ionization. In principle, there are an infinite number of such shake-ups which correspond to each primary ionization, but only a few will be intense enough to be observable.

In the simplest unrelaxed orbital independent particle model, the energy of this particular shake-up ionization I_s (Figure 14) would be approximated by

$$I_s \approx -[\epsilon_{2\sigma_u} + \Delta E(N_2^+; \pi_u \rightarrow \pi_g)] \qquad [54]$$

where the energy required to excite an electron from the $1\pi_u$ orbital to the $1\pi_g$ orbital in the simplest model is $\Delta E = \epsilon_{1\pi_g} - \epsilon_{1\pi_u} + \langle 1\pi_g 1\pi_u \| 1\pi_g 1\pi_u \rangle$ (see later). Such a description is much less satisfactory than for principal ionizations. First, the importance of correlation is likely to be greater because there will be correlation corrections for both the excitation and the ionization process. Second, the final state for a shake-up process can involve two or more important determinants in its description. In this example, the final state corresponds to a $^2\Sigma_g$ state, but this state requires the combination of determinants that correspond to the three spatial orbitals, $1\pi_g 1\pi_u 2\sigma_u$ with $\alpha\beta\alpha$, $\beta\alpha\alpha$, $\alpha\beta\beta$, and $\beta\alpha\beta$ spins to be a proper spin eigenfunction. Furthermore, there are independent combinations that can strongly mix, causing a splitting of the shake-up state energy and making it lower than that given by the single spin combination. Hence, the single determinant description of the final state is entirely lost

as a result of final state spin symmetry considerations. The correlated wavefunction, on the other hand, can in principle introduce all such determinants, thereby permitting the proper spin-adapted combination to be constructed.

A further inadequacy of the independent particle model pertains to another kind of mixing between configurations. For example, if we ionize the $2\sigma_u$ electron and then excite a $3\sigma_g$ electron to the $3\sigma_u$ orbital, we have a second spin-adapted configuration of the same symmetry as that involving the prior $1\pi_u$-to-$1\pi_g$ excitation, which should have a comparable energy. In the absence of other restrictions, it is likely that these two configurations will strongly mix in the final state wavefunction. If so, any attempt to describe the final state as a single electron excitation is doomed to fail. Clearly, correlation is a critical component of the description of shake-up ionization processes. In the particular case discussed above, the equation-of-motion method (discussed later) gives a shake-up frequency of 30.2 eV compared to the experimental value of 30.0 eV. Obviously, we can also identify shake-ups by computing the electronic excitations for the ion using the tools for predicting electronic spectra.

The next step in the evolution of methods for photoelectron spectra is to avoid making separate calculations for the neutral species and the various possible ions. By so doing, we take advantage of certain elements of the problem that are common for each species. To do this we will use some simple operator concepts that lead us to such a set of equations.

Define R_k as an operator whose action is to create from the neutral (n electron) molecule ground state wavefunction $\Psi_0(n)$ the kth ionized state, which has $n - 1$ electrons,

$$R_k\Psi_0(n) = \Psi_0(n - 1) \qquad [55]$$

(We actually have a plane-wave continuum type orbital for the outgoing electron with energy KE that preserves the number of electrons, but we need not worry about this explicitly. This fact facilitates the commutation implicit in Eq. [59], however.) Since $\Psi_0(n)$ is a solution of the Schrödinger equation for n particles, and $\Psi_k(n - 1)$ the solution for $n - 1$ particles, we have

$$H\Psi_0 = E_0\Psi_0 \qquad [56a]$$

$$H\,R_k\Psi_0 = E_kR_k\Psi_0 \qquad [56b]$$

Multiplying Eq. [56a] by R_k, and subtracting from Eq. [56b], we then obtain

$$(H\,R_k - R_kH)\Psi_0 = I_k\Psi_0 \qquad [57]$$

where $I_k = E_k(n - 1) - E_0(n)$. In this theory, the correlated $n - 1$ electron states are described by linear combinations of single, double, etc., excitations of the $n - 1$ electron determinants starting with $\Phi_k = \mathcal{A}\,(\varphi_1(1) \cdots \varphi_{k-1}(k - 1)\,\varphi_{k+1}(k) \cdots \varphi_{n-1}(n - 1))$, made up of neutral orbitals:

$$R_k\Phi_0 = \Phi_k + \sum_{i,a} r_i^a \Phi_i^a + \sum_{\substack{i<j \\ a<b}} r_{ij}^{ab} \Phi_{ij}^{ab} + \ldots \qquad [58]$$

The objective is to determine r_i^a, r_{ij}^{ab}, etc. Now, if we choose $\Psi_0 = \exp(T)\Phi_0$, and carry out some manipulations, it may be shown that Eq. [57] can be written as

$$\bar{H}\, R_k\Phi_0 = I_k R_k \Phi_0 \qquad [59]$$

where $\bar{H} = e^{-T}\, He^T$ and $R_k\bar{H}$ turns out to vanish. Just as in ordinary CC theory, the coefficients $r_i^a, r_{ij}^{ab}, \ldots$ are determined from successive projections on single and double excitations,

$$\bar{H}\mathrm{r}_k = \mathrm{r}_k I_k \qquad [60]$$

and we have for all n ionized (and shake-up) states the equation

$$\bar{H}\mathbf{R} = \mathbf{R}\mathbf{I} \qquad [61]$$

where I is the diagonal matrix of the n ionization (and shake-up) values, and

$$\mathbf{R} = (\mathrm{r}_1, \mathrm{r}_2, \ldots, \mathrm{r}_n) \qquad [62]$$

We call this the equation-of-motion coupled cluster (EOM-CC) method.[114-116] EOM-CC results are shown in Tables 18 and 19 for CH_2PH.[117]

For principal ionization potentials, EOM-CC is equivalent to a multireference approach referred to as the Fock space multireference coupled-cluster method (FS-MRCC);[27-30] both terminologies are used. Unlike the Fock space approach, EOM-CC computational strategies also provide a way to readily obtain "shake-up" eigenvalues. Comparison of FS-MRCCSD and EOM-CCSD results with ΔE_{MBPT} and ΔE_{CC} results for CH_2PH shows excellent agreement. Results as a function of basis show improved convergence for the $5a'$ level. The effect of triples as measured by the noniterative $T^*(3)$[118] is not too great.

To demonstrate results for an open-shell system, Table 20 reports results for O_2.[30] Intensities can also be obtained by considering the left eigenvector of the (non-Hermitian) operator $\bar{H}$, along with R_k, and such EOM-CC examples are shown for electronic excited states later.

Electron Affinities

Electron photodetachment experiments are not fundamentally different from photoionization; electrons are just ejected from an anion. Consequently, computing the energy for attaching an electron to a molecule $M + e^- \rightarrow M^-$

Table 18 Valence Ionization Potentials (eV) of CH_2PH Using Various Correlated Methods (DZP Basis)[a]

Orbital	MBPT(4)	CCSD	CCSDT-1	QRHF-CCSD	QRHF-CCSDT-1	EOM-CCSD	EOM-CCSD+T*(3)[b]
$1a''$	10.05	9.91	10.03	9.90	10.05	10.07	9.98
$5a'$	10.64	10.24	10.25	10.22	10.24	10.29	10.28
$4a'$				13.15	13.15	13.18	13.19
$3a'$				15.15		15.13	15.27

[a]Reference 117.
[b]Noniterative triple excitation correction. Reference 118.

Table 19 EOM-CCSD Ionization Potentials (eV) for CH_2PH as a Function of Basis Set[a]

	EOM-CCSD			
Orbital	DZ	DZP	TZP	Experimental
$1a''$	10.18	10.07	10.08	10.30
$5a'$	9.82	10.29	10.27	10.70
$4a'$	13.14	13.18	13.19	13.20
$3a'$	15.08	15.13	15.16	15.00

[a]Reference 117.

(the electron affinity, or E_A) poses many of the same methodological problems as the photoionization studies. Koopmans' theorem, ΔSCF, ΔE_{MBPT}, ΔE_{CC}, QRHF-CC or EOM-CC are all formally applicable; except that we require a description of the anion instead of the cation. There are two principal factors that make such studies more difficult:

1. An anion M^- requires a more extensive atomic basis set.
2. The extra electron in M^- introduces additional electron correlation effects.

In particular, this latter consideration makes the Koopmans estimate of E_A far worse than its estimate of a valence *I*p.

Depending on the system, the extra electron will occupy (in the independent particle description) either a partly empty valence orbital, an antibonding valence orbital, or a Rydberg orbital. In the latter two cases, a basis set chosen to describe the neutral will tend to favor M over M^-, causing E_A to be underestimated. Similarly, the additional correlation effects in M^- will tend to be underestimated at a given truncation of the FCI because higher excitation contributions will be more important. Consequently, computed E_A values are generally too small, although no rigorous bounds govern this behavior.

As an illustration consider :C=C=C=C: which is a triplet ($^3\Sigma_g^-$) with a π HOMO occupied by two electrons of parallel spin. Table 21 displays results obtained with several different levels of correlation and basis sets.[119] There are actually three different quantities that can be computed: the vertical electron detachment energy (VEDE, energy to eject electron at the geometry of the anion); the adiabatic electron affinity (AEA, when the neutral M is allowed to relax to its optimum geometry), and the vertical electron affinity (VEA, where the geometry of the neutral is assumed for the anion).

Three different experimental electron affinity values have been reported for C_4 (3.7, 3.88, and 3.79 eV). Exactly which measure of EA is being sampled is debatable, but it appears to be closest to AEA. The higher precision value of 3.88 eV would appear to offer the best comparison. Allowing for a correction of ~0.15 eV from VEDE values as obtained in the PVTZ UHF-CCSD(T) results, the larger, more diffuse basis values cluster near 3.8 eV for this quantity.

Table 20 Ionization Potentials of O_2 ($^3\Sigma_g^-$)[a]

Basis set	O_2^+			
	$^2\Pi_g$	$^4\Pi_u$	$^4\Sigma_g^-$	$^4\Sigma_u^-$
DZP	11.76	16.40	17.75	24.15
PVTZ	12.16	16.74	18.12	24.55
PVTZ++[b]	12.24	16.80	18.21	24.63
PVQZ[b]	12.34	16.90	18.31	24.71
PVQZ++[b]	12.37 (12.39)[c]	16.93 (16.76)[c]	18.34 (18.26)[c]	24.74 (24.82)[c]
Exp (vertical I_p's)[d]	12.35	16.85	18.33	24.66

[a] Reference 30.
[b] Augmented with two diffuse s and p functions.
[c] Value obtained by ΔE_{CCSD} results using UHF references for neutral and ion.
[d] Estimated vertical I_ps are extracted from adiabatic experimental values.

Table 21 Calculated Electron Affinities and Electron Detachment Energies (eV) of Linear C_4 and C_4^-[a]

Basis set	Method	VEA	AEA	VEDE
5s4p1d	UHF-CCSD	3.30		3.57
5s4p1d	UHF-CCSD+T(CCSD)	3.39		3.62
PVTZ	UHF-MBPT(2)	3.982	4.074	4.170
PVTZ	UHF-CCSD	3.482	3.628	3.779
PVTZ	ROHF-MBPT(2)	3.561	3.660	3.764
PVTZ	ROHF-CCSD	3.525	3.669	3.817
PVTZ	UHF-MBPT(2)	3.924	4.020	4.155
PVTZ	UHF-CCSD	3.442	3.579	3.738
PVTZ	UHF-CCSD+T(CCSD)	3.553	3.647	3.807
PVTZ	UHF-CCSD(T)	3.555	3.654	3.812
PVTZ+sp	UHF-MBPT(2)			4.288
PVTZ+sp	UHF-CCSD			3.852
PVTZ+sp	UHF-CCSD+T(CCSD)			3.933
PVTZ+sp	UHF-CCSD(T)			3.937
5s4p2d1f	UHF-CCSD			3.775
5s4p2d1f	UHF-CCSD+T(CCSD)			3.855
5s4p2d1f	UHF-CCSD(T)			3.860

[a]Reference 119.

In addition to the basis, the very important effect of triple excitations for obtaining highly accurate answers is apparent from this set of calculations.

Just as a spectrum of different ionizations is commonly observed, several bound electron attached states may exist. This can happen for a cation like MgF^+ because of the net positive charge. In an independent particle picture, different empty orbitals (see Figure 15) can be occupied at different E_{A_i} to give the corresponding electronic states of the neutral (see Table 22). These are the same states that could be obtained via electronic excitations of the neutral, but they also can be approached as an electron attachment problem using either EOM-CC or FS-MRCC. An electron adding to the 7σ orbital gives the $X^2\Sigma^+$ state of MgF; adding one to the 3π orbital gives the $A^2\Pi$ state, and adding one to the 8σ and 9σ orbitals provides the B and $C^2\Sigma^+$ states, respectively.

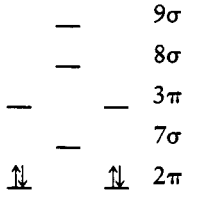

Figure 15 Orbital diagram of $MgF^+(1\sigma^2 2\sigma^2 3\sigma^2 1\pi^4 4\sigma^2 5\sigma^2 6\sigma^2 2\pi^4)$.

Table 22 Electronic Transition Energies (cm^{-1}) of MgF^+

	$A^2\Pi \leftarrow X^2\Sigma^+$	$B^2\Sigma^+ \leftarrow X^2\Sigma^+$	$C^2\Sigma^+ \leftarrow X^2\Sigma^+$
FSMRCCSD[a]	29,312.4		
QRHF-CCSD[a]	29,378.7		
FSMRCCSD[b]	27,851.2	37,831.4	45,537.5
Experimental	27,852.5	37,187.4	42.589.6

[a]Mg: 6-31G*, F: DZP, total: 35 Gaussian-type orbitals (GTOs).
[b]Mg: (12s9p12d/8s6p4d), F: (10s7p5d/6s5p4d), total: 95 GTOs.

ELECTRONIC SPECTRA

In electronic spectroscopy, processes that involve transitions between two distinct electronic states in atoms and molecules are studied. The energy typically required for these processes falls in the ultraviolet or visible range of the electromagnetic spectrum; the field is therefore also frequently called ultraviolet/visible (or UV/vis) spectroscopy. Due to availability of the requisite technology, this is the oldest branch of chemical spectroscopy and has been of interest to quantum chemists since the late 1920s. Indeed, many of the early successes of Mulliken's molecular orbital theory involved qualitative interpretations of electronic spectra. The advent of the Hückel molecular orbital treatment in the 1930s made semiquantitative calculations for conjugated organic molecules possible for the first time.[120] Two decades later, the semiempirical crystal field model was developed and applied with great success to calculate electronic energy levels in transition metal complexes.

Much of our qualitative understanding of electronic transitions and the language we use to describe them ultimately derives from the independent particle approximation. Typically, we interpret features in absorption spectra as "$n \rightarrow \pi^*$" or "$\sigma \rightarrow \sigma^*$" transitions, etc., in an attempt to describe these processes in terms of the simplest molecular orbital picture. However, we should be aware that the molecular orbital paradigm is approximate and that the actual excitation process is more complex. Within the Born–Oppenheimer approximation, the interaction between specific wavelengths of UV or visible radiation and molecules leads to transitions between quantum states that "belong" to two separate potential energy surfaces. In general, the absorption of a photon takes a state characterized by distinct electronic, vibrational, and rotational quantum numbers to another state having another set of quantum numbers. The energy required for transitions between different electronic states is typically much larger than spacings between vibrational and rotational states, so typically observed low resolution spectra are often characterized by blobs that grossly represent the electronic part of the transition, with the underlying vibrational and rotational features unresolved. Nevertheless, spectra having sufficiently good resolution often show vibrational and rotational "fine struc-

ture," with transitions between individual states visible within the absorption envelope. (The modern techniques of supersonic jet expansion and laser spectroscopy allow very high resolution spectra to be obtained, even for relatively large organic molecules.) These features are often useful for determining differences in equilibrium geometry between the ground and excited states of the molecule and other properties. Our objective here is to survey some methods that can be used to calculate energy differences between the adiabatic potential energy surfaces obtainable from quantum chemical calculations.

As in our discussion of photoelectron spectroscopy, a simple and conceptually appealing description of the excitation process can be developed as follows. We will assume that the molecular orbital picture is a valid first-order approximation and that the radiation field causes a single electron to be promoted from the occupied spin orbital i to orbital a, which is not occupied in the ground electronic state. Furthermore, in this simplest model we further require that the molecular orbitals in the ground and excited states must be the same. This treatment, which is based on a one-electron picture that neglects orbital relaxation effects, is the direct analog of Koopmans' theorem but for excitation processes. Evaluating the excited state expectation value for the single excitation Φ_i^a and for the Hartree–Fock ground state Φ_0, we obtain after some simplification,

$$\Delta E = \langle \Phi_i^a | H | \Phi_i^a \rangle - \langle \Phi_0 | H | \Phi_0 \rangle = \epsilon_a - \epsilon_i + \langle ai \| ai \rangle \qquad [63]$$

Note that unlike the simple Hückel method, this SCF-based approach does not predict that the excitation energy is given by a difference of orbital eigenvalues. Rather, this model allows for a certain amount of interaction between electrons and correctly predicts unequal energies for configurations that differ only in the spin of unpaired electrons. In the case that the ground state is a closed-shell singlet, this model predicts singlet and triplet excitation energies of

$$\Delta E_{\text{singlet}} = \epsilon_a - \epsilon_i + \langle ai | ai \rangle = \epsilon_a - \epsilon_i + (aa|ii) \qquad [64]$$

and

$$\Delta E_{\text{triplet}} = \epsilon_a - \epsilon_i + \langle ai | ai \rangle - \langle ai | ia \rangle = \epsilon_a - \epsilon_i + (aa|ii) - (ai|ai) \qquad [65]$$

The last terms of Eqs. [64] and [65] use the familiar Mulliken two-electron integral notation. Note that the singlet–triplet splitting predicted by this simplest model is given by the exchange integral between orbitals a and i. Since this term is always positive, the simple model presented here predicts that the triplet state is more stable, thereby providing a simple physical justification for Hund's rule.

Although the model described above may be qualitatively appealing, it

does not provide quantitatively satisfactory predictions of excitation energies even though the analogous Koopmans approximation works reasonably well for ionization potentials. Why should this be? The principal difference between the Koopmans approximation for ionization potentials and the present treatment of excitation energies is that the latter explicitly involves unoccupied SCF orbitals. This is the main problem with these calculations, inasmuch as the SCF procedure does not optimize the virtual orbitals and the frozen orbital approximation fails.

It is natural to ask whether a better theoretical approach to excitation processes exists, which does not discard the intuitively attractive one-electron picture. Indeed, such a method was invented nearly a half-century ago and is known as the Tamm–Dancoff approximation (TDA) or CI singles (i.e., CIS).[121] In this approach, the excited state is approximated by a linear combination of elementary frozen-orbital single excitations. TDA exploits a standard CI procedure. First, we take the set of single excitations and construct $\langle S|H|S\rangle = \mathbf{H}_{ss}$ and solve $\mathbf{H}_{ss}\mathbf{C}_k = \mathbf{C}_k E_k$. The eigenvalues of this matrix, E_k, represent the eigenvalues of the Schrödinger equation for excited states subject to the restrictions defined by the model, and the eigenvectors are the associated wavefunctions. The excitation energy is $E_k - E_{SCF}$, because single excitations do not mix with the UHF or RHF solution, Φ_0; the ground state energy is $E_0 = E_{SCF}$. In some respects, the term CIS is unfortunate because it suggests a method that offers some treatment of electron correlation effects. In fact, the terms "CI" and "electron correlation" are so often used interchangeably in the literature that it may be difficult to understand that a method called CIS completely neglects electron correlation! Hereafter, we will refer to this method as the TDA, with the understanding that is equivalent to CIS. (Both the ACES II and GAUSSIAN program systems have capabilities for performing TDA calculations.)

The discussion of orbital relaxation in the preceding section provides us with a clear way of understanding the shortcomings of the TDA. Recall that any Slater determinant formed from a particular set of basis functions may be obtained from any other Slater determinant that lies in the same basis by means of the exponential transformation

$$|\Phi'\rangle = \exp(T_1)|\Phi_0\rangle \qquad [66]$$

Let us now assume that the excited state wavefunction is given exactly by some Slater determinant. It should be clear that the TDA does not contain sufficient flexibility to describe this state in the general case because the excited state wavefunctions in this approximation are given by a linear combination of singly excited determinants

$$|\Phi_{excited}^{TDA}\rangle = \hat{C}_1|\Phi_0\rangle \qquad [67]$$

The flexibility missing from the TDA arises from its neglect of nonlinear terms in the exponential operator of Eq. [66], which would lead to the inclusion of very specific types of determinants "doubly," "triply" excited, etc., into the parameterization of the single determinant $|\Phi'\rangle$. It is very important to understand that $|\Phi'\rangle$ is still a single configuration wavefunction and that this inclusion of more highly excited determinants therefore is not an electron correlation effect. [This discussion is somewhat oversimplified for excited states that correspond to low spin electron configurations, such as open-shell singlets. In these cases, the "simplest" excited state wavefunction that retains the property of being a spin eigenfunction is $|\Phi_{\text{excited}}\rangle = 1/\sqrt{2}[\phi^{\alpha}_{i\to a} + \phi^{\beta}_{i\to a}]$, where $\phi^{\alpha}_{i\to a}$ and $\phi^{\beta}_{i\to b}$ are Slater determinants differing only in the spin of the excited electron. Within the Thouless parameterization, these determinants may be written as $\exp(T^{\alpha}_1)|\Phi_0\rangle$ and $\exp(T^{\beta}_1)|\Phi_0\rangle$, respectively. Nevertheless, the resulting excited state wavefunction corresponds to a single electronic configuration and contains no correlation.] After one understands the considerations above, it can be seen that the first way to improve the TDA is to extend its flexibility through a better treatment of the $\exp(T_1)$ operator. These effects are included, albeit in an approximate and somewhat indirect way, in what is called the *random phase approximation* (RPA).[121] [Again, to satisfy requirements of spin symmetry, we take $\exp(T_1)$ to be $\exp(T^{\alpha}_1 + T^{\beta}_1) = \exp(T^{\alpha}_1)\exp(T^{\beta}_1)$ in the following.]

We can derive this method in a nonstandard way[32] by considering the energy associated with $\Phi' = \exp(T_1)\Phi_0$, that is,

$$E = \frac{\langle\Phi'|H|\Phi'\rangle}{\langle\Phi'|\Phi'\rangle} = \frac{\langle\Phi|\exp(T_1^{\dagger})H\exp(T_1)|\Phi\rangle}{\langle\Phi|\exp(T_1^{\dagger})\exp(T_1)|\Phi\rangle}$$

and vary the energy with respect to $T_1^{\dagger}$, which leads us to the matrix equation that depends on the $\mathbf{H}_{ss}$ matrix, that is, the A matrix of RPA augmented by the B matrix ($\langle\Phi|H\hat{T}_1^2/2|\Phi\rangle$) that derives from quadratic T_1 terms. This alternative approach to the calculation of excitation energies allows for some effects of selected doubly excited configurations, and the RPA method is therefore somewhat more flexible than the TDA. It is often stated in the literature that the RPA method (which is equivalent to the time-dependent Hartree–Fock approximation) reduces to the coupled–perturbed Hartree–Fock approximation in the static case and contains electron correlation effects, but this is certainly untrue unless one adopts a nonstandard view of what is meant by correlation.

Excitation energies calculated with the RPA and TDA approaches for N_2 with a moderately large basis set are listed in Table 23. Both the RPA and TDA excitation energies are significantly lower than those obtained with the simplest frozen orbital approximation. All these approaches differ only in their treatment of the final state, and the pattern of predicted excitation energies shows this in a rather dramatic way. Both the RPA and TDA allow for a limited amount of relaxation and provide much improved predictions. Inclusion of the

Table 23 Excitation Energies for N_2 (5s3p1d Basis)

	Excitation energies (eV)		
Final state	TDA	RPA	Experimental
$a'^1\Sigma_u^-$	8.50	7.93	9.9
$\omega^1\Delta_u$	9.08	8.80	10.3
$a^1\Pi_g$	9.99	9.74	9.3
$b'^1\Sigma_u^+$	15.78	15.48	14.4

special "double" excitation effects discussed above in the RPA is reflected in a systematic lowering of the predicted excitation energies relative to the TDA.

Before concluding this discussion of the TDA and RPA approaches, one problem occasionally encountered in RPA calculations of excitation energies relative to a closed-shell ground state should be discussed. Within the RPA, excitation energies are intimately related to the dependence of the energy with respect to infinitesimal changes in the molecular orbitals. In some cases, Hartree–Fock solutions are "unstable," meaning that a small change in the orbitals results in a lowering of the electronic energy. Most frequently, the change that lowers the energy involves a breaking of the spin symmetry of α and β orbitals. Hence, the determinant is transformed from an RHF to a UHF wavefunction. The UHF energy is always lower than or equal to the RHF result because spin symmetry can be relaxed. If lower energy UHF solutions exist, we say the RHF is unstable. When this occurs, the RPA fails and predicts imaginary excitation energies for transitions to triplet excited states. The subject of Hartree–Fock instabilities is rather complicated and takes us too far afield from our discussion, but suffice it to say that these phenomena tend to occur in systems that are poorly described by a single determinant. Hence, in cases that should be suitable for the RPA (both ground and excited states are well represented by a single configuration), these pathological problems will not occur. However, this sort of instability is actually encountered fairly often; a simple example is C_2H_4. It should be expected to occur in any closed-shell system for which one can draw reasonable Lewis dot structures with two unpaired electrons such as for ozone (Figure 16). Molecules that fall into this category are frequently called *biradicals*. The nature of these systems and the problems associated with their theoretical description form an interesting subject, which is not discussed here.

A second type of instability is known as a "singlet" instability, which

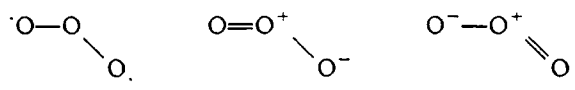

Figure 16 Resonance in ozone.

means that the SCF energy can be lowered by an in-phase rotation of α and β spin orbitals (i.e., there is a lower energy single determinant that is still a closed-shell singlet). This type of instability is not very common and is usually encountered only in exotic systems such as N_2 at very large internuclear separations and the anion O_2^{2-}. Fortunately, one is usually more interested in singlet excitation energies, and the scarcity of cases exhibiting this type of instability means that the RPA can usually be used for such studies.

When it is possible to describe an excited state by a single configuration wavefunction, the "best" uncorrelated approach would be via separate evaluation of SCF wavefunctions for both the ground and excited states. Subtraction of the resulting energies gives us excitation energies in a ΔE_{SCF} treatment analogous to that discussed previously for ionization potentials. However, the ΔE_{SCF} approach to excited states has a number of undesirable features that severely limit its applicability. First, most excited states cannot be adequately approximated by any single determinant (many are open-shell singlets), and one must resort to low spin ROHF approaches, which can be difficult to converge. Second, as in the case of ionization potentials, one encounters the problem of variational collapse. In fact, this represents even a greater problem in excitation energies than it does in the determination of ionization potentials because in the latter case we can at least determine the lowest ionization potential in this manner. In general, the same is not true for excitation energies. Consider a molecule with no elements of symmetry, such as FOOH. In such a case, it may not be possible to routinely obtain SCF solutions for any state other than the electronic ground state, prohibiting any attempt to calculate ΔE_{SCF} excitation energies.

Another desirable aspect of using the TDA and RPA approaches is that they both use a common set of molecular orbitals, which aids both in developing qualitative interpretations of the excitation process and also in calculating properties such as transition moments. The latter depends on $|\langle\psi_i|\mathbf{r}|\psi_f\rangle|^2$, where $\mathbf{r} = \Sigma_j \mathbf{r}_j$ is the dipole operator. It is easy to evaluate such a one-electron property provided ψ_i and ψ_f are described in terms of the same orthonormal orbital set. When different orbitals are used in ψ_i and ψ_f—typically to get the "best" possible solution for both states—the resultant nonorthogonality causes a number of complications. This is particularly true when an entire spectrum of electronic states is the objective and all transition moments are required. Nevertheless, all the methods discussed so far neglect electron correlation effects, and one must go beyond the single configuration approximation if quantitative accuracy is to be achieved.

Conceptually, one of the simplest ways to study excited states at the correlated level of theory is by means of ΔE methods, in which E is obtained with some post-HF method. While the problems of variational collapse discussed above severely complicate efforts to calculate excitation energies by ΔSCF methods, it is actually straightforward to obtain ΔCI excitation energies, provided the same reference function is used for both states. In this case, the

orbitals are usually optimized for the ground state. Correlated energies are then obtained by diagonalization of the Hamiltonian matrix in the basis of the reference determinant and some suitable subset of excited configurations. In this way, wavefunctions for the ground and excited states as well as excitation energies are easily obtained. Despite the conceptual simplicity of this approach, it is not often used in practice. Why is this? Once again, considerations of orbital relaxation come into play. Remember that all the CI wavefunctions are based on a common reference state, Φ_0, for each k, and that the orbitals making up Φ_0 are typically optimized for the ground state. Since computational considerations limit practical ΔCI approaches to the CISD approximation, insufficient orbital relaxation is included, and therefore the excited state is not described as well as the ground state. As a result of the unbalanced nature of the approach, ΔCISD excitation energies typically overestimate excitation energies; especially large differences can be expected to occur when the best one-electron descriptions (natural orbitals) for the ground and excited states are very different. In fact, TDA and RPA calculations are usually preferable to ΔCI because these approaches offer a more balanced description of the ground and excited states.

The "orbital problem" associated with ΔCI calculations can be circumvented by a number of means. First, modern developments in MCSCF orbital optimization strategies have made obtaining MCSCF solutions for both ground and excited states a fairly routine matter. In some calculations, the orbitals are indeed optimized for each state of interest, and the ground and excited states are treated in an even-handed way. Dynamic correlation can then be included by performing multireference configuration interaction calculations. This approach, which can be used to obtain very accurate excitation energies, has been used to study a number of small molecules. However, it is inconvenient for the study of several excited states because separate orbital optimizations and CI calculations are required for each state. Furthermore, the use of different orbitals for different states severely complicates the calculation of transition properties, which are needed to describe important physical phenomena such as oscillator strengths.

One way to include many of the advantageous features of both the ΔCI and ΔMCSCF-CI approaches is to use "state-averaged" orbitals. In these calculations, a common set of orbitals designed to describe a set of electronic states is used in a subsequent CI diagonalization. Such a procedure is relatively efficient and is expected to work well, provided the optimal orbitals for all the states of interest are not very different. However, the strategy used to obtain the state-averaged orbitals involves minimization of an energy functional that weighs the electronic states arbitrarily and is therefore not amenable to a black-box procedure. Furthermore, if there is a significant difference between the best one-electron picture of the electronic states, such a state-averaged scheme cannot work very well because all electronic states will be described poorly. In addition, the size of the configuration space required in these calculations is

larger than that needed for state-specific MCSCF calculations, resulting in great computational demands.

The considerations discussed above clearly show that multireference CI approaches to the study of excited states require great care and are not well suited to black-box applications. Ideally, one would like a method that retains the conceptual simplicity of the ΔCI approach while providing a better description of excited states. Since the problems associated with the ΔCI method are due to the use of a single determinant reference state for all electronic states, one might naturally wonder whether a "better" (more flexible) reference state can be used. In other words, we assume the same form of the excited state wavefunction

$$|\Psi_K\rangle = R_K|\Psi_0\rangle \qquad [68]$$

but no longer take $|\Psi_0\rangle$ to be a single determinant. Let us consider the case in which the reference function is the CC wavefunction

$$|\Psi_0\rangle = \exp(T)|\Phi_0\rangle \qquad [69]$$

where $|\Phi_0\rangle$ is the SCF determinant. After inserting this expression into the Schrödinger equation and carrying out a few manipulations similar to the EOM ionization problem, but here for the same number of electrons, and subtracting the ground state solution, one obtains

$$\exp(-T)\hat{H}\exp(T)R_K|\Phi_0\rangle = \Delta E_K R_K|\Phi_0\rangle \qquad [70]$$

or, equivalently,

$$\bar{H}\,R_K|\Phi_0\rangle = \Delta E_K R_K|\Phi_0\rangle \qquad [71]$$

There is a CI-like eigenvalue equation for the excitation energy, ΔE_K, except that the Hamiltonian $(\hat{H})$ has been replaced by $\bar{H}$ and includes the ground state correlation. Again, in practical calculations, the T operator must be truncated to a suitable level of excitation, typically, $T = T_1 + T_2$, which defines the CCSD model for the ground state. Such a reference is much more flexible than that used in ΔCI studies, yet this approach retains the feature of using a common set of orbitals to describe all states. Nevertheless, for finite truncations of T, the excited state wavefunction is more constrained than the ground state CC solution. One therefore expects some residual bias in favor of the ground state. However, the numerical consequences of this imbalance are necessarily smaller than those associated with single reference ΔCI approaches. This equation-of-motion, coupled-cluster (EOM-CC) method, with $T = T_1 + T_2$ and $\hat{R}_k = \hat{R}_{k_1} + \hat{R}_{k_2}$, has recently been implemented into the ACES II program system.[114-116,122] We believe that this method (and its closely

related Fock space MR-CCSD)[27-29,123] will eventually become the most commonly used high level approach for the study of excited states. (Unlike the case for ionization potentials and electron affinities, here these two methods do not give exactly the same answers. See also SAC-CI.[124])

Before discussing the numerical accuracy of various methods, some mention should be made of the special demands placed on basis sets in excited state calculations. Superficially, excited states can be grouped into two categories: valence type and Rydberg type. In the former category, the spatial extent of the electronic probability distribution is similar to that in the ground state, whereas Rydberg states have significantly more diffuse electronic wavefunctions. Because of the large difference in the character of the density between the ground and Rydberg-type excited states, basis set considerations are important. To properly describe Rydberg states, one is forced to use basis sets that contain at least a few diffuse functions, which are needed to describe the long-range features of the electronic charge cloud. Usually, Rydberg states are characterized by a hydrogen-atom-like designation ($n = 3$, $n = 4$, etc.) with energies that converge toward some ionization limit. In practice, a few diffuse functions usually provide a good description of the $n = 3$ levels, while more and more diffuse functions are required for accurate calculations of higher levels.

Some commonly used basis sets that contain diffuse functions are the augmented correlation consistent basis sets of Dunning (PVDZ+, PVTZ+, PVQZ+, etc.),[66] the atomic natural orbital basis sets of Widmark, Malmqvist, and Roos (WMR),[64] the polarized basis sets of Sadlej (POL1),[67] and augmented variants of the 6-31G and 6-311G basis sets[125] (6-31G+, 6-31G+(d,p), etc.). (All these basis sets are available in the ACES II program library.) For most routine calculations, we recommend use of the POL1 basis sets, which are relatively small and appear to provide reasonable results for valence transitions as well as the first level of Rydberg states. The amount of Rydberg character is easily monitored by comparing the second moment of the electronic charge distribution $\langle r^2 \rangle$ to that calculated for the ground state. These values can be obtained from the associated one-particle density matrices, which are evaluated in a straightforward way for all the approaches discussed here (TDA, RPA, ΔCI, EOM-CC).[116] For valence states, the standard basis sets usually used to compute energy differences and molecular geometries (6-31G*, DZP, TZ2P, etc.) should be acceptable because the ground and excited state electron densities have similar spatial extent.

The accurate prediction of excitation energies and associated excited state geometries and properties is one of the more challenging areas of quantum chemistry. All the methods that are easily applied to calculating a spectrum of excited states treat the ground state somewhat more completely than the excited states, so improvements in the level of theory usually tend to reduce the predicted excitation energies. Furthermore, for Rydberg-type excited states, basis set improvements also lead to a systematic lowering of the predicted values. Hence, although fortuitous cancellation of basis set and correlation

effects is observed in some applications of quantum chemistry (such as the prediction of equilibrium geometries and vibrational frequencies), these effects act in concert in excitation energy calculations.

We now turn to a brief survey of the numerical performance of various methods for singlet–singlet transitions from closed-shell ground states. (The EOM-CC implementation in ACES II is equally applicable to open-shell ground states, but we do not discuss excitation energies of open-shell molecules simply because very little experience has been gained thus far in these calculations.) Furthermore, since all optically allowed (and therefore most interesting) transitions from closed-shell ground states are of the singlet–singlet variety, we also do not consider singlet–triplet transitions. Nevertheless, the accuracy of excitation energies calculated for singlet–triplet processes will always be comparable to that for the corresponding singlet–singlet energy difference. However, these transitions are not allowed by spin and therefore carry no oscillator strength in the nonrelativistic Born–Oppenheimer approximation.

To "factor out" basis set effects, we first compare in Table 24 full configuration interaction (FCI) excitation energies and dipole strengths (the values in parentheses) to those obtained with the TDA, RPA, ΔCISD, and EOM-CCSD approximations. Because FCI is a very expensive method, which has a factorial dependence on the number of electrons, we are restricted to a small system and present comparisons only for the beryllium atom and the CH^+ molecule.[116]

The results in Table 24 clearly illustrate many of the points made in our earlier discussion. For most of the excitations considered here, the ΔCISD results are in the poorest agreement with the FCI excitation energies. All these values are much too large, reflecting the unbalanced nature of the method in favor of the ground state. The RPA and TDA results are in better agreement, with the former providing systematically lower excitation energies than the latter. Nevertheless, none of these three approaches can be said to provide quantitative predictions of the excitation energies.

The EOM-CCSD results, however, are in good agreement with the FCI calculations. Note that there is a clear negative correlation between the quality of the results obtained at this level and the values in the rightmost column under the heading "AEL" (approximate excitation level). These numbers provide a measure of the number of electrons that are "excited" in the transition between the ground and excited states. For excitations that are well described by single excitations (AEL values near 1.0), the EOM-CCSD excitation energies are in excellent agreement with the FCI values. However, larger errors are noted for transitions that have significant double-replacement character. Note also that the TDA and RPA approaches also fail completely for these transitions because they are ultimately one-electron models. The performance of EOM-CCSD for excitations with AEL values much larger than unity is relatively poor because the final state wavefunctions corresponding to these processes are constrained to a greater degree than those for nearly pure single excitations. Better results would be achieved by a more elaborate EOM-CC approach,

Table 24 Comparison of Different Methods for Excitation Energies (eV) and Dipole Strengths (in parentheses, atomic units) with Full CI for States of Be[a] and CH^+[b,c]

Final state symmetry	Method					AEL[d]
	TDA	RPA	ΔCISD	EOM-CCSD	FCI	
Be						
^1S	6.13	6.12	7.69	6.77	6.77	1.06
^1S	7.26	7.26	8.97	8.08	8.08	1.04
^1P	5.05 (2.548)	4.80	6.24	5.32 (3.564)	5.32 (3.549)	1.06
^1P	8.77 (0.101)	6.72	8.39	7.47 (0.021)	7.46 (0.022)	1.06
^1D	6.94	6.93	8.03	7.16	7.09	1.59
^1D	7.59	7.59	8.97	8.06	8.03	1.22
CH^+						
$^1\Sigma^+$	17.60 (0.102)	17.52 (0.195)	9.92	9.11 (0.025)	8.55 (0.025)	1.96
$^1\Sigma^+$	13.75 (0.986)	13.70 (0.933)	14.94	13.58 (1.073)	13.52 (1.080)	1.06
$^1\Pi$	2.93 (0.097)	2.65 (0.109)	4.46	3.26 (0.095)	3.23 (0.080)	1.03
$^1\Pi$	15.23 (0.585)	14.84 (0.891)	15.57	14.45 (0.692)	14.13 (0.588)	1.24
$^1\Delta$	49.03	49.02	8.44	7.89	6.96	1.98
$^1\Delta$	59.79	59.77	18.49	17.34	16.83	1.66

[a](9s9p5d) basis.
[b](14s5p1d) basis.
[c]Reference 116.
[d]Approximate excitation level (see text).

particularly one in which T is approximated by $T_1 + T_2 + T_3$. However, such calculations would scale with the eighth power of the number of basis functions and are not a practical method for routine applications. Approximate inclusion of T_3, as in CCSD(T) or CCSDT-1 should offer some improvement, however. Namely, when an excited state involves significant double excitations, the triple excitation operators (T_3 and R_3) would introduce correlation corrections analogous to those carried by T_2 and R_2 for "single" excitations.

For optically allowed transitions, dipole oscillator strengths predicted by the EOM-CCSD model are superior to those calculated at the RPA and TDA levels and are in relatively good agreement with the FCI results for all the transitions that have AEL values near 1.0. The behavior of the oscillator strengths versus the AEL diagnostic parallels that of the predicted excitation energies, as it should, because both quantities ultimately depend on the quality of the excited state wavefunction. The perfect agreement between the EOM-CCSD and FCI oscillator strengths for the nearly pure $^1\Sigma^+ \rightarrow {}^1\Sigma^+$ double excitation in CH^+ is clearly fortuitous.

In applications of the EOM-CCSD approach to chemical problems, two factors must be carefully considered. As discussed above, the method works best for processes that are well described by single electron transitions, so some degree of caution must be exercised when studying excitations that have a fair amount of double-excitation character (somewhat arbitrarily, we place the cutoff for this "dangerous" region at AEL values of 1.2 and larger). In addition, the basis set used in these calculations must be properly chosen. The latter point is particularly true for the study of Rydberg-like states, where basis sets containing diffuse functions (such as POL1) should be used.

Assume that a DZP basis is used to study excited states of water. If such a calculation is performed, the $\langle r^2 \rangle$ values for the excited states will be similar to the ground state value. This does not mean that the excited states of water are valence type! Indeed, the DZP basis is inherently incapable of describing Rydberg-type states because it does not contain diffuse functions. If a more flexible basis such as POL1 is used, the $\langle r^2 \rangle$ values for the excited state will be much larger than those of the ground state, showing that these are actually Rydberg states. Valence states may be identified as those for which expansion of the basis from a valence set, such as DZP, to a diffuse basis, such as POL1, does not significantly change the calculated values of $\langle r^2 \rangle$. To simplify matters and to make calculations less expensive, it is probably best to carry out TDA calculations with the two different types of basis set and identify the states as either Rydberg or valence. Then, an appropriate basis can be selected for the higher level calculations.

In Table 25 we present results of TDA and EOM-CCSD calculations for the ketene molecule. This system has an extraordinarily complex electronic spectrum, which has been the subject of a number of experimental and theoretical analyses. It also illustrates many features of excited state calculations.

Table 25 Excitation Energies of Ketene (eV) and Corresponding Dipole Oscillator Strengths (in parenthesis, atomic units)

	DZP basis				
Final state	TDA	EOM-CCSD		AEL	Experimental
$^1A_2$	4.38	4.04		1.08	3.84
$^1A_1$	8.63	8.15 (0.156)		1.08	6.78
$^1B_2$	9.64	8.98 (0.0006)		1.07	5.86
2^1A_2	9.97	9.60		1.10	
2^1B_2	10.94	10.34 (0.006)		1.07	
2^1A_1	11.34	10.95 (0.946)		1.09	
	POL1 basis				
Final state	TDA	EOM-CCSD	$\langle r^2 \rangle^a$	AEL	Experimental
$^1A_2$	4.32	3.98	40.18	1.08	3.84
$^1A_1$	7.83	7.22 (0.165)	48.3	1.08	6.78
$^1B_2$	6.41	5.89 (0.033)	48.8	1.07	5.86
2^1A_2	7.52	7.09	55.0	1.06	
2^1B_2	7.73	7.20 (0.008)	57.8	1.07	
2^1A_1	8.54	8.12 (0.033)	47.9	1.07	

[a]Ground state $\langle r^2 \rangle$ value is 41.0 au.

Reliable experimental results for the excitation energies of ketene are limited to the three lowest electronic states, which are believed to be $^1A_2$, $^1A_1$, and $^1B_2$, respectively. If we first look at the results obtained with the DZP basis set, we note that all AEL values are in the range 1.07–1.10, indicating that the EOM-CCSD model probably provides a good treatment of differential electron correlation between the ground and excited states. However, the second and third excitation energies predicted by these calculations are in very poor agreement with the experimental values. In fact, while the experimental value for the $X^1A_1 \rightarrow {}^1B_2$ transition is approximately 1 eV below that for excitation to the $^1A_1$ state, the EOM-CCSD results obtained in the DZP basis predict the opposite behavior, with a splitting of nearly 1 eV favoring the $^1A_1$ state. While it would be tempting to speculate that the errors are systematic and the ordering deduced from the experiments incorrect, it is also well known that Rydberg states are ubiquitous in multiply bonded organic molecules. Hence, before glibly jumping to conclusions, it is always worthwhile to use a larger basis set.

The results (Table 25) obtained with a basis suitable for the study of Rydberg states (the POL1 basis) are strikingly different from those obtained with DZP. Although the lowest energy $X^1A_1 \rightarrow {}^1A_2$ excitation does not change significantly, incorporation of diffuse functions into the basis set lowers some of the other excitation energies by as much as 3 eV! Differences between the excited and ground state $\langle r^2 \rangle$ values are roughly proportional to the energy lowerings brought about by incorporating diffuse functions in the basis set. In particular, note that the ordering of electronic energy levels is now in agreement with experimental assignments. Predicted excitation energies are still a bit on

the high side for the first and third transitions. Nearly perfect agreement is achieved for the $X^1A_1 \rightarrow {}^1B_2$ transition, with the EOM-CCSD result a mere 0.03 eV above the experimental value. It is significant to note that this is the most well-established experimental result in Table 25 and corresponds to a vertical excitation energy. The experimental values for excitation to the first and third levels are less certain and probably correspond more closely to adiabatic (equilibrium geometry to equilibrium geometry) than vertical excitation processes. This is another feature that must be carefully considered in studying excited states, since excitation energies obtained from experiment often are affected by changes in equilibrium geometries between the two states. Since the equilibrium geometry of the excited state is necessarily lower in energy than that associated with the vertical transition, adiabatic transition energies will always be lower than the vertical values.

In addition, all the ketene states discussed above are open-shell singlets, which require at least two determinants in a zeroth-order description as discussed earlier. An approach for an in-depth study specific to one of these states is offered by the two-determinant, TD-CCSD, multireference method.[31] In ketene, with a DZP basis the TD-CCSD vertical excitation energy is 3.83 for the $^1A_2$ state in excellent agreement with experiment, while the 2^1A_1 state is at 8.64 eV compared to the EOM-CCSD value of 8.15 eV. For the same two states, the Fock space MR-CCSD gives 3.83 and 7.89 eV. Other methods related to EOM-CC include polarization propagator (PP) procedures[38] built on a second order [MBPT(2)] ground state wavefunction (e.g., the SOPPA method) and more general methods of analysis that use a CC ground state reference (e.g., CCPPA).

It is hoped that this section provides a useful introduction to ab initio studies of excited states. In this challenging area in quantum chemistry, it is not always straightforward to compare results of such calculations with experimental values because information about molecular excited states (and, in particular, the associated potential energy surfaces) is very scarce. Indeed, while the prediction of infrared spectra has clearly been the most fruitful area of application for quantum chemical methods in the past decade, it is likely that theoretical studies of electronically excited states will continue to grow in importance. In particular, the availability of accurate (and therefore predictive) methods such as the EOM-CCSD approach in programs such as ACES II will serve to make accurate calculations of these systems accessible to a wide range of users.

MOLECULAR PROPERTIES

First-Order Properties

Properties of interest can be static or dynamic (i.e., time or frequency dependent); first, second, or higher order; and one- or two-particle type. First-order static one-electron properties (dipole and quadrupole moments, electric

field gradients, hyperfine coupling constants, etc.) are obtained by integrating over the molecular charge density.[126] That is, for some one-particle operator $\hat{\theta} = \Sigma_i \hat{\theta}(i)$ [e.g., for a dipole moment in atomic units $\hat{\theta} = \Sigma_i \mathbf{r}(i)$],

$$\langle \hat{\theta} \rangle = \int \Psi^*(12 \ldots n) \sum_i \hat{\theta}(i) \Psi(12 \ldots n) d\tau \qquad [72]$$

$$\langle \hat{\theta} \rangle = \int \hat{\theta}(1) \rho(1) d\tau \qquad [73]$$

where

$$\rho(1) = \int \Psi(12 \ldots n) \Psi^*(12 \ldots n) d\tau_2 d\tau_3 \ldots d\tau_n \qquad [74]$$

and $\rho(1)$ is the (spin-dependent) molecular charge density.

Another, more general way to define a property is via perturbation theory, where the usual electronic Hamiltonian, H (now $H(0)$) has a perturbation $\lambda\hat{\theta}$ added to it. (The "0" argument of H should be taken to mean that the Hamiltonian does not contain the perturbation of interest. It should not be confused with a Hamiltonian that ignores electron correlation.) Then

$$\mathcal{H} = H(0) + \lambda\hat{\theta} = H(0) + \lambda \frac{\partial \mathcal{H}}{\partial \lambda} \qquad [75]$$

and the Schrödinger equation for the perturbed Hamiltonian gives us

$$\mathcal{H}\Psi(\lambda) = E(\lambda)\Psi(\lambda) \qquad [76]$$

Then, expanding $\Psi(\lambda)$ and $E(\lambda)$ in a Taylor series,

$$\Psi(\lambda) = \Psi(0) + \frac{\partial \Psi}{\partial \lambda} \lambda + \frac{1}{2} \frac{\partial^2 \Psi}{\partial \lambda^2} \lambda^2 + \cdots \qquad [77]$$

$$E(\lambda) = E(0) + \frac{\partial E}{\partial \lambda} \lambda + \frac{1}{2} \frac{\partial^2 E}{\partial \lambda^2} \lambda^2 + \cdots \qquad [78]$$

Inserting Eqs. [77] and [78] into Eq. [76], and insisting that the coefficient of each power of λ be the same on both sides of the equation, we have

$$\frac{\partial E}{\partial \lambda} = \langle \Psi(0) | \theta | \Psi(0) \rangle + 2 \left\langle \frac{\partial \Psi}{\partial \lambda} | H(0) - E(0) | \Psi(0) \right\rangle \qquad [79]$$

Provided we know the solution to the unperturbed Schrödinger equation

$$H(0)\Psi(0) = E(0)\Psi(0) \qquad [80]$$

$$\frac{\partial E}{\partial \lambda} = \left\langle \Psi(0) \middle| \frac{\partial \mathcal{H}}{\partial \lambda} \middle| \Psi(0) \right\rangle = \langle \Psi(0) | \hat{\theta} | \Psi(0) \rangle = \langle \hat{\theta} \rangle \qquad [81]$$

there is an exact equivalence between the first derivative and the expectation value. The fact that we obtain the property from the first derivative of E, the first term in the power series, justifies the terminology "first-order" property. In the next section we will consider second-order properties.

Equation [81] is a statement of the Hellmann–Feynman theorem, which always holds when we have the exact solution for the unperturbed Schrödinger equation (Eq. [80]). However, the Hellmann–Feynman theorem is true only for certain classes of approximate wavefunctions. Except for energy derivatives as previously discussed, where the Gaussian basis is fixed to the nuclear centers in a molecule and therefore changes when the nuclei are displaced, basis functions are usually independent of the perturbation $\lambda\hat{\theta}$. (An exception occurs when field-dependent or gauge-including orbitals are employed, as in NMR and magnetic susceptibility calculations.) This causes the simple Hellmann–Feynman theorem, Eq. [81], to be satisfied for an SCF wavefunction. This follows because it may be shown that any wavefunction that is variationally optimum with respect to variation of all adjustable parameters satisfies the Hellmann–Feynman theorem. In MCSCF, both the MOs and CI coefficients are optimized, so it, too, satisfies Eq. [81] for ordinary properties. However, for CI wavefunctions, the configuration coefficients are variationally optimum but the MOs are not. Similarly, in MBPT or CC theory neither the configuration coefficients nor the MOs are optimum. For the latter cases, the second term in Eq. [79] has a role to play in the accurate treatment of properties and should be included.

In the SCF independent particle case, $\Psi(0) = \Phi_0$, and Eq. [74] becomes

$$\rho(1) = \sum_{i=1}^{n} \varphi_i(1)\varphi_i^*(1) \qquad [82]$$

so

$$\langle \hat{\theta} \rangle = \sum_{i=1}^{n} \langle \varphi_i | \hat{\theta} | \varphi_i \rangle = \mathrm{Tr}(\theta\rho) \qquad [83]$$

The SCF solution for a first-order, one-electron property is usually argued to be relatively accurate. The reason follows from the Møller–Plesset theorem.[4] Earlier we found that the first correlation correction to Φ_0 comes solely from double excitations, $\Phi_0 + \Phi^{(1)} = \Phi_0 + \Sigma_{\substack{i>j \\ a>b}} \Phi_{ij}^{ab} C_{ij}^{ab}$. However, $\langle \Phi_0 | \theta | \Phi_{ij}^{ab} \rangle = 0$

Table 26 Variation of Ground State Dipole Moments (au) of Selected Small Molecules with Different Basis Sets at the SCF Level[a]

Basis set	OC	H_2O	H_3N	H_2S	HF
STO-3G	0.0661	0.6791	0.7028	0.4026	0.5069
3-21G	−0.1552	0.9581	0.8552	0.7148	0.8479
6-31G	−0.2209	1.0349	0.9139	0.7315	0.9032
6-31G*	−0.1309	0.9595	0.7435	0.5418	0.7759
DZP	−0.0966	0.8604	0.7217	0.5025	0.8065
TZP	−0.1179	0.8671	0.7414	—	0.8063
POL1	−0.0989	0.7804	0.6366	0.4375	0.7566
Experimental	+0.044	0.721	0.578	0.401	0.708

[a]Dipole is positive with A^+B^- polarity.

for a one-electron property, so the quantity $\langle\hat{\theta}| = \langle\Phi_0 + \Phi^{(1)}|\hat{\theta}|\Phi_0 + \Phi^{(1)}\rangle = \langle\Phi_0|\hat{\theta}|\Phi_0\rangle + \langle\Phi^{(1)}|\hat{\theta}|\Phi^{(1)}\rangle$. Hence, all first-order correlation corrections to $\langle\hat{\theta}\rangle$ vanish for an SCF solution because the second term is second order in correlation. Tables 26, 27, and 28 show how well this works in practice for dipole moments, quadrupole moments, and field gradients. As is well known, the SCF dipole moment of CO has the wrong sign. Nevertheless, in the POL1 basis, which is good for such properties, SCF dipoles fall within about 10% of experiment.

When making comparisons to experimental properties, we must emphasize the role of the Gaussian basis set. Ab initio methods obtain answers that are only as reliable as the basis permits. A basis that is good for energy calculations is not usually appropriate without extension for other properties. This is easy to understand. The energy preferentially samples regions of space close to the nuclei via operators like $1/r$ while a dipole moment requires a description of $\hat{r}$ and a quadrupole moment $\hat{r}^2$. The latter are much more sensitive to the diffuse parts of the electronic density. A field gradient depends on the operator $\theta = \Sigma_i (3z_i^2 - r_i^2)/r_i^5$, so its $\sim 1/r^3$ dependence makes it particularly sensitive to regions of the density near the nucleus. Hyperfine coupling constants are derived from spin densities—that is, $A_{iso} = (8\pi/3h)g_e g_N \mu_e \mu_N [\rho^\alpha(0) - \rho^\beta(0)]$—and therefore depend on the density exactly at the nucleus. Hence, to describe

Table 27 Variation of Electric Quadrupole Moment (au) of Selected Small Molecules with Different Basis Sets at the SCF Level

Basis set	CO	H_2O	NH_3	H_2S	CO_2	HF
STO-3G	−2.2512	0.0081	0.5977	0.2329	−3.9096	0.9230
3-21G	−2.1529	−0.0622	0.8687	0.5148	−5.2684	1.5054
6-31G	−2.1331	−0.1213	0.9928	0.5416	−5.4341	1.5748
6-31G*	−1.6117	−0.1292	0.9558	0.6905	−4.0916	1.6525
DZP	−1.6494	−0.1043	1.0240	0.6755	−4.0932	1.6798
TZP	−1.7010	−0.1194	1.0920	—	−4.2469	1.7040
POL1	−1.5368	−0.0989	1.0637	0.7883	−3.8087	1.7426

Table 28 Variation of Electric Field Gradient (au) at Atomic Centers of Selected Small Molecules with Different Basis Sets at the SCF Level

Molecule	Center	STO-3G	3-21G	6-31G	6-31G*	DZP	TZP	POL1
CO	O	0.0683	−0.5323	−0.4268	−0.4674	−0.4371	−0.6813	−0.4812
	C	−0.4424	−0.8047	−0.8926	−0.9936	−0.9809	−1.0964	−1.0600
CO_2	O	1.3985	0.8574	1.0481	0.8633	0.9406	0.7776	0.8866
	C	0.1694	−0.3780	−0.4528	−0.5846	−0.5463	−0.6566	−0.6417
HF	H	0.5785	0.7165	0.6315	0.5704	0.5697	0.5784	0.5777
	F	3.8582	3.1783	3.1311	2.9803	2.9714	2.9168	2.8766
H_2S	S	1.2287	0.5398	0.5335	0.4021	0.4508	—	0.3580
	H	0.0609	0.0663	0.0657	0.0608	0.0630	—	0.0712
H_2O	O	0.3146	0.2267	0.2440	0.2116	0.2217	0.1877	0.2205
	H	0.0220	0.0298	0.0196	0.0239	0.0407	0.0388	0.0418
NH_3	N	0.7957	0.5361	0.5147	0.4844	0.4942	0.4899	0.4781
	H	0.2165	0.2341	0.2265	0.1990	0.2100	0.2098	0.2131

all the above equitably requires basis sets augmented in both the core and diffuse regions. Such simultaneous extensions are seldom practical, so different basis sets tailored to different properties are usually used in practice.

As we have seen in Tables 26–28, the nature of the basis set has a dramatic effect on a property at the SCF level, so that aspect needs to be under control[127] before we can reliably assess the role of electron correlation. Finally, we should also note that whereas the energy is variational and the wavefunction can be optimized to give the lowest energy, the same cannot be done for other properties (there are some useful bounds that pertain to second-order properties, however). As a result, we can never be certain that properties obtained at increasingly more complete levels of theory will systematically converge to the exact result.

Using the perturbation theory approach to properties, we can always evaluate a property by simply adding $\lambda\hat{\theta}$ to the electrostatic Hamiltonian, for some small value of λ, and solve directly for the $E(\lambda)$ in Eq. [76]. (Variants of the finite field procedure include placing the molecule in a field generated by point charges a long distance away rather than explicitly adding the finite field to the Hamiltonian as described above.) By repeating for the same small value of λ but with a negative sign, we obtain $E(-\lambda)$. Inasmuch as our objective is $\partial E/\partial\lambda$, we know

$$\frac{\partial E}{\partial \lambda} \approx \frac{E(\lambda) - E(-\lambda)}{2\lambda} \qquad [84]$$

and in the limit of $\lambda \rightarrow 0$, we obtain the exact derivative. Since each $E(\lambda)$ calculation would routinely be done by reoptimizing the MOs in the presence of the perturbation and, in the case of a correlated calculation, the configuration coefficients, in this procedure we are actually including the effects of the non-Hellmann–Feynman terms in Eq. [79]. Even though this approach seems to make good sense only for properties such as dipole moments, where $\lambda\theta = \Sigma_i \boldsymbol{\epsilon} \cdot \mathbf{r}_i$ and we can "turn on" the electric field strength vector $\boldsymbol{\epsilon}$, we can actually evaluate any first-order property in this way. For example, the spin density is not usually thought to be a field-dependent property, but we can add an operator to H and evaluate spin densities.[128] Hence, this "finite field" procedure is simply an artifice for indirectly calculating the property.

In finite field calculations we have to worry about numerical accuracy because the field strength must be large enough to cause an adequate change in the significant digits of $E(\lambda)$, but should also be small enough to make the numerical derivative accurate. Typically fields of 0.001 to 0.005 au are used for dipole moments and polarizabilities, but for the hyperpolarizabilities β and γ, which are third and fourth derivatives of the energy with respect to an electric field, the precision of finite-field calculations can be questioned. A field strength of $(0.001)^4 = 10^{-12}$ means that more than 12 significant digits in the

energy are necessary to evaluate γ accurately. This is typically beyond the precision of the molecular integral evaluation. Finally, of formal but generally not numerical significance, adding an electric field to the electrostatic Hamiltonian gives an $\mathcal{H}(\lambda)$ that is unbound. Its exact solution corresponds to the experimentally well-known field ionization, leading to a cation plus an electron. The use of a finite basis set makes the field-ionized solution, which requires a continuum description of the free electron, inaccessible, so practical finite field calculations should not run into this difficulty.

The solution to all the foregoing reservations lies in analytical evaluation of first-order properties. The critical quantity is the "relaxed" density[84,129] $D(1) = \Sigma_{p,q}\, \varphi_p(1) D_{pq} \varphi_q^*(1)$ when D_{pq} consists of the one-particle response density and the MO relaxation part. This is the same density used in analytical gradients, but the final form of the equations for ordinary properties is just $\langle\hat{\theta}\rangle = \int\hat{\theta}(1)D(1)d\tau = \Sigma_{p,q}\, \hat{\theta}_{pq} D_{pq}$. The finite field procedure is clearly less desirable than a calculation based on "relaxed density" because once $D(1)$ has been obtained, all one-electron properties can be rapidly evaluated by just multiplying D_{pq} with the appropriate integral θ_{pq} and summing. Alternatively, many separate finite field calculations would be needed to get all properties. We will thus have a D_{pq} for all levels of theory where analytical gradients have been implemented (MBPT(2), MBPT(3), MBPT(4), CCSD, CCSD(T), QCISD(T), etc.) in ACES II. With the aid of this quantity, we can investigate the role of electron correlation on molecular properties.

Results for dipole moments are shown in Table 29.[130] Clearly, coupled with good basis sets, correlated methods can do quite well for this property. Elsewhere, we have used relaxed density-based CC and MBPT methods to study spin densities[129] and the related hyperfine coupling constants; to evaluate relativistic corrections (Darwin and mass–velocity term) when important;[131] and to evaluate highly accurate electric field gradients to extract nuclear quadruple moments.[132]

Table 29 Variation of Ground State Dipole Moments (au) of Selected Small Molecules with Different Basis Sets and Correlated Methods

Basis set	OC	H_2O	H_3N	H_2S	HF
DZP-MBPT(2)	0.1447	0.8229	0.7102	0.4902	0.7642
DZP-CCSD	0.0585	0.8163	0.6990	0.4626	0.7602
DZP-CCSD(T)	0.0752	0.8114	0.6963	0.4599	0.7564
TZP-MBPT(2)	0.1222	0.8387	0.7368	—	0.7671
TZP-CCSD	0.0344	0.8294	0.7249	—	0.7625
TZP-CCSD(T)	0.0558	0.8248	0.7229	—	0.7580
POL1-MBPT(2)	0.1208	0.7297	0.5994	0.4053	0.7079
POL1-CCSD	0.0421	0.7287	0.5975	0.3924	0.7079
POL1-CCSD(T)	0.0581	0.7215	0.5904	0.3857	0.7014
Experimental	+0.044	0.721	0.578	0.401	0.708

Second-Order Properties

Second order properties derive from the second derivative term in Eq. [78]. For the most general case we should also allow for a second-order perturbation, $\mathcal{H}(\lambda) = H(0) + (\partial\mathcal{H}/\partial\lambda)\lambda + \frac{1}{2}(\partial^2\mathcal{H}/\partial\lambda^2)\lambda^2$ from which differentiation of the Schrödinger equation gives

$$\frac{\partial^2 E}{\partial\lambda^2} = \left\langle \Psi(0)\left|\frac{\partial^2\mathcal{H}}{\partial\lambda^2}\right|\Psi(0)\right\rangle + 2\left\langle \frac{\partial\Psi(0)}{\partial\lambda}\left|\frac{\partial\mathcal{H}}{\partial\lambda} - \frac{\partial E}{\partial\lambda}\right|\Psi(0)\right\rangle + 2\left\langle \frac{\partial^2\Psi}{\partial\lambda^2}\left|H(0) - E(0)\right|\Psi(0)\right\rangle \quad [85]$$

[Allowing λ to be a vector would define all nine components of the second derivative tensor $(\partial^2 E/\partial\lambda_i\partial\lambda_j)$.] For the polarizability tensor where $\lambda\theta = \Sigma_i \boldsymbol{\epsilon}\cdot\mathbf{r}_i$ and many other examples, there is no $\partial^2\mathcal{H}/\partial\lambda^2$ perturbation. Once again, if we cannot solve Eq. [80] exactly (or have all parameters optimum), a non-Hellmann–Feynman term that depends on the second derivative (i.e., second order) perturbed wavefunction must be considered. When the theorem is satisfied, the new information we require is only the first-order perturbed wavefunction, $\partial\Psi/\partial\lambda$. This quantity is equivalent to $\psi^{(1)}$ in Eq. [29b], when $V = \partial\mathcal{H}/\partial\lambda$ and $E^{(1)} = \partial E/\partial\lambda$. We can solve for $\partial\Psi/\partial\lambda$ in the same way as before, by the textbook expedient of expanding in the complete set of solutions to $H(0)$, which means all the excited electronic states, which as eigenfunctions of $H(0)$, are orthogonal to the ground state. Using the zz component of the polarizability as an example,

$$\alpha_{zz} = -2\sum_{k\neq 0}^{\infty} |\langle\Psi_0|z|\Psi_k\rangle|^2 / (E_0 - E_k) \quad [86]$$

Equation [86] is sometimes useful, e.g., when a knowledge of the excitation energies and polarized components of the transition moments for a few states could be used to estimate the α tensor from experiment. However, this sum-over-states formula is computationally about the worst approach to the theoretical evaluation of second-order quantities. To use it directly would require computing all the excited states the finite basis permits and the appropriate transition moments. It can be solved indirectly, however.[133]

The superior approach is to simply compute the second derivative (Hessian) matrix analytically.[134] Just as for force constants, this is the most accurate and efficient procedure when the second-derivative formulas have been programmed. Furthermore, any residual dependence on $\partial^2\Psi/\partial\lambda^2$ is alleviated, just

Table 30 Dipole Polarizabilities (au) for Molecules (POL1 Basis)[a]

	CO_2		N_2		C_2H_4		CO	
	$\bar{\alpha}$[b]	$\Delta\alpha$[c]	$\bar{\alpha}$	$\Delta\alpha$	$\bar{\alpha}$	$\Delta\alpha$	$\bar{\alpha}$	$\Delta\alpha$
SCF	15.8	12.1	11.4	5.4	28.0	12.6	12.2	3.4
MBPT(2)	17.9	15.0	11.5	4.4	27.4	10.2	13.1	3.9
CCSD	17.4	14.4	11.6	4.8	26.9	10.7	12.9	4.0
CCSD(T)	17.6	14.5	11.8	4.9	27.1	10.5	13.0	3.9
Experimental	17.5	13.8	11.8	4.7	28.7	11.0	31.1	3.7
	HF		H_2O		NH_3		H_2S	
	$\bar{\alpha}$	$\Delta\alpha$	$\bar{\alpha}$	$\Delta\alpha$	$\bar{\alpha}$	$\Delta\alpha$	$\bar{\alpha}$	$\Delta\alpha$
SCF	4.9	1.3	8.5	1.1	12.9	0.5	23.6	0.4
MBPT(2)	5.7	1.1	9.8	0.4	14.4	1.9	24.5	0.9
CCSD	5.6	1.2	9.6	0.6	14.1	1.7	24.3	0.9
Experimental	5.5	1.3	9.8	0.6	14.6	1.9	25.5	

[a] Reference 130.
[b] $\bar{\alpha} = 1/3\ (\alpha_{xx} + \alpha_{yy} + \alpha_{zz}) = 1/3\ \mathrm{Tr}(\boldsymbol{\alpha})$.
[c] $\Delta\alpha = 1/\sqrt{2}\ [(\alpha_{xx} - \alpha_{yy})^2 + (\alpha_{xx} - \alpha_{zz})^2 + (\alpha_{yy} - \alpha_{zz})^2]^{1/2}$.

as in the gradient case, by introducing the configuration response (via Λ) and the molecular orbital relaxation contribution. [This can be done for open (UHF[92] and ROHF[93]) and closed shells at the MBPT(2) level in ACES II.] To obtain polarizabilities at higher correlated levels, the dipole moment is computed as a function of a finite field $\mu(\boldsymbol{\lambda})$, from which numerical differentiation provides the tensor $\boldsymbol{\alpha}$. Similarly, a second numerical differentiation gives $\boldsymbol{\beta}$ and a third, $\boldsymbol{\gamma}$.[130] The accuracy for $\boldsymbol{\alpha}$ at several levels of theory is shown in Table 30.

NUCLEAR MAGNETIC RESONANCE

Although evaluations of harmonic force constants ($\partial^2 E/\partial q_i \partial q_j$), electric polarizabilities ($\partial^2 E/\partial \epsilon_i \partial \epsilon_j$), and dipole moment derivatives ($\partial^2 E/\partial \epsilon_i \partial q_j$) are perhaps the most common applications of second-order properties (or, equivalently, second derivatives), other areas of interest to chemists can be treated with these techniques. One such field of application that holds great promise for the future is the calculation of nuclear magnetic resonance chemical shifts.

The theoretical study of NMR shifts has a relatively long history. Calculations of magnetic properties inherently suffer from a "gauge origin" problem, which simply means that the results depend on the choice of origin of the coordinate system (e.g., the calculated NMR shifts for water will change if the molecule is "translated" along an axis). This clearly unphysical behavior can be avoided by assigning a local gauge origin to each basis function, which is

known as a "gauge-including atomic orbital" (GIAO).[135] This approach was first tried nearly 20 years ago, but a straightforward implementation requires evaluation of difficult integrals, which involve complex quantities, and did not find wide acceptance. Subsequently, a number of methods designed to minimize the gauge origin problem were suggested—the IGLO[136] and LORG[137] techniques—but these still do not completely do away with the problem. Eventually, it was realized that analytic second-derivative techniques could be used to avoid many of the complicated steps involving the GIAO basis function integrals, and a number of applications of the GIAO approach were carried out at the SCF level.[138] In particular, when the second derivatives are evaluated analytically, no arithmetic involving complex numbers needs to be performed.

Elements of the chemical shift tensor σ for a particular nucleus η are given by the mixed second derivative of the energy with respect to the nuclear magnetic moments $[I_{q_i}(\eta)]$ and the magnetic field $[B_j]$

$$\sigma_{ij} = \frac{\partial^2 E}{\partial I_{q_i} \partial B_{q_j}} \qquad [87]$$

The chemical shift is then given by $\frac{1}{3}Tr(\sigma)$.

Applications of the GIAO approach at the SCF level are now relatively routine, but correlated calculations are more difficult because the most convenient implementations of this approach require the analytic evaluation of the second derivatives. Therefore, correlated studies using GIAO basis functions are effectively limited to levels of theory for which analytic second-derivative methods are available. Although the number of calculations thus far carried out on chemical shifts is far too small to give us a clear picture of basis set and correlation effects, the initial results of GIAO-MBPT(2) calculations[139] suggest that correlation is indeed important for these phenomena. In Table 31 are results from a few representative calculations of ^{17}O chemical shifts.

From these results and a limited number of other studies, it appears that the correlation effects are most pronounced for systems with multiple bonds, which should come as no surprise. In addition, it appears that basis set and correlation effects tend to act in different directions, which, of course, can lead

Table 31 ^{17}O Chemical Shifts

Molecule	Basis set	SCF	MBPT(2)	Experimental
H_2O	DZP	331.7	345.4	344.0
	TZ2P	323.2	339.8	344.0
CO_2	DZP	216.9	253.0	243.4
	TZ2P	200.4	236.4	243.4
CO	DZP	−96.7	−27.3	−42.3
	TZ2P	−113.5	−54.1	−42.3

to fortuitous cancellation and the appearance of Pauling points. However, since the GIAO method is currently limited to the SCF and MBPT(2) levels, the effect of higher order correlation corrections on the calculated chemical shifts are not yet known.

ACKNOWLEDGMENTS

Many other members of our research group have significantly contributed to this chapter. All the CASSCF-CI calculations were performed by Dr. Peter Szalay using the COLUMBUS program system. Dr. John Watts provided the CCSDT results for the N_2 curve among several other calculations. Dr. Stanislaw Kucharski provided the CISDT and CISDTQ results. Dr. Anna Balkova is responsible for the TD-CCSD results. Mr. Steve Gwaltney computed some of the vibrational frequencies. Ms. Suely Meth did the MgF^+ calculation. Mr. Ajith Perera computed the first-order properties. Dr. Hideo Sekino did the polarizability calculations. Dr. Jürgen Gauss is responsible for the NMR results. Mr. Sullivan Beck, Mr. Dave Bernholdt, and Dr. Don Comeau offered invaluable help with computer graphics. Finally, Mrs. Sue Linsley typed this long chapter, despite extensive, illegible revisions from the authors. This work has been supported by the Air Force Office of Scientific Research and the Office of Naval Research. We acknowledge the Florida Supercomputer Center and the Ohio Supercomputer Center for their generous allocation of computer resources.

APPENDIX

Quadratic Configuration Interaction (QCI)

What is QCI? To answer this question we need to consider the relationship between CI and CC theory in a little more detail. Since the exact CI wavefunction is $\Psi_{CI} = (1 + \hat{C}_1 + \hat{C}_2 + \hat{C}_3 + \cdots + \hat{C}_n)\Phi_0$ and $\Psi_{CC} = \exp(\hat{T}_1 + \hat{T}_2 + \cdots + \hat{T}_n)\Phi_0$, it follows that $\hat{C}_1 = \hat{T}_1$, $\hat{C}_2 = \hat{T}_2 + \hat{T}_1^2/2$, $\hat{C}_3 = \hat{T}_3 + \hat{T}_1\hat{T}_2 + \hat{T}_1^3/3!$ and $\hat{C}_4 = \hat{T}_4 + \hat{T}_2^2/2 + \hat{T}_1^2\hat{T}_2/2 + \hat{T}_1\hat{T}_3 + \hat{T}_1^4/4!$ etc. The inclusion of $\hat{T}_2^2/2$ in even the simplest CCD model explains why CCD is usually better than CID, CISD, or even CISDT. Once we have CISDTQ, this term is picked up along with several others showing that CISDTQ $\approx$ CCSD(T) (e.g., as shown in Table 4). In operator form, the CISD equations in the canonical SCF case are

$$\langle \Phi_i^a | H_N(\hat{C}_1 + \hat{C}_2)|\Phi_0\rangle = \Delta E \langle \Phi_i^a | \hat{C}_1 | \Phi_0\rangle$$

$$\langle \Phi_{ij}^{ab} | H_N(1 + \hat{C}_1 + \hat{C}_2)|\Phi_0\rangle = \Delta E \langle \Phi_{ij}^{ab} | \hat{C}_2 | \Phi_0\rangle$$

$$\Delta E = \langle \Phi_0 | H_N \hat{C}_2 | \Phi_0\rangle$$

In contrast, in terms of $\hat{C}_p$, the CCSD equations are

$$\langle \Phi_i^a | H_N (\hat{C}_1 + \hat{C}_2 + \hat{C}_3') | \Phi_0 \rangle = \Delta E \langle \Phi_i^a | \hat{C}_1 | \Phi_0 \rangle \qquad [88]$$

$$\langle \Phi_{ij}^{ab} | H_N (1 + \hat{C}_1 + \hat{C}_2 + \hat{C}_3' + \hat{C}_4') | \Phi_0 \rangle = \Delta E \langle \Phi_{ij}^{ab} | \hat{C}_2 | \Phi_0 \rangle \qquad [89]$$

$$\Delta E = \langle \Phi_0 | H_N \hat{C}_2 | \Phi_0 \rangle$$

where $\hat{C}_3' = C_3 - T_3$ and $\hat{C}_4' = C_4 - \hat{T}_4 - \hat{T}_1 \hat{T}_3$. Remember, while the ΔE remains in CI, it has to disappear from extensive methods. Algebraic analysis shows that $\Delta E \langle \Phi_i^a | \hat{C}_1 | \Phi_0 \rangle$ (which is an unlinked term) is equal to a term derived from $\hat{T}_1 \hat{T}_2$ in C_3' in Eq. [88]. Similarly, $\Delta E \langle \Phi_{ij}^{ab} | \hat{C}_2 | \Phi_0 \rangle$ equals a term arising from the $\hat{T}_2^2/2 + \hat{T}_1^2 \hat{T}_2/2$ terms in C_4' in Eq. [89]. Eliminating the corresponding terms from the equations eliminates ΔE, making the CCSD method extensive.

The idea of QCI is to replace these essential terms by the closest CI coefficient analog. Namely, $\hat{C}_1 \hat{C}_2 = \hat{T}_1 \hat{T}_2 + \hat{T}_1^3/2$ and $\hat{C}_2^2/2 = \hat{T}_2^2/2 + \hat{T}_1^2 T_2/2 + \hat{T}_1^4/4$. Hence, the QCISD equations are

$$\langle \Phi_i^a | H_N (\hat{C}_1 + \hat{C}_2 + \hat{C}_1 \hat{C}_2) | \Phi_0 \rangle = \Delta E \langle \Phi_i^a | \hat{C}_1 | \phi_0 \rangle$$

$$\left\langle \Phi_{ij}^{ab} | H_N \left(1 + \hat{C}_1 + \hat{C}_2 + \hat{C}_2^2/2 \right) | \Phi_0 \right\rangle = \Delta E \langle \Phi_{ij}^{ab} | \hat{C}_2 | \Phi_0 \rangle \qquad [90]$$

$$\Delta E = \langle \Phi_0 | H_N \hat{C}_2 | \Phi_0 \rangle$$

These differ from CCSD via the C_3' term in the double-excitation equation and the different numerical factors in the $\hat{T}_1^3$ and $\hat{T}_1^4$ terms, but none of these terms is required to cancel unlinked terms. Also, none of these terms contributes before the fifth-order energy in the canonical SCF case. So usually QCISD $\approx$ CCSD (see Table 32). QCISD's mean error of 6.41 compares with 7.06 for CCSD. Also, since nonlinear T terms tend to raise the correlation energy, their neglect in QCISD will usually cause E(QCISD) $<$ E(CCSD) slightly. If we restrict ourselves to just CCD, then QCID = CCD. Also, it is apparent from the derivation above that QCISD is an extensive (i.e., many-body) method. It is also clear that for two electrons, CISD = QCISD = CCSD. Unlike CCSD, QCISD is defined only in the canonical SCF case. Besides keeping the effects of $\hat{T}_1$ small because of the Brillouin theorem, this is necessary to maintain the extensive property of the method: otherwise, $\Delta E = \langle \Phi_0 | H_N (\hat{C}_1 + \hat{C}_2) | \Phi_0 \rangle$ and adding the additional $C_1 C_2$ term to Eq. [90] and $\hat{C}_1^2/2$ in the single excitation equation can lead to residual unlinked terms in the wavefunction. This is also why there is no extensive QCISDT method.[140]

Noniterative T_3 contributions can be added to QCISD just as in the CCSD case. The contribution from double excitations to T_3 is formally exactly the same T(CCSD) term, except that it is evaluated using QCISD coefficients, that is, T(QCISD). QCISD(T) further adds a single excitation term like CCSD(T), but it needs to be multiplied by 2 compared to CCSD because the C_3' term remaining in Eq. [89] introduces this term once and iteratively in CCSD.

Table 32 Differences (millihartrees) Between QCI and Full CI Energies (DZP Basis Set)

Method	BH			FH			H_2O			Mean absolute error
	R_e	1.5 R_e	2.0 R_e	R_e	1.5 R_e	2.0 R_e	R_e	1.5 R_e	2.0 R_e	
QCISD	1.75	2.35	3.84	2.57	4.14	8.40	3.88	9.37	21.38	6.41
QCISD(T)	0.40	0.41	0.12	0.24	0.66	1.38	0.62	1.81	−1.26	0.77
QCISD(TQ*)[a]	0.05	−0.09	−0.85	0.17	0.34	0.87	0.09	−0.13	−1.08	0.41

[a]QCISD(TQ*) = QCISD + TQ*(QCISD) from reference 49.

Unlike CI, where $\Psi_{CISD} = (1 + \hat{C}_1 + \hat{C}_2)\Phi_0$, and CCSD, where $\Psi_{CCSD} = \exp(\hat{T}_1 + \hat{T}_2)\Phi_0$, the Ψ_{QCISD} wavefunction cannot be simply represented. It is an approximate truncation of $\exp(\hat{T}_1 + \hat{T}_2)\Phi_0$ that is *different for the single and double excitation projections.* The QCISD(T) mean error of 0.77 compares to 1.15 for CCSD(T). Also adding T_4 effects gives QCISD(TQ*), whose mean error of 0.41 is close to that of CC5SD(TQ*), 0.44. QCISD and QCISD(T) are simply approximate versions of the CCSD and CCSD(T) equations; therefore all the analytical gradient and other methods in ACES II contain QCI as a special case.

REFERENCES

1. This chapter presents the kind of information communicated to participants of workshops on applied molecular orbital theory and to new graduate students. The choice of topics is based on our experience with these groups.
2. D. B. Boyd, in *Reviews in Computational Chemistry,* Vol. 4, K. B. Lipkowitz and D. B. Boyd, Eds., VCH Publishers, New York, 1993, pp. 229–257. Compendium of Software for Molecular Modeling.
3. J. F. Stanton, J. Gauss, J. D. Watts, W. J. Lauderdale, and R. J. Bartlett, *Int. J. Quantum Chem.,* S26, 879 (1992). The ACES II Program System.
4. A. Szabo and N. S. Ostlund, *Modern Quantum Chemistry,* Macmillan, New York, 1990.
5. R. J. Bartlett, *Annu. Rev. Phys. Chem.,* 32, 359 (1981). Many-Body Perturbation Theory and Coupled Cluster Theory for Electron Correlation in Molecules.
6. R. J. Bartlett, *J. Phys. Chem.,* 93, 1697 (1989). Coupled-Cluster Approach to Molecular Structure and Spectra: A Step Toward Predictive Quantum Chemistry.
7. P. Carsky and M. Urban, *Ab Initio Calculations,* Springer-Verlag, Berlin, 1980.
8. W. J. Hehre, J. A. Pople, P. v. R. Schleyer, and L. Radom, *Ab Initio Molecular Orbital Theory,* Wiley, New York, 1986. (This book offers a wealth of comparisons of SCF results and those from perturbation theory in a variety of basis sets.)
9. I. Shavitt, in *Methods of Electronic Structure Theory,* H. F. Schaefer, III, Ed., Plenum, New York, 1977, p. 189. The Method of Configuration Interaction.
10. F. W. Bobrowicz and W. A. Goddard, III, in *Modern Theoretical Chemistry III,* H. F. Schaefer, III, Ed., Plenum, New York, 1977, p. 79. The Self-Consistent Field Equations for Generalized Valence Bond and Open-Shell Hartree–Fock.
11. J. Čížek and J. Paldus, *Physica Scripta,* 21, 251 (1980). Coupled-Cluster Approach.
12. R. J. Bartlett, C. E. Dykstra, and J. Paldus, in *Advanced Theories and Computational Approaches to the Electronic Structure of Molecules,* C. E. Dykstra, Ed., Reidel, Dordrecht, 1984, p. 127. Coupled-Cluster Methods for Molecular Calculations.
13. J. A. Pople, M. Head-Gordon, and K. Raghavachari, *J. Chem. Phys.,* 87, 5968 (1987). Quadratic Configuration Interaction. A General Technique for Determining Electron Correlation Energies.
14. B. O. Roos, *Adv. Chem. Phys.,* 69, 399 (1987). The Complete Active Space Self-Consistent Field Method and Its Application in Electronic Structure Calculations.
15. I. N. Levine, *Quantum Chemistry,* Prentice-Hall, Englewood Cliffs, NJ, 1991 (especially Chapters 15 and 17).
16. W. Kutzelnigg and W. Klopper, *J. Chem. Phys.,* 94, 1985 (1991). Wavefunctions with Terms Linear in the Interelectronic Coordinates to Take Care of the Correlation Cusp. I. General Theory.

17. D. H. Magers, R. J. Harrison, and R. J. Bartlett, *J. Chem. Phys.*, 84, 3284 (1986). Isomers and Excitation Energies of C_4. (Approximate determination of open-shell singlet energies with triplet information.)
18. B. O. Roos, in: *Methods in Computational Physics*, Vol. 1, G. H. F. Diercksen and S. Wilson, Eds., Reidel, Dordrecht, 1983, p. 161. The Multiconfigurational (MC) SCF Method.
19. R. Shepard, *Adv. Chem. Phys.*, 69, 63 (1987). The Multiconfiguration Self-Consistent-Field Method.
20. T. H. Dunning, Jr., D. C. Cartwright, W. J. Hunt, P. J. Hay, and F. W. Bobrowicz, *J. Chem. Phys.*, 64, 4755 (1976). Generalized Valence Bond Calculations on the Ground State ($X^1\Sigma_g^+$) of Nitrogen.
21. G. D. Purvis, III, and R. J. Bartlett, *J. Chem. Phys.*, 76, 1910 (1982). A Full Coupled-Cluster Singles and Doubles Model: The Inclusion of Disconnected Triples. (CCSD.)
22. J. Noga and R. J. Bartlett, *J. Chem. Phys.*, 86, 7041 (1987). The Full CCSDT Model for Molecular Electronic Structure. Ibid., 89, 3401 (1988). Erratum.
23. K. Ruedenberg, M. W. Schmidt, M. M. Gilbert, and S. T. Elbert, *Chem. Phys.*, 71, 41 (1982). Are Atoms Intrinsic to Molecular Wavefunctions? I. The FORS Model.
24. G. Hose and U. Kaldor, *J. Phys., B: Atom. Mol. Phys.*, 12, 3827 (1979). Diagrammatic Many-Body Perturbation Theory for General Model Spaces.
25. M. G. Shepard and K. F. Freed, *J. Chem. Phys.*, 75, 4525 (1981). Convergence Studies of the Effective Valence Shell Hamiltonian for Correlation Energies of the Fluorine Atom and Its Ions Using Third Order Quasidegenerate Many-Body Perturbation Theory.
26. S. Kucharski and R. J. Bartlett, *Int. J. Quantum Chem. Symp.*, 22, 383 (1988). Multi-Reference Many-Body Perturbation Theory.
27. D. Mukherjee and S. Pal, *Adv. Quantum Chem.*, 20, 292 (1989). Use of Cluster Expansion Methods in the Open-Shell Correlation Problem.
28. U. Kaldor, *Theor. Chim. Acta*, 80, 427 (1991). The Fock Space Coupled Cluster Method: Theory and Application.
29. S. Pal, M. Rittby, R. J. Bartlett, D. Dinha, and D. Mukherjee, *J. Chem. Phys.*, 88, 4357 (1988). Molecular Applications of Multireference Coupled-Cluster Methods Using an Incomplete Model Space. Direct Calculation of Excitation Energies. (FS-MRCCSD.)
30. J. F. Stanton, R. J. Bartlett, and C. M. L. Rittby, *J. Chem. Phys.*, 97, 5560 (1992). Fock Space Multireference Coupled-Cluster Theory for General Single Determinant Reference Functions.
31. A. Balkova and R. J. Bartlett, *Chem. Phys. Lett.*, 193, 364 (1992). Coupled-Cluster Method for Open-Shell Singlet States.
32. J. Paldus, in *Methods in Computational Molecular Physics*, Vol. 1, S. Wilson and G. H. F. Diercksen, Eds., Plenum, New York, 1992, p. 99. Coupled Cluster Theory.
33. R. J. Bartlett and G. D. Purvis, III, *Int. J. Quantum Chem.*, 14, 561 (1978). Many-Body Perturbation Theory, Coupled Pair Many-Electron Theory, and the Importance of Quadruple Excitations for the Correlation Problem. [SDQ-MBPT(4), CCD].
34. S. R. Langhoff and E. R. Davidson, *Int. J. Quantum Chem.*, 8, 61 (1974). Configuration Interaction Calculations on the Nitrogen Molecule.
35. C. W. Bauschlicher, Jr., and P. R. Taylor, *J. Chem. Phys.*, 85, 2779 (1986). Benchmark Full Configuration Interaction Calculations on H_2O, F, and F^-.
36. R. J. Harrison, *J. Chem. Phys.*, 94, 5020 (1991). Approximating Full Configuration Interaction with Selected Configuration Interaction and Perturbation Theory.
37. W. von Niessen, J. Schirmer, and L. S. Cederbaum, *Comput. Phys. Rep.*, 1, 59 (1984). Computational Methods for the One-Particle Green's Function.
38. J. Oddershede, P. Jørgensen, and D. L. Yeager, *Comput. Phys. Rep.*, 2, 25 (1984). Polarization Propagator Methods in Atomic and Molecular Calculations.
39. C. W. Bauschlicher, Jr., S. R. Langhoff, P. R. Taylor, N. C. Handy, and P. J. Knowles, *J. Chem. Phys.*, 85, 1469 (1986). Benchmark Full Configuration-Interaction Calculations on HF and NH_2.

40. R. J. Harrison and N. C. Handy, *Chem. Phys. Lett.*, **95**, 386 (1983). Full CI Calculations on BH, H_2O, NH_3, and HF.
41. R. J. Bartlett and D. M. Silver, *Int. J. Quantum Chem. Symp.*, **9**, 183 (1975). Some Aspects of Diagrammatic Perturbation Theory.
42. R. J. Bartlett and D. M. Silver, *Phys. Rev.*, **A10**, 1927 (1974). Pair-Correlation Energies in Sodium Hydride with Many-Body Perturbation Theory; *Chem. Phys. Lett.*, **29**, 199 (1974). Many-Body Perturbation Theory Applied to Hydrogen Fluoride.
43. R. J. Bartlett and I. Shavitt, *Chem. Phys. Lett.*, **50**, 190 (1977). Comparison of High-Order Many-Body Perturbation Theory and Configuration Interaction for H_2O.
44. S. A. Kucharski, J. Noga, and R. J. Bartlett, *J. Chem. Phys.*, **90**, 7282 (1989). Fifth-Order Many-Body Perturbation Theory for Molecular Correlation Energies.
45. J. Paldus and J. Čížek, *Adv. Quantum Chem.*, **9**, 105 (1975). Time-Independent Diagrammatic Approach to Perturbation Theory of Fermion Systems.
46. J. Cizek, *Adv. Chem. Phys.*, **14**, 35 (1969). On the Use of the Cluster Expansion and the Technique of Diagrams in Calculations of the Correlations Effects in Atoms and Molecules.
47. M. Urban, J. Noga, S. J. Cole, and R. J. Bartlett, *J. Chem. Phys.*, **83**, 4041 (1985). Towards a Full CCSDT Model for Electron Correlation. [CCSD + T(CCSD).]
48. K. Raghavachari, G. W. Trucks, M. Head-Gordon, and J. A. Pople, *Chem. Phys. Lett.*, **157**, 479 (1989). A Fifth-Order Perturbation Comparison of Electron Correlation Theories.
49. R. J. Bartlett, J. D. Watts, S. A. Kucharski, and J. Noga, *Chem. Phys. Lett.*, **165**, 513 (1990). Non-Iterative Fifth-Order Triple and Quadruple Excitation Energy Correlations in Correlated Methods. [CCSD(T), CCSD + TQ*(CCSD).] Ibid., **167**, 609 (1990). Erratum.
50. A. C. Hurley, *Electron Correlations in Small Molecules*, Academic Press, San Francisco, 1976.
51. S. A. Kucharski and R. J. Bartlett, *J. Chem. Phys.*, **97**, 4282 (1992). The Coupled-Cluster Single, Double, Triple, and Quadruple Excitation Method.
52. Y. S. Lee, S. A. Kucharski, and R. J. Bartlett, *J. Chem. Phys.*, **81**, 5906 (1984). A Coupled-Cluster Approach with Triple Excitations. (CCSDT-1.)
53. S. A. Kucharski and R. J. Bartlett, *Chem. Phys. Lett.*, **206**, 574 (1993). Coupled Cluster Methods Correct Through Sixth Order.
54. R. A. Chiles and C. E. Dykstra, *J. Chem. Phys.*, **74**, 4544 (1981). An Electron Pair Operator Approach to Coupled-Cluster Wavefunctions. Applications to He_2, Be_2, and Mg_2 and Comparison with CEPA Methods.
55. N. C. Handy, J. A. Pople, M. Head-Gordon, K. Raghavachari and G. W. Trucks, *Chem. Phys. Lett.*, **164**, 185 (1989). Size-Consistent Brueckner Theory Limited to Double Substitutions.
56. J. F. Stanton, J. Gauss, and R. J. Bartlett, *J. Chem. Phys.*, **97**, 5554 (1992). On the Choice of Orbitals for Symmetry Breaking Problems with Application to NO_3. [Brueckner-CCD(T), QRHF-CCSD(T).]
57. D. Feller and E. R. Davidson, in *Reviews in Computational Chemistry*, Vol. 1, K. B. Lipkowitz and D. B. Boyd, Eds. VCH Publishers, New York, 1990, p. 1. Basis Sets for Ab Initio Molecular Orbital Calculations and Intermolecular Interactions.
58. P. C. Hariharan and J. A. Pople, *Theor. Chim. Acta*, **28**, 213 (1973). The Influence of Polarization Functions on Molecular Orbital Hydrogeneration Energies. (6-31G*.)
59. J. S. Binkley, J. A. Pople, and W. J. Hehre, *J. Am. Chem. Soc.*, **102**, 939 (1980). Self-Consistent Molecular Orbital Methods. 21. Small Split-Valence Basis Sets for First Row Elements. (6-31G**.)
60. T. H. Dunning, Jr., *J. Chem. Phys.*, **53**, 2823 (1970). Gaussian Basis Functions for Use in Molecular Calculations. I. Contraction of (9s,5p) Atomic Basis Sets for the First-Row Atoms. (DZ, TZ.)
61. S. Huzinaga, *Comput. Phys. Rep.*, **2**, 279 (1985). Basis Sets for Molecular Calculations.

62. L. T. Redmon, G. D. Purvis, III, and R. J. Bartlett, *J. Am. Chem. Soc.*, **101**, 2856 (1979). Accurate Binding Energies of Diborane, Borane Carbonyl, and Borazane Determined by Many-Body Perturbation Theory. (Correlated polarization exponents for DZP basis sets.)

63. T. H. Dunning, Jr., *J. Chem. Phys.*, **55**, 716 (1971). Gaussian Basis Functions for Use in Molecular Calculations. III. Contraction of (10s,6p) Atomic Basis Sets for First-Row Atoms. (TZ.)

64. P. O. Widmark, P. A. Malmqvist, and B. O. Roos, *Theor. Chim. Acta*, **77**, 291 (1990). Density Matrix Averaged Atomic Natural Orbital (ANO) Basis Sets for Correlated Molecular Wavefunctions. I. First-Row Atoms.

65. J. Almlöf and P. R. Taylor, *Adv. Quantum Chem.*, **22**, 301 (1991). Atomic Natural Orbital (ANO) Basis Sets for Quantum Chemical Calculations.

66. T. H. Dunning, Jr., *J. Chem. Phys.*, **90**, 1007 (1989). Gaussian Basis Functions for Use in Related Molecular Calculations I. The Atoms Boron Through Neon and Hydrogen. (ccPVDZ, ccPVTZ, ccPVQZ.)

67. A. Sadlej, *Theor. Chim. Acta*, **79**, 123 (1991). Medium-Size Polarized Basis Sets for High-Level Correlated Calculations of Molecular Electric Properties. I. First-Row Atoms: H Through F. (POL1 basis.)

68. J. F. Stanton, J. Gauss, J. D. Watts, and R. J. Bartlett, *J. Chem. Phys.*, **94**, 4334 (1991). A Direct Product Decomposition Approach for Symmetry Exploitation in Many-Body Methods. I. Energy Calculations.

69. L. R. Khan, P. Baybutt, and D. G. Truhlar, *J. Chem Phys.*, **65**, 3826 (1976). Ab Initio Effective Core Potentials. Reduction of All-Electron Molecular Structure Calculations to Calculations Involving Only Valence Electrons.

70. P. J. Hay and W. R. Wadt, *J. Chem. Phys.*, **82**, 270 (1985). Ab Initio Effective Core Potentials for Molecular Calculations. Potentials for Transition Metal Atoms Sc to Hg.

71. M. M. Hurley, L. Pacios, P. A. Christiansen, R. B. Ross, and W. C. Ermler, *J. Chem Phys.*, **84**, 6840 (1986). Ab Initio Relativistic Effective Potentials with Spin-Orbit Operators II; K Through Kr.

72. P. Pulay, *Adv. Chem. Phys.*, **69**, 241 (1987). Analytical Derivative Methods in Quantum Chemistry.

73. G. Fogarasi and P. Pulay, *Annu. Rev. Phys. Chem.*, **35**, 191 (1984). Ab initio Vibrational Force Fields.

74. R. J. Bartlett, J. F. Stanton, and J. D. Watts, in *Advances in Molecular Vibrations and Collision Dynamics*, Vol. 1, J. Bowman, Ed., JAI Press, Greenwich, CT, 1991, p. 139. Analytic MBPT(2) Energy Derivatives: A Powerful Tool for the Interpretation and Prediction of Vibrational Spectra for Unusual Molecules.

75. C. E. Dykstra, J. D. Augspurger, B. Kirtman, and D. J. Malik, in *Reviews in Computational Chemistry*, Vol. 1, K. B. Lipkowitz and D. B. Boyd, Eds., VCH Publishers, New York, 1990, p. 83. Properties of Molecules by Direct Calculation.

76. J. Gauss and D. Cremer, *Adv. Quantum Chem.*, **23**, 206 (1992). Analytical Energy Gradients in Møller–Plesset Perturbation Theory and Quadratic Configuration Interaction Methods: Theory and Application.

77. J. Gauss, J. F. Stanton, and R. J. Bartlett, *J. Chem. Phys.*, **95**, 2623 (1991). Coupled-Cluster Open-Shell Analytic Gradients: Implementation of the Direct Product Decomposition Approach in Energy Gradient Calculations.

78. J. Gauss, J. F. Stanton, and R. J. Bartlett, *J. Chem. Phys.*, **95**, 2639 (1991). Analytic Evaluation of Energy Gradients at the Coupled-Cluster Singles and Doubles Level Using Quasi-Restricted Hartree–Fock Open-Shell Reference Functions.

79. J. Gauss, W. J. Lauderdale, J. F. Stanton, J. D. Watts, and R. J. Bartlett, *Chem. Phys. Lett.*, **182**, 207 (1991). Analytic Energy Gradients for Open-Shell Coupled-Cluster Singles and Doubles (CCSD) Calculations Using Restricted Open-Shell Hartree–Fock (ROHF) Reference Functions.

80. W. J. Lauderdale, J. F. Stanton, J. Gauss, J. D. Watts, and R. J. Bartlett, *J. Chem. Phys.*, **97**, 6606 (1992). Restricted Open-Shell Hartree–Fock Based Many-Body Perturbation Theory. Theory and Application of Energy and Gradient Calculations.

81. J. D. Watts, G. W. Trucks, and R. J. Bartlett, *Chem. Phys. Lett.*, **164**, 502 (1989). Coupled-Cluster, Unitary Coupled-Cluster and MBPT(4) Open-Shell Analytical Gradient Methods.

82. J. D. Watts, J. Gauss, and R. J. Bartlett, *Chem. Phys. Lett.*, **200**, 1 (1992). Open-Shell Analytical Energy Gradients for Triple Excitation Many-Body Coupled-Cluster Methods. MBPT(4), CCSD + T(CCSD), CCSD(T) and QCISDT(T). (UHF-CC/MBPT gradients.)

83. J. D. Watts, J. Gauss, and R. J. Bartlett, *J. Chem. Phys.*, **98**, 8718 (1993). Coupled-Cluster Methods with Non-Iterative Triple Excitations for Restricted Open-Shell Hartree–Fock and Other General Single Determinant Reference Functions. Energies and Analytical Gradients. (ROHF-CCSD(T) gradients.)

84. E. A. Salter, G. W. Trucks, and R. J. Bartlett, *J. Chem. Phys.*, **90**, 1752 (1989). Analytic Energy Derivatives in Many-Body Methods. I. First Derivatives.

85. J. F. Stanton, J. D. Watts, and R. J. Bartlett, *J. Chem. Phys.*, **94**, 404 (1991). Harmonic Vibrational Frequencies and Infrared Intensities from Analytic Fourth-Order Many-Body Perturbation Theory Gradients.

86. B. H. Besler, G. E. Scuseria, A. C. Scheiner, and H. F. Schaefer, III, *J. Chem. Phys.*, **89**, 360 (1988). A Systematic Theoretical Study of Harmonic Vibrational Frequencies: The Single and Double Excitation Coupled Cluster Model.

87. J. R. Thomas, J. B. DeLeeuw, G. Vacek, and H. F. Schaefer, III, *J. Chem. Phys.*, **98**, 1336 (1993). A Systematic Study of the Harmonic Vibrational Frequencies for Polyatomic Molecules. The Single, Double, and Perturbative Triple Excitation Coupled-Cluster [CCSD(T)] Method.

88. J. D. Head and M. C. Zerner, *Adv. Quantum Chem.*, **20**, 241 (1988). Newton-Based Optimization Methods for Obtaining Molecular Conformation.

89. T. Schlick, in *Reviews in Computational Chemistry*, Vol. 3, K. B. Lipkowitz and D. B. Boyd, Eds., VCH Publishers, New York, 1992, pp. 1–71. Optimization Methods in Computational Chemistry.

90. R. Hoffmann and R. B. Woodward, *Acc. Chem. Res.* **1**, 17 (1968). The Conservation of Orbital Symmetry.

91. N. C. Handy, R. D. Amos, J. F. Gaw, J. E. Rice, E. D. Simandiras, T. J. Lee, R. J. Harrison, W. D. Laidig, G. B. Fitzgerald, and R. J. Bartlett, *Geometrical Derivatives of Energy Surfaces and Molecular Properties*, P. Jørgensen and J. Simons, Eds., Reidel, Dordrecht, 1986, p. 179. Techniques Used in Evaluating Orbital and Wavefunction Coefficients and Property Derivatives [e.g., the evaluation of M(B)P(T)-2 second derivatives].

92. J. F. Stanton, J. Gauss, and R. J. Bartlett, *Chem. Phys. Lett.*, **195**, 194 (1992). Analytic Evaluation of Second Derivatives Using Second-Order Many-Body Perturbation Theory and Unrestricted Hartree–Fock Reference Functions.

93. J. Gauss, J. F. Stanton, and R. J. Bartlett, *J. Chem. Phys.*, **97**, 7825 (1992). Analytic (ROHF)-MBPT(2) Second Derivatives.

94. D. H. Magers, E. A. Salter, R. J. Bartlett, C. Salter, B. A. Hess, and L. J. Schaad, *J. Am. Chem. Soc.*, **110**, 3435 (1988). Do Stable Isomers of N_3H_3 Exist?

95. K. F. Ferris and R. J. Bartlett, *J. Am. Chem. Soc.*, **114**, 8302 (1992). Hydrogen Pentazole: Does It Exist?

96. T. R. Burkholder, L. Andrews, and R. J. Bartlett, *J. Phys. Chem.*, **97**, 3500 (1993). Reaction of Boron Atoms with Carbon Dioxide. Matrix and Ab Initio Calculated Infrared Spectra of OBCO.

97. W. H. Green, A. Willetts, D. Jayatilaka, and N. C. Handy, *Chem. Phys. Lett.*, **169**, 127 (1990). Ab Initio Prediction of Fundamental, Overtone and Combination Band Infrared Intensities.

98. Y. Yamaguchi, M. Frisch, J. Gaw, H. F. Schaefer, III, and J. S. Binkley, *J. Chem. Phys.*, **84**, 2262 (1986). Analytic Evaluation and Basis Set Dependence of Intensities of Infrared Spectra.

99. S. R. Gwaltney and R. J. Bartlett, *J. Chem. Phys.*, in press. Comment on: The Relation Between Intensity and Dipole Moment for Bending Modes in Linear Molecules.

100. E. D. Simandiras, J. E. Rice, T. J. Lee, R. D. Amos, and N. C. Handy, *J. Chem. Phys.*, **88**, 3187 (1988). On the Necessity of f-Basis Functions for Bending Frequencies.

101. M. E. Jacox, *J. Phys. Chem.*, **91**, 6595 (1987). Vibrational and Electronic Spectra of the H+HCN Reaction Products Trapped in Argon.

102. J. F. Stanton, W. N. Lipscomb, D. H. Magers, and R. J. Bartlett, *J. Chem. Phys.*, **90**, 1077 (1989). Highly Correlated Single-Reference Studies of the O_3 Potential Surface. I. Effects of High Order Excitations on the Equilibrium Structure and Harmonic Force Field of Ozone.

103. T. J. Lee, W. D. Allen, and H. F. Schaefer, III, *J. Chem. Phys.*, **87**, 7063 (1987). The Analytic Evaluation of Energy First Derivatives for Two-Configuration Self-Consistent Field Configuration Interaction Wavefunctions. Applications to Ozone and Ethylene.

104. S. M. Alder-Golden, S. R. Langhoff, C. W. Bauschlicher, and G. D. Carney, *J. Chem. Phys.*, **83**, 255 (1985). Theoretical Calculation of Ozone Vibrational Frequencies (CASSCF).

105. K. Raghavachari, G. W. Trucks, J. A. Pople, and E. Replogle, *Chem. Phys. Lett.*, **158**, 207 (1989). Highly Correlated Systems: Structure, Binding Energy and Harmonic Vibrational Frequencies of Ozone.

106. J. D. Watts, J. F. Stanton, and R. J. Bartlett, *Chem. Phys. Lett.*, **178**, 471 (1991). A Benchmark Coupled-Cluster Single, Double, and Triple Excitation (CCSDT) Study of the Structure and Harmonic Vibrational Frequencies of the Ozone Molecule.

107. D. H. Magers, W. N. Lipscomb, R. J. Bartlett, and J. F. Stanton, *J. Chem. Phys.*, **91**, 1945 (1989). The Equilibrium Structure and Harmonic Vibrational Frequencies of Ozone: Coupled-Cluster Results Including Triple Excitations.

108. T. J. Lee and G. E. Scuseria, *J. Chem. Phys.*, **93**, 489 (1990). Vibrational Frequencies of Ozone.

109. R. J. Bartlett, I. Shavitt, and G. D. Purvis, III, *J. Chem. Phys.*, **71**, 281 (1979). The Quartic Force Field of H_2O Determined by Many-Body Methods That Include Quadruple Excitation Effects.

110. R. J. Bartlett, S. J. Cole, G. D. Purvis, III, W. C. Ermler, H. C. Hsieh, and I. Shavitt, *J. Chem. Phys.*, **87**, 6579 (1987). The Quartic Force Field of H_2O Determined by Many-Body Methods. II. Effects of Triple Excitations.

111. J. M. Bowman, A. Wierzbicki, and J. Zuniga, *Chem. Phys. Lett.*, **150**, 269 (1988). Exact Vibrational Energies of Non-Rotating H_2O and D_2O Using an Accurate Ab Initio Potential.

112. M. Rittby and R. J. Bartlett, *J. Phys. Chem.*, **92**, 3033 (1988). An Open-Shell Spin-Restricted Coupled Cluster Method: Application to Ionization Potentials in N_2. (ROHF-CCSD, ROHF-CCSDT-1, QRHF-CCSD.)

113. R. L. Martin and D. A. Shirley, in *Electron Spectroscopy: Theory, Techniques and Applications*, C. R. Brundle and A. D. Baker, Eds., Academic Press, New York, 1977, p. 75. Many-Electron Theory of Photoemission.

114. J. Geertsen, C. M. L. Rittby, and R. J. Bartlett, *Chem. Phys. Lett.*, **164**, 57 (1989). The Equation-of-Motion Coupled-Cluster Method: Excitation Energies of Be and CO.

115. D. C. Comeau and R. J. Bartlett, *Chem. Phys. Lett.*, **207**, 414 (1993). The Equation-of-Motion Coupled-Cluster Method: Application to Open- and Closed-Shell Reference States.

116. J. F. Stanton and R. J. Bartlett, *J. Chem. Phys.*, **98**, 7029 (1993). The Equation-of-Motion Coupled-Cluster Method. A Systematic Biorthogonal Approach to Molecular Excitation Energies, Transition Probabilities and Excited State Properties.

117. J. D. Watts, M. Rittby, and R. J. Bartlett, *J. Am. Chem. Soc.*, **111**, 4155 (1989). Calculation of Molecular Ionization Potentials Using Single- and Multi-reference Coupled-Cluster Methods. Application to Methylenimine, CH_2NH and Methylenephosphine, CH_2PH.

118. S. Pal, M. Rittby, and R. J. Bartlett, *Chem. Phys. Lett.*, 160, 212 (1989). Multi-Reference Coupled-Cluster Methods of Ionization Potentials with Partial Inclusion of Triple Excitations.

119. J. D. Watts, J. Gauss, J. F. Stanton, and R. J. Bartlett, *J. Chem. Phys.*, 97, 8372 (1992). Linear and Cyclic Isomers of C_4. A Theoretical Study with Coupled-Cluster Methods and Large Basis Sets.

120. J. D. Bolcer and R. B. Hermann, this volume.

121. C. W. McCurdy, Jr., T. N. Rescigno, D. L. Yeager, and V. McKoy, in *Modern Theoretical Chemistry III*, H. F. Schaefer, III, Ed., Plenum, New York, 1977. The Equation of Motion Method: An Approach to the Dynamical Properties of Atoms and Molecules.

122. J. F. Stanton and R. J. Bartlett, *J. Chem. Phys.*, 98, 9335 (1993). Does Chlorine Peroxide Exhibit a Strong Ultraviolet Absorption Near 250 nm? (EOM-CCSD for excitation energies.)

123. C. M. L. Rittby and R. J. Bartlett, *Theor. Chim. Acta*, 80, 469 (1991). Multireference Coupled-Cluster Theory in Fock Space With an Application to s-Tetrazine.

124. H. Nakatsuji, *Acta Chimica Hungarica. Models in Chemistry*, 129, 719 (1992). Electronic Structures of Ground, Excited, Ionized and Anion States Studied by the SAC/SAC-CI Theory.

125. R. Krishnan, J. S. Binkley, R. Seeger, and J. A. Pople, *J. Chem. Phys.*, 72, 650 (1988). A Basis Set for Correlated Wavefunctions. (6-311G**).

126. R. McWeeny, in *Molecules in Physics, Chemistry, and Biology*, J. Maruani, Ed., Reidel, Dordrecht, 1989, p. 1. The Molecule as a Many-Electron System: Electron Densities and Molecular Properties.

127. D. Feller, C. M. Boyle, and E. R. Davidson, *J. Chem. Phys.*, 86, 3424 (1987). One-Electron Properties of Several Small Molecules Using Near-Hartree–Fock Limit Basis Sets.

128. H. Sekino and R. J. Bartlett, *J. Chem. Phys.*, 82, 4225 (1985). Spin Density of Radicals by Finite Field Many-Body Methods.

129. S. A. Perera, J. D. Watts, and R. J. Bartlett, to be published. Analytical Coupled-Cluster Evaluation of Spin Densities.

130. H. Sekino and R. J. Bartlett, *J. Chem. Phys.*, 98, 3022 (1993). Molecular Hyperpolarizabilities.

131. S. A. Perera and R. J. Bartlett, *Chem. Phys. Lett.*, in press. Relativistic Effects at the Correlated Level: An Application to Interhalogens.

132. S. A. Perera and R. J. Bartlett, *Phys. Rev.*, submitted. Nuclear Quadrupole Moments from Accurate Coupled-Cluster Electric Field Gradients.

133. J. F. Stanton and R. J. Bartlett, *J. Chem. Phys.*, in press. A Coupled-Cluster Based Effective Hamiltonian Method for Dynamic Electric Polarizabilities.

134. R. D. Amos, *Adv. Chem. Phys.*, 67, 99 (1987). Molecular Property Derivatives.

135. R. Ditchfield, *Mol. Phys.*, 27, 789 (1974). Self-Consistent Perturbation Theory of Diamagnetism. I. A Gauge-Invariant LCAO Method for NMR Chemical Shifts.

136. M. Schindler and W. Kutzelnigg, *J. Chem. Phys.*, 76, 1919 (1982). Theory of Magnetic Susceptibilities and NMR Chemical Shifts in Terms of Localized Quantities. II. Application to Some Simple Molecules.

137. T. D. Bouman and A. E. Hansen, *Int. J. Quantum Chem. Symp.*, 23, 381 (1989). Linear Response Calculations of Molecular Optical and Magnetic Properties Using Program RPAC: NMR Shielding Tensors of Pyridine and *n*-Azines.

138. K. Wolinski, J. F. Hinton, and P. Pulay, *J. Am. Chem. Soc.*, 112, 8251 (1990). Efficient Implementation of the Gauge-Independent Atomic Orbital Method for NMR Chemical Shift Calculations.

139. J. Gauss, *Chem. Phys. Lett.*, **191**, 614 (1992). Calculation of NMR Chemical Shifts as Second-Order Many-Body Perturbation Theory Using Gauge Including Atomic Orbitals.

140. J. Paldus, J. Čížek, and B. Jeziorski, *J. Chem. Phys.*, 90, 4356 (1989). Coupled-Cluster Approach or Quadratic Configuration Interaction?